Journal of CO2 Utilization 80 (2024) 102693

Contents lists available at ScienceDirect

Journal of CO2 Utilization

journal homepage: www.elsevier.com/locate/jcou

Review article

Recent advances in processes and catalysts for glycerol carbonate production via direct and indirect use of CO_2

Patcharaporn Inrirai [a], John Keogh [a], Ander Centeno-Pedrazo [a], Nancy Artioli [a,b], Haresh Manyar [a,*]

[a] School of Chemistry and Chemical Engineering, Queen's University Belfast, David-Keir Building, Stranmillis Road, Belfast BT9 5AG, UK
[b] Department of Civil, Environmental, Architectural Engineering and Mathematics, University of Brescia, Via Branze, 43, Brescia 25123, Italy

ARTICLE INFO

Keywords:
Carbon dioxide utilization
CCUS
Net zero
Bio-fuels
Glycerol
Glycerol carbonate

ABSTRACT

Glycerol can be utilised as a renewable feedstock in several chemical reactions, including carbonation, carbonylation, transesterification, and oxidation. Among the several conversions, the production of glycerol carbonate is environmentally most attractive, as it also utilises CO_2 as the carbon source, as C1 feedstock, a key to accelerate the pursuit of decarbonization and the net-zero goals. The glycerol carbonate production can be divided into two main pathways i.e., direct and indirect route based on the utilisation of CO_2. There has been much interest in the direct conversion of glycerol with molecular CO_2, due to its potential for sustainability and ecological advantages. Moreover, this process could be directly minimising CO_2 levels in atmosphere. The indirect pathways involve the utilisation of CO_2 as a source for the synthesis of reactants, for instance organic carbonates and urea. These reactants are employed as raw materials in the process of glycerol carbonate production. It is important to note that each reaction route has its own set of advantages and drawbacks. However, the important factor for all processes lies in the high catalytic performance of the suitable catalyst and the optimal reaction conditions to enhance the yield of glycerol carbonate. This review aims to evaluate the recent progress made on the catalyst design and process conditions to produce glycerol carbonate via both the direct and indirect reaction pathways. In each route, the catalytic systems based on the heterogenous catalysts, the reaction condition and catalytic performance are considered. Finally, suggested perspectives for the future direction in glycerol carbonate production focusing on the utilisation of molecular CO_2 are presented.

1. Introduction

Considering the projected global population growth of 50 % by the year 2040, there will be a resulting rise in energy demand [1]. Fossil fuels, such as natural gas, oil, and coal, account for about 80 % of the global energy source. Fossil fuels have emerged as the major source of energy over the past decade. The extensive consumption of products derived from fossil fuels in the past few years has given rise to an energy depletion crisis and pollution [2]. Annual increases in carbon dioxide (CO_2) concentrations in the atmosphere have been documented by statistical data. In comparison to 2021, global CO_2 emissions rose by 1.5 % in 2022, leading to 36.1 $GtCO_2$ [3]. The sectoral analysis of CO_2 emissions in 2022 demonstrates that each consumption pattern following as: 39.3 % of the total CO_2 emissions were attributed to power, 28.9 % to

Abbreviations: ACN, Acetonitrile; [APmim]OH, 1-aminopropyl-3-methylimidazole hydroxide; BET, Brunauer–Emmett–Teller; COF, Covalent organic framework; CTAB, Cetyltrimethylammonium bromide; DABCO, 1,4-diazabicyclo[2.2.2]octane; DEC, Diethyl carbonate; DMAP, 4-(dimethylamino)pyridine; DMC, Dimethyl carbonate; DMF, Dimethylformamide; DMSO, Dimethyl sulfoxide; EC, Ethylene carbonate; ETS-10, microporous titanosilicate; FTIR, Fourier-transform infrared; HT, Hydrothermal; HMS, hexagonal mesoporous; LDHs, Layered double hydroxides; LSHV, Liquid hourly space velocity; MCM-41, 2D hexagonal mesoporous silica; MIPCA, *Mangifera indica* peel calcined ash; MMOs, Mixed metal oxides; MO, Metal oxide; NaTNT, Pristinedosium titanate nanotube; NDW, Ni-modified distillation waste; NHC, N-Heterocyclic carbene; NMP, *N*-methyl-2-pyrrolidone; OSC, Oxygen storage capacity; PC, Propylene carbonate; PEG, Polyethylene glycol; PMDTA, *N,N,N′,N″,N″*-pentamethyldiethylene triamine PT, Precipitation; PVP, polyvinylpyrrolidone; SA, Sodium aluminate; SBA-15, Uniform hexagonal mesoporous silica; SG, Sol-gel; SNS, Snail shell; SNS-AP, Snail shell apatite; TNT, Titanium nanotubes; TMEDA, *N,N,N′,N′*-tetramethylethane-1,2-diamine; TPR, Temperature programmed reduction; TUD-1, 3D mesoporous silica; $V_O^{\cdot}$, Oxygen vacancies; ZIF-8, Zeolitic imidazolate framework-8; ZSM-5, Zeolite socony mobil-5.

* Corresponding author.
E-mail address: h.manyar@qub.ac.uk (H. Manyar).

https://doi.org/10.1016/j.jcou.2024.102693
Received 5 November 2023; Received in revised form 2 January 2024; Accepted 26 January 2024
Available online 5 February 2024

industry, 17.9 % to ground transportation, 9.9 % to residential, 3.1 % to international bunkers (international aviation and shipping), and 0.9 % to domestic aviation [3]. It is critical in this situation to develop new fuels with properties comparable to those of fossil fuels. Biodiesel is one of the most crucial fuels for the replacement of fossil fuels [2,4]. In contrast to petro-diesel, biodiesel fuel has several beneficial features such as the absence of sulfur and aromatic compounds, non-toxicity, renewability, and a high flash point [2]. Additionally, the use of a biodiesel/diesel blend in vehicles could effectively reduce air pollution. Recent life cycle assessment studies indicate that the utilisation of biodiesel can result in a reduction of carbon dioxide (CO_2) and carbon monoxide (CO) emissions by 8–41 % [5,6]. Consequently, the growing market demand for biodiesel has resulted in an excessive amount of glycerol, leading to a significant decrease in its price. The manufacturing of biodiesel results in the by-product of glycerol, which constitutes 10 % w/w of the total output. It is necessary to find a suitable application for this glycerol to enhance the economic viability of the biodiesel production process [7,8].

Glycerol is considered a valuable by-product due to its extensive utilisation in various industrial sectors. Currently, glycerol exhibits a wide range of applications, particularly within the fields of pharmaceuticals, personal care products, food industry, and cosmetics [9]. Moreover, it possesses significant promise as a primary chemical reactant in the synthesis of several organic molecules. Glycerol has the potential to undergo several transformations resulting in the production of many derivatives with added value. These derivatives include glycerol esters, 1,2-propanediol, mesoxalic acid, glycerol 1,3-bromo- and iodohydrins, dihydroxyacetone, glyceric acid, oxalic acid, tartronic acid, syngas, hydrogen, and glycerol carbonate [10]. Glycerol carbonate (GC) (IUPAC: 4-hydroxymethyl-1,3-dioxolan-2-one, CAS: 931–40-8) contains two different reactive sites, namely a cyclic carbonate group and a hydroxyl group, resulting in an attractive starting material. These reactive sites of glycerol carbonate have potential uses as a green solvent for chemicals, additives for cosmetic (nail paint) [11], alkylating agent for production of β-Aryloxy alcohols [12], skincare products, and medicine. Glycerol carbonate was also used as raw material for the synthesis of chemical intermediates and various polymers, including polyesters, polycarbonates, and polyurethanes for the production of coatings, adhesives, foams, and lubricants [7,8].

In continuation of our group's interest in CO_2 utilisation, biofuels and environmental catalysis [13–26], herein we have attempted to review the recent progress made in the development of various direct and indirect processes for production of glycerol carbonate. The synthesis of glycerol carbonate has been recently noted using various processes, which can be divided into two categories, indirect and direct route [27]. For the direct process, glycerol carbonate can be synthesised by carbonation reaction of glycerol with CO_2 in the presence of catalysts as shown in Fig. 1. The reaction utilised catalysts that were metal-free, heterogeneous, and homogeneous, as reported by Lukato et al. [28]. While the heterogeneous catalyst seems to exhibit good catalytic performance, moreover, a dehydrating agent might enhance the reaction by breaking the thermodynamic limit.

Glycerol carbonate can also be synthesised via oxidative carbonation of glycerol with carbon monoxide and oxygen process in the presence of catalysts or other reactants, which is an indirect pathway as shown in Fig. 2. The utilisation of the given synthesis pathway was restricted due to the hazardous nature of carbon monoxide and the inherent challenges associated with its safe handling, both in laboratory and industrial manufacturing [29].

For other the indirect routes, glycerol carbonate can also be produced by following three reactions, (1) Transcarbonation of glycerol with phosgene, (2) Carbonylation with urea and (3) Transesterification of glycerol with different carbonate sources as shown in Figs. 3–5 [27, 29]. Moreover, Glycidol is a product from transesterification between glycerol with dimethyl carbonate (DMC) and can use as a starting reactant with CO_2 for production glycerol carbonate [30].

The synthesis process of glycerol with phosgene has been discontinued due to its high toxicity and unsafe reactants [29,35]. Additionally, the carbonylation of glycerol with urea results in the generation of environmentally harmful by-products, namely isocyanic acid and biuret and it is necessary to eliminate ammonia throughout the reaction process [36]. So that, the objective of synthesising glycerol carbonate, either direct or indirect process, is to minimise the environmental impact from carbon dioxide by using and reducing its amount in atmosphere, hence enhancing its potential for utilisation. Furthermore, using glycerol as a reagent for producing value-added products has the potential to minimise the amount of waste glycerol, are generated by biodiesel manufacturing [37]. In addition, utilising carbon dioxide (CO_2) as a feedstock to produce value-added chemicals is a more environment friendly approach to carbon reduction compared to its deep underground storage [38]. Furthermore, the utilisation of CO_2 as a reactant in the direct carbonation of glycerol is widely regarded as a very promising process for the energy-efficient, waste-minimising, and atom-efficient synthesis of glycerol carbonates [27,38,39]. Theoretically, this reaction has the potential to be classified as a green reaction [27].

2. Direct synthetic route for glycerol carbonate production

2.1. Mechanism

Glycerol carbonate can be synthesised through the reaction of glycerol with carbon dioxide in the presence of catalysts. In recent years, there have been an increasing number of reports on heterogeneous catalysts used in the synthesis of glycerol carbonate from glycerol and CO_2. Among these, the metal oxide catalyst exhibited good results.

Liu et al. [40] have suggested the possible reaction of glycerol and carbon dioxide to produce glycerol carbonate over CeO_2 based catalysts, which involves four steps as follows:

(i) Formation of Cerium glyceroxide – the hydroxyl (OH) group of glycerol undergoes adsorption onto the Lewis basic sites (Ce^{4+}) present on the catalysts.

(ii) Carbon dioxide (CO_2) was activated in the form of chelating bidentate carbonate species.

(iii) A seven-membered ring of esters was synthesised by directly inserting activated carbon dioxide into cerium alkoxides.

(iv) Formation of glycerol carbonate - an intramolecular nucleophilic attack, where the alkoxy group (located close to Ce) reacted with the carbonyl carbon atoms.

The absorption of water molecule on the cerium alkoxide occurred during the synthesis of seven-membered ring of esters, 2-cyanopyridine interacted with this molecule to generate 2-picolinamide. Eliminating water from the process may break the thermodynamic limitation of the reaction, resulting in an enhanced yield of glycerol carbonate. The reaction mechanism for the formation of glycerol carbonate between glycerol and CO_2 in the presence of dehydrating agent, is shown in

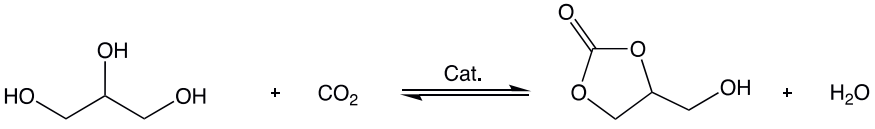

Fig. 1. Reaction scheme for carbonation of glycerol with carbon dioxide [29].

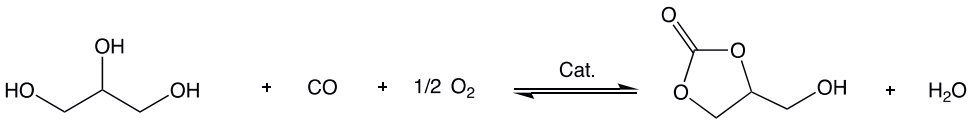

Fig. 2. Reaction scheme for oxidative carbonation with carbon monoxide and oxygen [29].

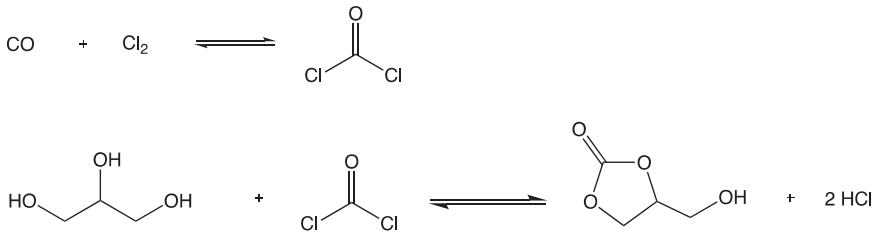

Fig. 3. Reaction scheme for transcarbonation of glycerol with phosgene [29,31].

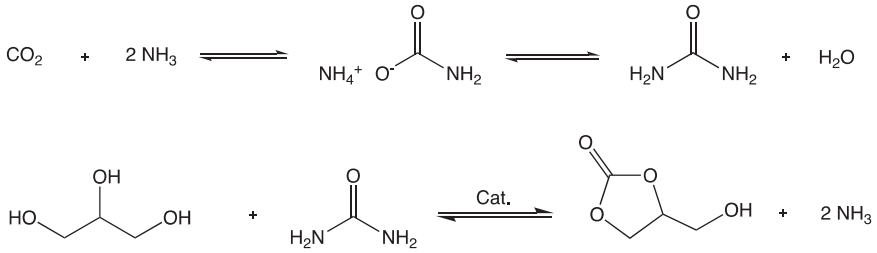

Fig. 4. Reaction scheme for carbonylation with urea [29,32,33].

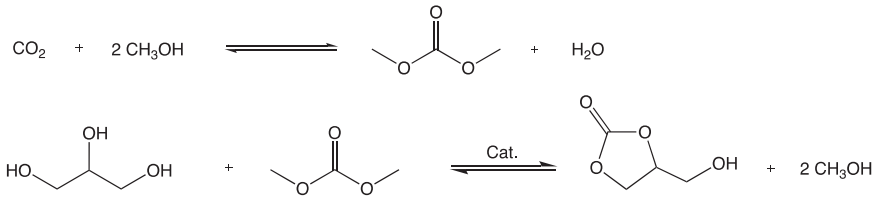

Fig. 5. Reaction scheme for transesterification of glycerol with dimethyl carbonate [29,34].

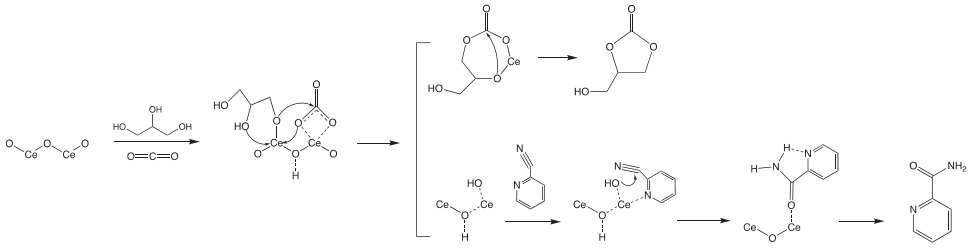

Fig. 6. The possible reaction mechanism over CeO_2- based catalysts [40].

Fig. 6.

2.2. Single component metal oxide

Five metal oxides (ZnO, SnO_2, Fe_2O_3, La_2O_3 and CeO_2) were synthesised by sol-gel method. Ozorio and Mota [41] observed that zinc oxides (ZnO) presented better catalytic activity compared to other metal oxides in the absence of a dehydrating agent. Under conditions of 180 °C, 15 MPa, and a reaction time of 12 h, they achieved a glycerol carbonate yield of 8.1 %. The yields of Fe_2O_3 and La_2O_3 were similar, both approximately 7 %. The CeO_2 catalyst resulted in a yield of 6 % for glycerol carbonate. Furthermore, Su et al. [42] examined to enhance catalytic performance of ZnO in the presence of a dehydrating agent. The production of glycerol carbonate resulted in a yield of 11.9 % when undertook at 170 °C for 12 h with a CO_2 pressure of 10 MPa. ZnO is a light-harvesting component. Li et al. [43] conducted a transformation of glycerol and CO_2 with light irradiation. By comparison of two methods, the light transformation process yielded a larger amount (1.5 %) of glycerol carbonate compared to the thermal-driven reaction (1.1 %), which is the same as $La_2O_2CO_3$. The production of glycerol carbonate significantly rose from 1.7 % to 3.0 % while using the $La_2O_2CO_3$ with light irradiation method. In addition, Liu and He [44] synthesised ZnO using the hydrothermal technique. The BET surface area measured 24.3 m^2/g with acid and basic sites totaling 0.1843 mmol/g and

0.4247 mmol/g, respectively. The ZnO catalyst achieved a glycerol carbonate yield of 2.3 % under the conditions of operating at a temperature of 150 °C for 6 h with a CO_2 pressure of 5 MPa in the DMF solvent.

The catalytic performance of Ti, Zr, and Al oxides was also examined, as reported by Su et al. [42]. All catalysts exhibited a yield of glycerol carbonate < 11 %. During the investigation, CeO_2 had a greater yield of 14.2 % compared to other metal oxides. It exhibited more effectiveness and selectivity in the process of carbonylation.

Among the wide range of metal oxides, cerium dioxide (CeO_2) seems to exhibit great potential as a catalyst for improving the conversion of biomass feedstocks. Cerium dioxide (CeO_2) and catalysts based on cerium were previously recognized as crucial materials in the process of carbon dioxide (CO_2) transformation reactions. The main reason for using ceria as a catalyst is its oxygen storage capacity (OSC), which enables it to release oxygen in a reduced atmosphere and fill oxygen vacancies in an oxidising atmosphere [45,46].

Cerium (IV) oxide is more commonly referred to as ceria (CeO_2). The cubic fluorite structure of stoichiometric CeO_2 is an ideal crystal arrangement. This structure is composed of unit cells that have a face-centered cubic configuration. Within this structure, it can be observed that each Ce^{4+} ion has a coordination number of eight oxygen ions, whereas each O^{2-} ion is coordinated by four Ce^{4+} ions. The presence of oxygen vacancies (Vo) on the surface and in the bulk is often accompanied by the structure of cerium, leading to the reversible charge transfer between Ce^{4+} and Ce^{3+} stages of Ce^{3+} cations. The presence of oxygen vacancy defects and Ce^{3+} ions in ceria has been found to enhance the adsorption and activation of carbon dioxide gas, as well as improve oxygen self-diffusion inside the lattice of nonstoichiometric ceria. These defects and ions play a significant role in increasing the efficiency of redox processes and catalytic reactions. Moreover, ceria exhibits unique acid and basic properties due to its amphoteric nature. According to current research, it is widely accepted that CeO_2 acts as a weak Lewis acid and a moderately strong Lewis base [46–48].

There are several methods have been reported for the synthesis of nanostructured ceria, including hydrothermal/solvothermal technique, precipitation, surfactant-assisted synthesis, template approach, sol-gel method, thermal decomposition, and microwave-assisted synthesis [49]. These methods provide different surface morphologies, textural properties, and crystalline sizes. The catalyst's surface morphology is one of the key factors that influence its catalytic activity [47]. Liu et al. [50] conducted the synthesis of CeO_2 via three different methods. The nanorod (CeO_2-HT-400) was synthesised by a hydrothermal process, which yielded a significantly greater BET surface area (89.0 m^2/g), pore volumes (0.31 cm^3/g), and average pore diameter (26.36 nm) compared to two other preparation techniques (-PT and -SG). However, the average crystalline size of the nanorod (9.3 nm) was found to be smaller than that of CeO_2 catalyst generated using the other two methods. The glycerol conversion and glycerol carbonate yield obtained with a nanorod catalyst were 38.0 % and 33.3 %, respectively. The experimental conditions for this reaction involved the use of 10 mmol of glycerol, 30 mmol of 2-cyanopyridine, 0.52 g of catalyst, and 10 mL of DMF at 150 °C for 5 h with CO_2 pressure of 4.0 MPa. The correlation between the conversion of glycerol and the yield of glycerol carbonate seems to be dependent on the surface area. However, it is important to note that the correlations between the rate of conversion and the rate of glycerol carbonate formation were not linear, as shown in Table 1. According to the data, the activity and selectivity of the catalysts appeared to be affected by variables other than their surface area. In general, the defect and acid-base sites are considered as the active centers.

Additionally, Liu et al. [50] reported that the basicity of CeO_2 increased from 55 mmol/g for CeO_2 nanoparticles to 113 mmol/g for sponge-like CeO_2 nanorods and 251 mmol/g for nanorods CeO_2. The oxygen vacancy density could be derived from the H_2 consumption below 600 °C, which was ranked as follows: CeO_2-HT-400 > CeO_2-PT-400 > CeO_2-SG-400. This suggests that the nanorods possess the greatest capacity for oxygen storage and release, while the sponge-like CeO_2 exhibits the least. Although CeO_2-HT-400 exhibited a notable glycerol conversion and glycerol carbonate yield, which may be related to its increased surface area, however, the basic site of the catalyst and the presence of oxygen vacancies have been observed to significantly influence its activity.

Table 1
Physicochemical properties, rate of glycerol conversion and glycerol carbonate formation of CeO_2 catalyst prepared by different methods [50].

Catalyst	BET surface area (m^2/g)	Total basic site amount (mmol CO_2/g catalyst)	Rate (mmol/ (m^2 h))	
			Glycerol conversion	Glycerol carbonate formation
CeO_2-PT-400	59.4	0.055	1.99×10^{-2}	1.90×10^{-2}
CeO_2-HT-400	89.0	0.251	1.67×10^{-2}	1.43×10^{-2}
CeO_2-SG-400	40.6	0.113	1.96×10^{-2}	1.94×10^{-2}

Gao et al. [38] produced CeO_2 with various morphologies, including octahedral, nanorod, and nanocubes structures, using the hydrothermal technique. The nanooctahedra of CeO_2 have sizes ranging from 200 to 500 nm. Both nanorods have a diameter of 10 – 15 nm, while their length ranges from 150 to 500 nm. The nanocubes have a regular shape with edge lengths ranging from 150 – 200 nm. Both the nanorods exhibited much greater BET surface areas, with values of 84.64 m^2/g and 56.67 m^2/s, compared to the nanocubes and octahedral structures. However, it was observed that the CeO_2 octahedral structure exhibited the highest amount of basic sites and acid sites, measuring 0.0631 μmol/m^2 and 0.3123 μmol/m^2, respectively, as shown in Table 2. The CeO_2 nanorods exhibited a higher amount of acidic sites but a smaller amount of basic sites in comparison to the nanocubes. The rate of glycerol carbonate formation per unit surface area was investigated with different CeO_2 catalysts under conditions of 160 °C for 24 h with 4 MPa of CO_2. The CeO_2 nanooctahedra exhibited a cumulative formation rate of 1.548 mmol/m^2, while the two CeO_2 nanorods displayed significantly lower cumulative formation rates of 0.155 mmol/m^2 and 0.134 mmol/m^2, respectively. The CeO_2 nanocubes revealed a formation rate of 0.988 mmol/m^2. The catalytic efficacy, indicated by the rate of glycerol carbonate formation, seems to be linearly dependent not on acidity or the acidity-to-basicity ratio, but on the density of basic sites. The Lewis basic sites occupied by the oxygen anions on the CeO_2 surface play an important role for the adsorption and activation of CO_2.

Su et al. [42] revealed five different crystal structures of CeO_2, namely mesoporous, nanocubes, nanorods, nanowires, and nanopolyhedra. The CeO_2 nanopolyhedra exhibited the maximum efficiency in producing glycerol carbonate and achieving the highest conversion

Table 2
Physicochemical properties and catalytic performance of the CeO_2 nanocrystals prepared by different methods [38].

Catalysts	Size (nm)	BET surface area (m^2/g)	Basic sites (μmol/m^2)	Acid sites (μmol/m^2)	Glycerol carbonate formation rate (mmol/m^2)
Octahedron	200-500	5.677	0.0631	0.3126	1.548
Cube	150-200	7.816	0.0433	0.0253	0.988
Rod-N	(10-15) x (150-500)	84.64	0.0237	0.1030	0.155
Rod-C	(10-15) x (150-500)	75.46	0.0232	0.1228	0.134

rate. Subsequently, the crystal structure of CeO_2 was also examined. The CeO_2 nanopolyhedra catalyst presented a maximum yield of 14.2 % and conversion of 35.5 % when 2-cyanopyridine was present, greater than the yield of 0.8 % and conversion of 1.6 % obtained in the absence of a dehydrating agent.(Tables 3 and 4).

2.3. Mixed metal oxide

2.3.1. Binary system

Binary mixed metal oxides are formed by combining two metal oxides to create beneficial functions and features that are suitable for the direct conversion of glycerol and CO_2. Lanthanum dioxycarbonate ($La_2O_3CO_3$) is easily produced when lanthanum is exposed to water (H_2O) and carbon dioxide (CO_2) at high temperature conditions. The reaction of glycerol and CO_2 to form glycerol carbonate was carried out using $La_2O_3CO_3$ catalysts and acetonitrile (CN_3CN) was used as the solvent and dehydration agent in this process [51]. La-Zn mixed oxide with different molar ratio was prepared a co-precipitation method [51]. Increasing the size of the bigger ions relative to the smaller ions inhibits the diffusivity t of the supporting material and prevents the formation of aggregates. Increasing the La component leads to a significant rise in the specific surface area of the La-Zn catalysts, from 8.3 m^2/g to 47.4 m^2/g. The oxygen atoms present on the surface lattice can be identified as Lewis basic sites. The introduction of $La_2O_3CO_3$ resulted in an increase in the quantity of lactic oxygen, suggesting that this leads to a greater quantity of basic sites and consequently favors CO_2. La–Zn catalysts resulted in the formation of moderately more basic sites, which increased as the La content rose; $La_2O_3CO_3$-ZnO calcined at 500 °C in a 0.25 molar ratio contained more basic sites than the other samples. According to Li et al. [51], the combination of $La_2O_2CO_3$ and ZnO resulted in a 14.3 % production of glycerol carbonate at a temperature of 170 °C for 12 h. A further investigation on the La-Zn oxide catalyst was conducted by Li et al. [52]. This catalyst was obtained by the process of calcination of hydrotalcite precursors. The uncalcined catalyst, consisting of La^{3+}: Zn^{2+} in a 1:4 at. ratio, had a BET surface area of 20.6 m^2/g. Its basicity was characterised as moderately basic sites resulting from the formation of $La_2O_3CO_3$. A glycerol carbonate yield of 10.8 % and a selectivity of 50.5 were achieved using a (1:4) La-Zn catalyst, which was greater than the yield produced using a (2:1) Al-Zn catalyst under the same conditions (170 °C, 12 h). La–Zn catalysts was also synthesised by Hu et al. [53]. The catalyst with a La/ZnO weight ratio of 7 % exhibited excellent catalytic activity when CH_3CN was used as the dehydrating agent. In addition, Li et al. [43] utilised $La_2O_3CO_3$-ZnO (hydrothermal) for photo-thermal transformation. The total amount of basic sites was determined by including weak and moderate basic sites, resulting in a value of 29.8 μmol CO_2/g for ZnO. The density of basic sites on the catalysts rose from 1.9 μmol CO_2/m^2 for ZnO to 5.3 μmol CO_2/m^2 for 50 % $La_2O_3CO_3$–ZnO, indicating that the presence of $La_2O_3CO_3$ in combination with ZnO slightly improved the density of basic sites. The glycerol conversion reached a yield of 6.1 % under reaction conditions of 150 °C, 5.5 MPa CO_2, with a reaction time of 6 h. This conversion was obtained using a catalyst consisting of 20 % $La_2O_2CO_3$–ZnO.

Zhang and He [54] examined the use of the impregnation method to load varying amounts of Cu onto lanthanum oxide (La_2O_3). The BET surface area of Cu/ La_2O_3 exhibited a slight decrease in comparison to pure La_2O_3, which had a surface area of 21 m^2/g. Furthermore, the amount of basic sites reduced with the introduction of Cu, particularly for the high-strength basic sites. Following the loading of Cu into La_2O_3, ranging from 0 % to 13.4 %, the amount of basic sites decreased from 173 μmol CO_2/g to 84 μmol CO_2/g. When employing a catalyst consisting of 3 %Cu/La_2O_3, the glycerol conversion, glycerol carbonate yield, and selectivity were 33.4 %, 15.2 %, and 45.4 %, respectively. Zhang and He [55] investigated the loading of Cu into several metal oxide supports (La_2O_3, CaO, MgO, Al_2O_3, and ZrO_2) using impregnation. The acid-base properties analysis revealed that Cu/ La_2O_3, Cu/CaO, and Cu/MgO did not possess any acid sites on their surfaces, but Cu/Al_2O_3 and Cu/ZrO_2 showed both acid and basic sites on their surfaces. These catalysts were ranked based on their basicity as follows: Cu/CaO > Cu/MgO > Cu/ La_2O_3 > Cu/Al_2O_3 > Cu/ZrO_2. On the contrary, Cu/Al_2O_3 exhibited the maximum surface area, measuring 197.4 m^2/g, while Cu/CaO had the lowest surface area. The utilisation of CH_3CN as a dehydrating agent resulted in a greater conversion of acetic acid when acid catalysts were used, compared to the conversion obtained with base catalysts. Al-kurdhi and Wang [56] conducted the reaction of CuO with Al_2O_3 support in the presence of 2-cyanopyridine. The catalyst consisting of 30 % CuO supported on Al_2O_33, which was calcined at 700 °C, exhibited great catalytic performance due to its high surface area of 170 m^2/g and a greater number of basic sites (1.082 mmol/g). At a pressure of 4.0 MPa of CO_2 and a temperature of 150 °C for 5 h, the glycerol conversion and glycerol yield may reach values as high as 41.3 % and 17.5 %, respectively.

$ZnWO_4$-ZnO catalysts were synthesised using the wet impregnation procedure, with varying amounts of WO_3 content [44]. Upon loading 10

Table 3
Catalyst characterisation of single component metal oxide catalyst for direct carbonation of glycerol with CO_2.

Catalyst	Morphology	BET surface area (m^2/g)	Pore Volume (cm^3/g)	Average Pore diameter (nm)	Crystalline size (nm)	H_2-TPR (mmol)	Total acid site amount (mmol NH_3/g catalyst)	Total basic site amount (mmol CO_2/g catalyst)	Ref.
ZnO	–	15.4	0.0277	12.7	–	–	–	0.0293	[43]
ZnO - hydrothermal	uniform nanoparticle	24.3	0.048	17.0	–	0.210	0.184	0.424	[44]
$La_2O_2CO_3$	–	5.1	0.0076	8.4	–	–	–	0.0073	[43]
CeO_2- Precipitation Calcined at 400 °C for 5 h	nanoparticles	59.4	0.16	9.94	11.7	0.072	–	0.055	[50]
CeO_2- hydrothermal Calcined at 400 °C for 5 h	nanoroads	89.0	0.31	26.36	9.3	0.135	–	0.251	[50]
CeO_2- sol-gel method Calcined at 400 °C for 5 h	sponge-like	40.6	0.09	7.61	9.9	0.027	–	0.113	[50]
CeO_2 – hydrothermal Calcined at 400 °C for 5 h	nanorods	69.4	0.23	14.0	15.0	0.0626	0.025	0.063	[40]
CeO_2 - mixed	cubes and spheroidal	9.5	–	–	12.1	–	–	–	[45]
CeO_2 - cube	nanocubes	25.7	–	–	11.6	–	–	–	[45]
CeO_2 – rod	nanorods	85.8	–	–	9.3	–	–	–	[45]

Table 4
Reaction conditions and catalyst performance of single component metal oxide catalysts for direct carbonation of glycerol with CO_2.

Catalyst	Operating Parameters							performance	Ref.
	Temp. (°C)	Time (h)	mole ratio of glycerol to dehydrating agent	Catalyst loading	Solvent	Pressure CO_2 (MPa)	Dehydration agent		
ZnO	180	12	25.2 g Gly	2 mmol	–	15	–	Y = 8.1 %	[41]
ZnO	170	12	1:2	0.085 g	DMF 2 mL	10	2-cyanopyridine	Y = 11.9 % C = 41.3 %	[42]
ZnO – light irradiate	150	6	0.92 g Gly	0.50 g	DMF 20 mL	5.5	–	Y = 1.5 % C = 1.6 %	[43]
ZnO - hydrothermal	150	6	0.92 g Gly	0.50 g	DMF 20 mL	5	–	C = 2.3 % S = 100 %	[44]
La_2O_3	180	12	25.2 g Gly	2 mmol	–	15	–	Y = 7 %	[41]
$La_2O_2CO_3$ – light irradiate	150	6	0.92 g Gly	0.50 g	DMF 20 mL	5.5	–	Y = 3.0 % C = 3.6 %	[43]
Fe_2O_3	180	12	25.2 g Gly	2 mmol	–	15	–	Y = 7 %	[43]
TiO_2	170	12	1:2	0.085 g	DMF 2 mL	10	2-cyanopyridine	Y = 10.9 % C = 30.9 %	[42]
Al_2O_3	170	12	1:2	0.085 g	DMF 2 mL	10	2-cyanopyridine	Y = 10.5 % C = 34.5 %	[42]
ZrO_2	170	12	1:2	0.085 g	DMF 2 mL	10	2-cyanopyridine	Y = 10.4 % C = 37.2 %	[42]
CeO_2	180	12	25.2 g Gly	2 mmol	-	15	-	Y = 6 %	[41]
CeO_2-nanoparticle	150	5	1:3	1.72 g	DMF 10 mL	4.0	2-cyanopyridine	Y = 79.8 %	[50]
CeO_2 - mixed	150	5	1:3	0.17 g	DMF 10 mL	4.0	2-cyanopyridine	Y = 4.1 % C = 4.2 % S = 98.7 %	[45]
CeO_2 - cube	150	5	1:3	0.17 g	DMF 10 mL	4.0	2-cyanopyridine	Y = 4.6 % C = 4.7 % S = 98.4 %	[45]
CeO_2 - rod	150	5	1:3	0.17 g	DMF 10 mL	4.0	2-cyanopyridine	Y = 9.1 % C = 9.2 % S = 99.0 %	[45]
CeO_2 - nanopolyhedra	170	12	1:2	0.085 g	DMF 2 mL	10	2-cyanopyridine	Y = 14.2 % C = 35.5 %	[42]
CeO_2 - mesoporous	170	12	1:2	0.085 g	DMF 2 mL	10	2-cyanopyridine	Y = 10.3 % C = 29.3 %	[42]
CeO_2 - nanocubes	170	12	1:2	0.085 g	DMF 2 mL	10	2-cyanopyridine	Y = 10.4 % C = 34.4 %	[42]
CeO_2 - nanorods	170	12	1:2	0.085 g	DMF 2 mL	10	2-cyanopyridine	Y = 12.9 % C = 28.1 %	[42]
CeO_2 - nanowires	170	12	1:2	0.085 g	DMF 2 mL	10	2-cyanopyridine	Y = 13.5 % C = 38.2 %	[42]

Note: Y = yield of glycerol carbonate, C = conversion of glycerol, S = selectivity of glycerol carbonate, DMF = Dimethylformamide, Gly = Glycerol

% WO_3 into ZnO, the BET surface area, total acid sites, and total basic sites decreased to 20.0 m^2/g, 0.137 mmol/g, and 0.359 mmol/g, respectively, in comparison to pure ZnO. The interaction between $ZnWO_4$ and ZnO results in an improved moderate acidic characteristic. In their study, Lei and He [44] found that the use of a 10 % $ZnWO_4$-ZnO catalyst resulted in a glycerol carbonate yield of 6.5 %. Furthermore, at the optimal reaction conditions of 150 °C for 6 h with 5 MPa CO_2, the selectivity of glycerol carbonate was almost 100 %.

Specific catalytic properties are attributed to metal oxide catalysts, which are utilised in the majority of industrial processes. These properties include acidity (Lewis or Brønsted types), basicity, and redox properties (when transition metal ions are present) [57]. The catalytic performance of cerium dioxide (CeO_2) is considerably influenced by the ratio of Ce^{3+}/Ce^{4+} and the concentration of oxygen vacancies (Vo). One method for adjusting the oxygen vacancy concentration on the surface of CeO_2 involves element doping and metal loading. This technique has been shown to greatly enhance the redox properties of CeO_2.

According to the results reported by Kehoe et al. [58], the introduction of divalent dopant ions into ceria (CeO_2) has been shown to enhance both the reducibility and the oxygen storage capacity (OSC). The main purpose of the dopant is to induce lattice distortion, thereby breaking the MO bonds and producing weakly or undercoordinated oxygen atoms that may be easily eliminated. The doping of larger dopants, such as Mg, Ca, Sr, and Ba, induces slightly distortion in the lattice structure. However, this distortion does not exhibit a substantial reduction in the energy required for the reducibility. While the size of the dopant ion does play a role, the main factor influencing the system is the distortion resulting from the electronic structure required by the dopants.

Zirconia (Zr) was introduced as a dopant onto the CeO_2 nanorod using the hydrothermal technique, with varying atomic ratios. In their study, Liu et al. [40] found an increase in surface area to 102.9 m^2/g and a decrease in crystalline size to 8.1 nm when the mole percentage of Zr was 0.02. The doping of Zr to CeO_2 resulted in a noticeable shift in reduction peaks. Specifically, the low-temperature peak exhibited a shift towards higher temperatures, whilst the high-temperature peak showed a shift towards lower positions compared to pure CeO_2. The increase in H_2 consumption observed in the low-temperature peak of H_2-TPR curves indicates a gradual improvement in the oxygen storage capacity. The Zr concentration of 0.02 (x) had the highest amount of acid sites, at 42 μmol NH_3/g. The catalytic efficacy of $Ce_{1-x}Zr_xO_2$ was observed to exhibit improvement in comparison with pure CeO_2 during the glycerol carbonate synthesis process. There was an increase in the conversion rate of glycerol, which rose from 25.5 % to 40.9 %. Additionally, the

yield of glycerol carbonate showed an increase, from 21.4 % to 36.3 %. These increases were observed as the molar fraction of Zr (x) increased gradually from 0 to 0.02. The catalytic performance did not show a strictly linear relationship with the surface area. Nevertheless, an increase in surface area could enhance catalytic properties by promoting exposure to more active sites. The reaction activities are influenced by various factors, including the BET surface area, crystallite size, redox, and acid-base properties, as well as the surface ratio of Ce^{4+} /Ce^{3+}.

Divalent transition metal ions (Zn, Cu and Ni) were doped on the CeO_2 nanorod by hydrothermal method. Kulal et al. [45] found that the activity of the catalyst increased in the order Zn/CeO_2 > Ni/CeO_2 > $CuCeO_2$ > CeO_2 nanorod. Raman spectroscopy revealed that an increasing concentration of Zn on CeO_2 resulted in shifting of peak to the higher wavenumber is observed. It indicated that the formation of these oxygen vacancies. Furthermore, Zn doping at concentrations ranging from 0 to 10.5 % resulted in a noted increase in surface area, reaching a value of 106.4 m^2/g. Importantly, the increase in Zn doping did not induce any significant changes in the morphology of CeO_2, as it retained its nanorod structure. In addition, the CeO_2 nanorod doped with metal exhibits a higher concentration of oxygen vacancies compared to the undoped CeO_2 nanorod, hence promoting the formation of a bent CO_2 intermediate. Kulal et al. [45] also reported that 10.5 % Zn/CeO_2 catalyst exhibited the best results in the process under investigation. This catalyst had a glycerol conversion of 90.4 % and a glycerol carbonate yield of 89.5 % when operated at a temperature of 150 °C for 5 h with a CO_2 pressure of 4 MPa.

2.3.2. Non-binary system

Ternary or quaternary mixed metal oxide catalysts can consist of three or four different metal components. Trimetallic based catalysts (Cu, Ce, and Zn metal oxide) have also been prepared through the co-precipitation method. Pandey and Pawar [59] reported that CeO_2 and ZnO showed high yield of glycerol carbonate, glycerol conversion, and selectivity, compared with other monometallic oxides (ZrO and CuO_2) for the catalyst screening step. In addition, CeO_2/ZnO (bimetallic oxide) enhanced the catalyst activity and obtained higher yield of glycerol carbonate than monometallic oxides are shown as Table 5. A 3 %wt of binary and trinary oxides catalyst gave 19.5 % and 29.3 % of glycerol carbonate yield, respectively, were higher than their parent catalysts (ZnO, CeO_2, and CuO) in the same reaction condition. Subsequently, 5 % wt loading was the optimized amount of CeO_2 and CuO loading catalyst for synthesis mixed metal oxides. A 5 % CeO_2/ZnO exhibited the highest catalytic activity, resulting in a conversion rate of 23.34 %, a yield of 23.35 %, and a selectivity of 100 %. The non-uniform dispersion of CeO_2 when loading it over 5 % on ZnO may result in the formation of side reaction products, namely monoacetin and diacetin. Pandey and Pawar also observed that a catalyst consisting of 5 % wt CuO/CeO_2/ZnO had favourable catalytic performance. The loading of CeO_2 and CuO onto ZnO resulted in a reduction in the average crystalline size, decreasing from 15 nm to 12 nm and 10 nm, respectively. Conversely, the surface area decreased from 68 m^2/g to 64 m^2/g after loading 5 % wt CuO on CeO_2/ZnO support. The highest conversion of glycerol observed after 6 h at 100 °C and 6 MPa CO_2 was with 5 %wt CuO/CeO_2/ZnO of 57.2 %, with a yield of glycerol carbonate of 57.2 % and selectivity of 100 %. The Trimetallic based catalysts exhibited an increase in glycerol conversion from their parent catalysts.

Table 5
Catalytic performance of Zn, Ce, and Cu oxides catalysts for direct carbonation of CO_2 into glycerol carbonate.

Catalyst	Glycerol conversion (%)	Glycerol carbonate yield (%)	Glycerol carbonate selectivity (%)
ZnO	17.0	17.0	100
CeO_2	13.8	14.0	100
CuO	8.4	8.4	100
3 % wt CeO_2/ZnO	19.5	19.5	100
3 % wt CuO/CeO_2/ZnO	29.3	29.3	100

Reaction condition: 2.0 g glycerol, 0.067 feed/solvent ratio, 3 MPa CO_2, 0.1 g catalyst at 150 °C for 5 h

Another ternary MMOs catalyst was studied in previous research, was Zn/Al/La catalysts with different molar ratios. Li et al. [52] prepared by calcination of hydrotalcite precursors. The BET surface area increased from 36.4 to 168 m^2/g as the Al content increased. The production of $La_2O_3CO_3$ results in the formation of Zn/Al/La, which possesses moderately basic sites. Furthermore, the amount of metal-oxygen pairs, such as Zn-O, Al-O, and La-O, associated with the moderately basic sites, rises as the amount of Al increases. Thus, the catalyst with a molar ratio of Zn:La:Al of 4:1:1 exhibited excellent performance. The Zn:La:Al catalyst provides a glycerol conversion of 30.4 %, resulting in a maximum glycerol carbonate yield of 13.3 % and a selectivity of 43.8 %. Li et al. [52] examined the catalysts that consisted of quaternary mixed metal oxides by modifying Li, Mg, and Zr with Zn:La:Al hydrotalcites and calcined at 500 °C. Modifying Li, Mg, and Zr onto Zn:La:Al results in an increase in the binding energy of $Zn2p_{3/2}$ and La3d species, whereas the binding energy of Al2p decreases. The XPS analysis of the sample revealed three peaks related to oxygen species ions within the crystal lattice, absorbed oxygen ions, and hydroxyl and carbonate species. The presence of Li, Mg, and Zr leads to an increase in the amount of lattice oxygen species. The lattice oxygen in metal oxides can be defined as a Lewis basic site. The activity of the catalyst is enhanced by the introduction of Li, Mg, and Ze, particularly when Li was modified on Zn:La:Al, compared to the Zn:La:Al catalyst. The Zn:La:Al – Li catalyst achieves a glycerol conversion of 30.4 % and a selectivity of 43.8 %, resulting in a maximum glycerol carbonate yield of 13.3 %. Zhang and He [55] investigated the process of loading Cu on the Mg-Al-Zr support using impregnation method. The catalyst gave a BET surface area of 244.8 m^2/g. The Cu/Mg-Al-Zr catalyst exhibited a total of 285 μmol NH_3/g of acid sites and 243 μmol CO_2/g of basic sites. The acid and basic site density on Mg-Al-Zr could be changed by varying the Zr ratio. The glycerol conversion and selectivity were 11.5 % and 20.9 % respectively over Cu/Mg-Al-Zr catalyst at 150 °C, 7 MPa CO_2, with a reaction time of 3 h. Nevertheless, the synthesis of monocaetin and diacetin may be seen in the process when CH_3CN is present. The esterification of glycerol with acetic acid exhibited a higher level of favourable when acid catalysts were utilised. The Mg-Al-Zr catalyst exhibited a conversion rate of 66.2 % for acetic acid and a selectivity of 96.1 % for monoacetin. The esterification of glycerol with acetic acid was more favorable when using acid catalysts. The Mg-Al-Zr catalyst exhibited a conversion rate of 66.2 % for acetic acid and a selectivity of 96.1 % for monoacetin.(Tables 6 and 7).

2.4. Silicate materials

Rice husk may be utilised as a silica source to produce hexagonal mesoporous silica (MCM-41). In a prior investigation, Appaturi et al. [60] reported the great catalytic efficacy of immobilised bromine (Br), chlorine (Cl), and iodine (I) on the MCM-41 for the production of glycerol carbonate through the reaction between carbon dioxide (CO_2) and glycidol. All three catalysts revealed a yield over 97.2 % and a glycerol conversion rate above 99.0 % under the conditions of 90 °C, 2 MPa CO_2, with a reaction time of 3 h. MCM-41 was employed as the support for a Cu-based catalyst in the conversion of glycerol with CO_2. Zhang and He [55] reported that Cu/MCM-41 exhibited only the diffraction peaks related to amorphous silica, with a BET surface area of 1050.3 m^2/g. The Cu/MCM-41 catalyst did not have a basic site, but it had very weak acid sites as a result of the adsorption of hydroxy groups. The Cu/MCM-41 exhibited the greatest glycerol conversion rate at 18.7 %, however, the selectivity for glycerol carbonate was rather low at 9.8 %. This could be caused by the presence of a strong BrØnsted acid, which may have affected the activity of Cu/MCM-41. In addition, Zhang and

Table 6
Catalyst characterisation of mixed metal oxide catalysts for direct carbonation of glycerol with CO_2.

Catalyst	Morphology	BET surface area (m^2/g)	Pore Volume (cm^3/g)	Average Pore diameter (nm)	Crystalline size (nm)	H_2-TPR (mmol)	Total acid site amount (mmol NH_3/g catalyst)	Total basic site amount (mmol CO_2/g catalyst)	Ref.
(1:4) $La_2O_3CO_3$-ZnO - Calcined at 500 °C	–	20.6	0.13	18.8	–	–	–	–	[51]
(1:4) La-Zn	–	20.6	0.14	–	–	–	–	–	[52]
20 % $La_2O_3CO_3$-ZnO - light irradiation	–	6.3	0.0091	10.0	–	–	0.140	0.023	[43]
(2:1) Al-Zn	plate shape	62.5	0.082	–	–	–	–	–	[52]
2.3 % Cu/La_2O_3	nanorod	20	0.08	24	–	–	–	0.140	[54]
Cu/CaO	Blocky shape	0.60	0.06	29.9	–	–	0	0.183	[55]
Cu/MgO	–	24.2	0.10	28.2	–	–	0	0.148	[55]
Cu/La_2O_3	–	20.8	0.08	24.4	–	–	0	0.140	[55]
Cu/Al_2O_3	–	197.4	0.42	11.3	–	–	0.310	0.131	[55]
Cu/ZrO_2	–	63.0	0.26	13.3	–	–	0.125	0.080	[55]
30 %CuO/Al_2O_3 - Calcined at 700 °C	large nutty	170.5	0.277	6.65	–	–	–	0.1082	[56]
10 % $ZnWO_4$-ZnO	Irregular concretion	24.8	0.058	23.5	–	0.1527	0.0628	0.0478	[44]
11 % Ni/CeO_2	nanorods	66.1	–	–	10.5	–	–	–	[45]
9.5 % Cu/CeO_2	nanorods	75.7	–	–	9.9	–	–	–	[45]
10.5 % Zn/CeO_2	nanorods	89.5	–	–	8.9	–	–	–	[45]
5 %wt CeO_2/ZnO	Irregular granular shape	68	–	5-20	12	–	–	–	[59]
5 %wt CuO/CeO_2/ZnO	Irregular granular shape	64	–	5-20	10	–	–	–	[59]
$Ce_{0.98}Zr_{0.02}O_2$	nanorods	102.9	0.35	14.1	8.9	0.0862	0.042	0.074	[40]
(4:1:1) Zn:Al:La	–	36.4	0.069	–	–	–	–	–	[52]
(4:1:1) Zn:Al:La - Li	–	47.4	0.20	–	–	–	–	–	[52]
Cu/Mg-Al-Zr	–	244.8	1.38	1.38	–	–	0.285	0.243	[55]

He [55] prepared a Cu-based catalyst using HZSM-5 support. The XRD spectra of Cu/HZSM-5 displayed the diffraction peaks associated with zeolite HZSM-5. The BET surface area of Cu/HZSM-5 was measured to be 360.1 m^2/g. The Cu/HZSM-5 catalysts did not have any base sites on their surface, while it exhibited the largest and strongest of acid sites, as evidenced by the presence of two desorption peaks of ammonia (1123 μmol NH_3/g). This can be attributed to the presence of both Lewis and BrØnsted acid sites on the surface of HZSM-5. The Cu/HZSM-5 catalyst exhibited dramatically low activity, with a glycerol conversion rate of 0.5 % and a selectivity of 14.6 %.

2.5. Zeolites

Zeolites are characterised by a high specific surface area and adjustable acid/basic sites [61]. Zeolitic imidazolate framework-8 (ZIF-8) was reported to catalyse glycerol with CO_2 for glycerol carbonate production. Hu et al. [53] synthesised lanthanum (La)-modified ZIF-8 using different weight ratios. The increase in La content in ZIF-8 resulted in a decrease in surface area, which may be related to the surface covering by La2O3 nanoclusters. Conversely, the presence of La in ZIF-8 resulted in an increase in both acidic and basic sites. Specifically, the 5 %wt La/ZIF-8 sample shown a greater amount of acidic and basic sites compared to the control group (ZIF-8). This suggests that the modification of ZIF-8 with La enhances its acidity and basicity, which may improve the activation of CO_2. When using CH_3CN as a dehydrating agent, the greatest conversion and yield obtained for 5 %wt La/ZIF-8 were 46.5 % and 35.5 %, respectively. Furthermore, the selectivity exceeded 92 % when MgCO3 replaced CH_3CN as the dehydrating agent.

Tectosilicate zeolite (ETS-10) with approximately 4 % active metal (Co, Zr, Zn, Ce, Fe, Cu and Ni) introduced by an impregnation method [61]. The comparison of ETS-10 with several metal-based catalysts revealed significant alterations in the desorption temperature distribution, particularly in the higher range. The sample consisting of metal exhibited a temperature distribution that was lower than 600 °C, whereas the desorption peak of ETS-10 occurred at 620 °C. Among a range of metal-introduced ETS-10 catalysts, Co/ETS-10 exhibited the lowest CO_2 desorption amount of 0.44 mmol/g. However, all ETS-10 based catalysts showed greater basic sites compared to pure ETS-10. Among all support catalysts, most of them exhibited greater glycerol conversion and glycerol carbonate production compared to the metal-free catalysts, except for Ni/ETS-10. This unexpected result can be due to the excessive basicity of Ni/ETS-10 (1.41 mmol/g). Co/ETS-10 and Zn/ETS-10 exhibited the highest glycerol conversion and glycerol carbonate selectivity, respectively. The Cu/ETS-10, Ce/ETS-10, and Fe/ETS-10 catalysts showed great potential in converting glycerol, but their ability to improve glycerol selectivity was not as effective as Co/ETS-10 catalyst. Co/ETS-10 exhibited better catalytic activity, with a glycerol conversion of 35.0 % and a glycerol carbonate yield of 12.7 %.

Table 7
Reaction conditions and catalyst performance of mixed metal oxide catalysts for direct carbonation of glycerol with CO_2.

Catalyst	Operating Parameters							performance	Ref.
	Temp. (°C)	Time (h)	mole ratio of glycerol to dehydrating agent	Catalyst loading	Solvent	Pressure CO_2 (MPa)	Dehydration agent		
(1:4) $La_2O_3CO_3$-ZnO - Calcined at 500 °C	170	12	2:1	0.23 g	–	4	ACN 5 mL	Y = 14.3 % C = 30.3 %	[51]
(1:4) La-Zn	170	12	4.60 g Gly	0.14 g	–	4	ACN 5 mL	Y = 10.8 % C = 25.1 % S = 43.2 %	[52]
20 % $La_2O_3CO_3$-ZnO - light irradiation	150	6	0.92 g Gly	0.50 g	DMF 20 mL	5.5	–	Y = 6.1 % C = 6.9 %	[43]
(2:1) Al-Zn	170	12	4.60 g Gly	0.14 g	–	4	ACN 5 mL	Y = 10.4 % C = 23.2 % S = 45.1 %	[52]
2.3 % Cu/La_2O_3	150	12	4.60 g Gly	0.23 g	–	7	ACN 10 mL	Y = 15.2 % C = 33.4 % S = 45.4 %	[54]
Cu/CaO	150	3	4.60 g Gly	0.08 g	–	7.0	ACN 10 mL	C = 0.3 % S = 8.4 %	[55]
Cu/MgO	150	3	4.60 g Gly	0.08 g	–	7.0	ACN 10 mL	C = 8.6 % S = 26.1 %	[55]
Cu/La_2O_3	150	3	4.60 g Gly	0.08 g	–	7.0	ACN 10 mL	C = 8.9 % S = 29.3 %	[55]
Cu/Al_2O_3	150	3	4.60 g Gly	0.08 g	–	7.0	ACN 10 mL	C = 13.6 % S = 8.7 %	[55]
Cu/ZrO_2	150	3	4.60 g Gly	0.08 g	–	7.0	ACN 10 mL	C = 11.2 % S = 18.6 %	[55]
Catalyst	Operating Parameters							performance	Ref.
	Temp. (°C)	Time (h)	mole ratio of glycerol to dehydrating agent	Catalyst loading	Solvent	Pressure CO_2 (MPa)	Dehydration agent		
30 %CuO/Al_2O_3 - Calcined at 700 °C	150	5	2.30 g Gly	1.0 g	DMF 19.0 g	4.0	2-cyanopyridine 6.32 g	Y = 17.5 % C = 41.3 % S = 42.4 %	[56]
10 % $ZnWO_4$-ZnO	150	6	0.92 g Gly	0.50 g	DMF 20 mL	5.0	–	Y = 6.5 % S ~100 %	[44]
11 % Ni/CeO_2	150	5	1:3	0.17 g	DMF 10 mL	4.0	2-cyanopyridine	Y = 12.5 % C = 12.7 % S = 98.5 %	[45]
9.5 % Cu/CeO_2	150	5	1:3	0.17 g	DMF 10 mL	4.0	2-cyanopyridine	Y = 9.9 % C = 10.0 % S = 99.1 %	[45]
10.5% Zn/CeO_2	150	5	1:3	1.09 g	DMF 10 mL	4.0	2-cyanopyridine	Y = 89.5 % C = 90.4 % S = 99.0 %	[45]
5%wt CeO_2/ZnO	140	4	1:3	5% wt	–	3.0	ACN 30 mL	Y = 23.35 % C = 23.34 % S = 100 %	[59]
5%wt CuO/CeO_2/ZnO	160	6	0.067	10% wt	–	6.0	ACN 30 mL	Y = 57.2 % C = 57.2 % S = 100 %	[59]
$Ce_{0.98}Zr_{0.02}O_2$	150	5	1:3	0.52 g	DMF 10 mL	4.0	2-cyanopyridine	Y = 36.3 % C = 40.9 %	[40]
(4:1:1) Zn:Al:La	170	12	4.60 g Gly	0.14 g	–	4	ACN 5 mL	Y = 13.3 % C = 30.4 % S = 43.8 %	[52]
Catalyst	Operating Parameters							performance	Ref.
	Temp. (°C)	Time (h)	mole ratio of glycerol to dehydrating agent	Catalyst loading	Solvent	Pressure CO_2 (MPa)	Dehydration agent		
(4:1:1) Zn:Al:La - Li	170	12	4.60 g Gly	0.14 g	–	4	ACN 5 mL	Y = 15.1 % C = 35.7 % S = 42.2 %	[52]
Cu/Mg-Al-Zr	150	3	4.60 g Gly	0.08 g	–	7.0	ACN 10 mL	C = 11.5 % S = 20.9 %	[55]

Note: Y = yield of glycerol carbonate, C = conversion of glycerol, S = selectivity of glycerol carbonate, DMF = Dimethylformamide, Gly = Glycerol

2.6. Other

Carbon nanotube (CNTs) was used as a support for Cu-cased catalyst in the direct reaction, was reported by Zhang and He [55]. When loading Cu onto CNTs, it was observed that Cu/CNTs catalysts had no acid sites on their surface and the BET surface area of these catalysts was 195.4 m^2/g. The glycerol conversion and glycerol carbonate selectivity achieved 7.3 % and 17.8 %, respectively, using a Cu/CNTs catalyst

under the condition of 150 °C, 7 MPa of CO_2 pressure, and 6 h in the presence of CH_3CN as dehydrating agent.

Ionic liquids (ILs) have been shown to be efficient catalysts and reaction media for the chemical fixation of CO_2 due to their unique structures with high designability [62]. The protic ionic liquids (ILs) were produced by a neutralisation process. The production of value-added glycerol carbonate and by-products styrene glycol (SG) and styrene carbonate (SC) may be received by the one-pot reaction of CO_2, glycerol, and styrene oxide (SO), catalysed by protic ionic liquids (protic ILs). Among all the prepared protic ILs, HDBUI exhibited highest yields of glycerol carbonate at 86 %, as well as a yield of 39 % for styrene carbonate and 34 % for styrene glycol, based on styrene oxide. The catalytic activity exhibited the following order: HDBNI > HDBNBr > HDBNCl. The I– anion's good catalytic activity might be related to its improved nucleophilicity and alkalinity. In addition, George et al. [63] utilised a 1 mol % $^{n}Bu_2SnO$ catalyst in the reaction between glycerol and carbon dioxide. The obtained yield of 1,2-glycerol carbonate was 35 % when the reaction was conducted at 120 °C for 4 h and at a pressure of 13.8 MPa CO_2.(Tables 8 and 9).

2.7. Effect of dehydrating agent and solvent in reaction

In order to break the thermodynamic limit of the reaction, a dehydrating agent or coupling reagent was used. In the previous study, several dehydration agents were used in this process, including nitrile solvents and inorganic dehydrating agents. Several dehydrating agents were employed to remove water from the reaction between glycerol and CO_2. Nevertheless, it is important to take into account the possibility of side reactions caused by each dehydrating agent. Some dehydrating agents may lead to unwanted side reactions that might negatively impact the selectivity of glycerol carbonate and increase the production of by-products [53].

In a study conducted by Liu et al. [50], it was shown that the use of 30 mmol of 2-cyanopyridine and 10 mL of DMF resulted in a significant increase in glycerol carbonate yield when compared to other dehydrating agents such as acetonitrile, valeronitrile, benzonitrile, and phenylacetonitrile. According to Su et al. [42], several nitrogen-containing dehydrating agents were investigated in the absence of catalysts. The results of the yield of glycerol carbonate and glycerol conversion are shown in Table 10. In the absence of a dehydrating agent, the production of glycerol carbonate was only 0.7 %. Additionally, 2-cyanopyridine exhibited higher glycerol conversion and glycerol carbonate yield compared to acetonitrile. A 2-cyanopyridine has notable alkaline properties and is able of forming intramolecular hydrogen bonds within the resulting amide product. The hydrolytic activity of 2-cyanopyridine exhibited a significant association with the concentration of oxygen vacancies (defect site), as well as the quantity of basic sites.

Furthermore, Su et al. [42] argued that 2-cyanopyridine serves two roles in the reaction, acting not only as a dehydrating agent to promote the reaction, but also as a catalyst for the carbonylation by activating the carbonyl bond of CO_2. The effect of the cyano group's stereo-position inside the dehydrating reagent is noteworthy in relation to the ongoing carbonylation process. The glycerol carbonate achieved the maximum yield (18.7 %) when subjected to direct carbonylation with carbon dioxide (CO_2) at a temperature of 180 °C for 12 h and 15 MPa CO_2, without the presence of a catalyst. In the study, Su et al. [42] found that there are two possible ways of interaction between CO_2 and 2-cyanopyridine. One of them occurs at site-a, which refers to the nitrogen atom in the pyridine ring. Another way occurs at site-b, which is related to the nitrogen atom in the cyano group -C≡N). These interactions were seen for three different types of cyanopyridine. A 2-cyanopyridine exhibits a third form of interaction, wherein a CO_2 molecule simultaneously interacts with one nitrogen in the cyano group and the other nitrogen in the pyridine ring. This results in the formation of a five-membered ring intermediate (2c-T), as shown in Fig. 7. The FITR spectra revealed the presence of new peaks, indicating the coordination between CO_2 and 2-cyanopyridine and the formation of a five-membered ring intermediate.

An intermediate species might form through the interaction between a CO_2 molecule and a 2-cyanopyridine molecule, as shown in Fig. 8. The structure had the same result as reported by Su et al. [42], where a mixture of glycerol + DMF + 2-cyanopyridine was able to activate CO_2, as previously described by Al-Kurdhani and Wang [56].

Su et al. [42] have suggested that the possible reaction route for the activation of CO_2 with 2-cyanopyridine, which involves two steps as follows:

(i) The carbonyl group of carbon dioxide is absorbed onto the nitrogen atom in pyridine.
(ii) Formation of five-membered ring intermediate: oxygen ion undergoes absorption on to the N in the cyano group.

Table 8
Catalyst characterisation of silicate materials, zeolites, and other catalysts for direct carbonation of glycerol with CO_2.

Catalyst	Morphology	BET surface area (m^2/g)	Pore Volume (cm^3/g)	Average Pore diameter (nm)	Crystalline size (nm)	H_2-TPR (mmol)	Total acid site amount (mmol NH_3/g catalyst)	Total basic site amount (mmol CO_2/g catalyst)	Ref.
Silicate materials									
Cu/MCM-41	–	1050.3	0.99	3.00	–	–	0.028	0	[55]
Cu/HZSM-5	–	360.1	0.77	0.5	–	–	1.123	0	[55]
Zeolites									
ZIF-8	hexagonal	1830	–	<1	–	–	0.121	0.158	[53]
5 %wt La/ZIF	Circular-hexagonal	1700	–	<1	–	–	0.305	0.582	[53]
ETS-10	bipyramidal truncated	324.4	–	–	–	–	–	0.37	[61]
Co/ETS-10	bipyramidal truncated	302.3	–	–	–	–	–	0.44	[61]
Zn/ETS-10	–	283.4	–	–	–	–	–	0.50	[61]
Cu/ETS-10	–	310.6	–	–	–	–	–	0.74	[61]
Fe/ETS-10	–	307.9	–	–	–	–	–	0.74	[61]
Ni/ETS-10	–	309.4	–	–	–	–	–	1.41	[61]
Zr/ETS-10	–	299.4	–	–	–	–	–	0.61	[61]
Ce/ETS-10	–	309.7	–	–	–	–	–	0.68	[61]
Other									
Cu/CNTs	–	195.4	1.32	18.6	–	–	0	0	[55]

Table 9
Reaction conditions and catalyst performance of silicate materials, zeolites and other catalysts for direct carbonation of glycerol with CO_2.

Catalyst	Operating Parameters							performance	Ref.
	Temp. (°C)	Time (h)	mole ratio of glycerol to dehydrating agent	Catalyst loading	Solvent	Pressure CO_2 (MPa)	Dehydration agent		
Silicate materials									
Cu/MCM-41	150	3	4.60 g Gly	0.08 g	-	7.0	ACN 10 mL	C = 18.7 % S = 9.8 %	[55]
Cu/HZSM-5	150	3	4.60 g Gly	0.08 g	-	7.0	ACN 10 mL	C = 0.5 % S = 14.6 %	[55]
Zeolites									
ZIF-8	150	6	15 mL Gly	0.1 g	-	0.7	ACN 5 mL	C = 24 % S = 56 %	[53]
5 %wt La/ZIF	150	15	15 mL Gly	0.1 g	-	0.7	ACN 5 mL	Y = 35.5 % C = 46.5 %	[53]
5 %wt La/ZIF	150	15	15 mL Gly	0.1 g	-	0.7	$MgCO_3$ 0.05 g	Y = 34.8 % C = 36.6 %	[53]
5 %wt La/ZIF	150	15	15 mL Gly	0.1 g	-	0.7	$CaCO_3$ 0.05 g	Y = 16.6 % C = 18.5 %	[53]
ETS-10	170	6	4.6 g Gly	0.25 g	-	4	ACN 5 mL	Y = 4.7 % C = 33.6 % S = 13.9 %	[61]
Co/ETS-10	170	6	4.6 g Gly	0.25 g	-	4	ACN 5 mL	Y = 12.7 % C = 35.0 % S = 36.3 %	[61]
Zn/ETS-10	170	6	4.6 g Gly	0.25 g	-	4	ACN 5 mL	Y = 11.7 % C = 32.7 % S = 32.7 %	[61]
Cu/ETS-10	170	6	4.6 g Gly	0.25 g	-	4	ACN 5 mL	Y = 8.5 % C = 35.6 % S = 23.9 %	[61]
Fe/ETS-10	170	6	4.6 g Gly	0.25 g	-	4	ACN 5 mL	Y = 8.7 % C = 33.4 % S = 25.9 %	[61]
Ni/ETS-10	170	6	4.6 g Gly	0.25 g	-	4	ACN 5 mL	Y = 4.3 % C = 29.6 % S = 14.1 %	[61]
Zr/ETS-10	170	6	4.6 g Gly	0.25 g	-	4	ACN 5 mL	Y = 4.7 % C = 33.6 % S = 14.1 %	[61]
Ce/ETS-10	170	6	4.6 g Gly	0.25 g	-	4	ACN 5 mL	Y = 9.8 % C = 32.7 % S = 29.9 %	[61]
Other									
Cu/CNTs	150	3	4.60 g Gly	0.08 g	-	7.0	ACN 10 mL	C = 7.3 % S = 17.8 %	[55]

Note: Y = yield of glycerol carbonate, C = conversion of glycerol, S = selectivity of glycerol carbonate, DMF = Dimethylformamide, Gly = Glycerol

Table 10
The carbonation of glycerol with CO_2 using different dehydrating agents [42].

Dehydrating agent	Conversion (%)	Yield (%)
None	1.4	0.7
Acetonitrile	11.1	1.5
2-cyanopyridine	31.1	11.4
3-cyanopyridine	37.7	5.3
4-cyanopyridine	46.7	3.8

Note: Reaction conditions: glycerol 1.15 g, dehydrating agent/glycerol (mole ratio) 2:1, CO_2 10 MPa, 170 °C, 12 h

Liu et al. [40] also investigated possible reaction pathways and catalytic mechanisms, pure 2-cyanopyridine, DMF, glycerol, and their mixture were treated with CO_2 (4 MPa) under continuous stirring conditions at 150 °C for 5 h in the autoclave. FTIR spectra revealed the presence of additional bands resulting from the interaction between 2-cyanopyridine and CO_2 at 150 °C, indicating that a five-membered ring intermediate was formed from this reaction for the purpose to activation of CO_2 as shown in Fig. 9. The formations of different CO_2 absorption species are originated from basic sites with different of strengths. The main adsorption pattern observed for CeO_2 was the chelation of bidentate carbonate species, which required the existence of an adjacent M^{n+} -O^{2-} pair. This preference for chelating bidentate carbonate can be attributed to its greater stability compared to bridging bidentate carbonate. Álvarez et al. [64] reported that CO_2 is attracted by the basic sites on solid surfaces. CO_2 undergoes or reacts over acid–base materials, leading to the formation of three forms: (i) carbonate, which is produced by reacting with O, (ii) bicarbonate, which is formed through the reaction with surface hydroxyl groups (OH), and (iii) linear adsorption. Acid–base catalysts are commonly recognized as non-reductive catalysts. The process of non-reductive carbon dioxide (CO_2) transformation involves the synthesis of cyclic and linear organic carbonates. This transformation occurs when CO_2 is activated by surface oxygen defect sites, resulting in its dissociation into CO and O, or its interaction with more reactive species, leading to the formation of reaction intermediates.

To eliminate the water produced in the reaction between glycerol and CO_2 in the presence of CH_3CN, the hydrolysis of CH_3CN can be used to break the thermodynamic limitation. Therefore, the hydrolysis of

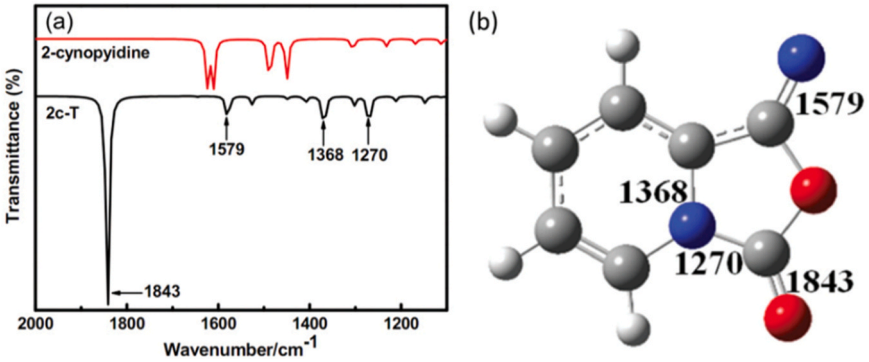

Fig. 7. (a) FTIR spectra of 2-cyanopyridine and 2c-T (b) possible five-membered ring intermediate [42].

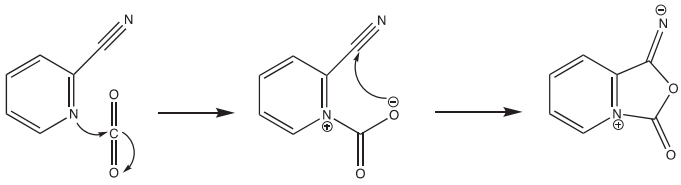

Fig. 8. The interaction of CO_2 with 2-cyanopyridine to form an intermediate [42,56].

CH_3CN might potentially provide acetic acid, which could react with glycerol to produce the by-products (monoacetin and diacetin) [55]. Li et al. [52] reported that increasing the amount of CH_3CN resulted in enhanced catalytic activity. Hence, the by product of acetins may be an issue to concern. The higher selectivity of acetins compared to glycerol carbonate can be attributed to the presence of water in the reagents (glycerol and acetonitrile), which were used as analytical agents. It is important to note that no dehydration process was involved in the reaction, as shown in Fig. 10. The moderated basic sites can enhance both the activation of CO_2 and the hydrolysis of acetonitrile. Consequently, an increased production of acetic acid resulted in a higher selectivity for acetins (as a byproduct) and a lower selectivity for glycerol carbonate.

Calcium carbide (CaC_2) is a renewable chemical derived from the abundant calcium found in the Earth's crust. Zhang et al. [65] used CaC_2 as a desiccating agent to produce glycerol carbonate, employing a zinc-based catalyst with 1,10-phenanthroline (phen) as the catalyst. In the absence of a catalyst, the process produced a yield of 16 % when 0.5 mmol of glycerol, 2.5 mmol of CaC_2, and 5 MPa of CO_2 were used in 3 mL of NMP as the solvent. The use of $Zn(OTf)_2$/phen and CaC_2 resulted in a glycerol carbonate yield of 92 %. Thus, CaC_2 could be one of a sacrificial dehydrating agent [66]. The use of sacrificial dehydrating agents has the disadvantage, was not ecologically sustainable. In addition, Takeuchi et al. [66] showed that Calcium oxides may be used as a dehydrating agent. CaO may be easily and inexpensively synthesised from limestone. The dehydration process of limestone yields calcium hydroxide ($Ca(OH)_2$), which can be regenerated back into CaO. It is important to note that $Ca(OH)_2$ does not react with glycerol carbonate, which prevents a decrease in yield [65]. The yield of glycerol carbonate using 0.5 mmol glycerol, 5 mmol CaO, and 3 MPa CO_2 in 3 mL NMP (solvent) was 40 % when introducing the $Zn(OTf)_2$/phen catalyst previously reported by Zhang et al. [65].

Using inorganic dehydrating agent, including $MgCO_3$ and $CaCO_3$ were reported by Hu et al. [53]. Consequently, the reaction in the

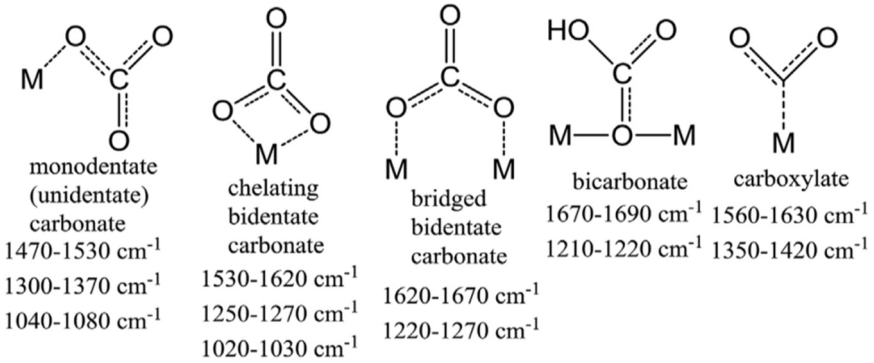

Fig. 9. CO_2 adsorption model [40].

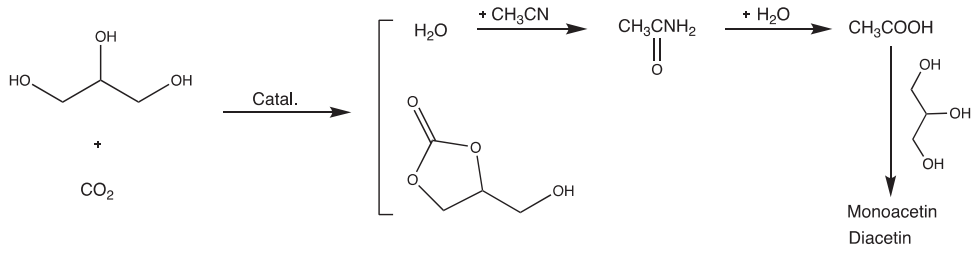

Fig. 10. The reaction scheme for glycerol carbonate and acetins (by-product) in the presence of acetronitrile [52].

presence of CH_3CN exhibited a greater glycerol conversion compared to the inorganic dehydrating agents. However, the best selectivity was achieved with $MgCO_3$. Furthermore, the use of $MgCO_3$ and $CaCO_3$ as dehydrating agents resulted in a decrease of undesirable reactions and improved catalytic performance, leading to higher production and selectivity of glycerol carbonate. When the 5La/ZiF-8 catalyst is used, the conversion, yield, and selectivity reach over 36 %, 34 %, and 9 % respectively. Furthermore, the selectivity exceeded 89 % when $CaCO_3$ was used as the dehydrating agent. Due to its very acidic nature, the use of H_2SO_4 in the ZIF-8 catalyst system was unsuitable since it caused instability and reduced the catalytic efficiency of ZIF-8. The activation energy of the reaction was determined using the Arrhenius equation. It was found that acetonitrile had a higher activation energy compared to $MgCO_3$. This suggests that acetonitrile required more external energy to activate the reaction.

Additionally, the presence of a solvent had a crucial role in determining the catalytic activity. According to Liu et al. [50], the largest yield of glycerol carbonate was obtained using dimethylformamide (DMF) of 20.8 %. Dimethylsulfoxide (DMSO) yielded a lower amount of glycerol carbonate as a secondary result. The yield of glycerol carbonate produced from the process conducted by Su et al. [42] was found to be 11.6 % and 10.1 % when N-methylpyrrolidone (NMP) and DMF were used as solvents, respectively.

Methanol has been reported as a solvent in a previous study. The interaction between glycerol and CO_2 used $^{n}Bu_2SnO$ and $^{n}Bu_2Sn(OMe)_2$ as homogeneous catalysts. The tin-glycerol complex acted as an intermediate [67]. However, the conversion of glycerol was only 2.3 % under the reaction conditions (6 h, 5 MPa, 180 °C). The use of methanol as a solvent and 13X zeolite as a dehydrant resulted in an enhanced yield of glycerol carbonate, reaching 35 %. This reaction was catalysed by nBu_2SnO at 120 °C for 4 h and 13.8 MPa CO_2 [63]. Therefore, Liu et al. [50] suggested that the solubility of CO_2 in these solvents might also be an important factor. The considerable solubility of carbon dioxide (CO_2) may potentially offer advantages in terms of enhancing the concentration of CO_2 at the catalyst surface, hence resulting in positive effects for the reaction. However, the selection of these solvents should be carefully considered in terms of their toxicity, environmental impact, and health and safety effects.

3. Indirect synthetic routes for glycerol carbonate production

3.1. Transcarbonation glycerol with phosgene

The utilisation of phosgene in transcarbonation seems to be a simple but effective technique for the synthesis of organic carbonates. Franklin [68] documented the method by which carbonate chloroformate ester was synthesised in 1948. A chemical reaction between glycerol and liquid phosgene. Glycerol and liquid phosgene were added slowly while vigorously stirring at 30 °C for 6 h. Approximately 90 % carbonate chloroformate ester was reported as a yield. Nevertheless, due to the concerns relating to handling of this extremely hazardous gas, the utilisation of phosgene was significantly restricted [29]. Many nations have prohibited its use in the sector because of safety concerns, making this technique uncommonly utilised owing to its negative impacts. Phosgene is typically present as a gas, although it may form as a liquid under certain pressure and temperature conditions. Phosgene must be handled cautiously during the process, as accidental release could have severe environmental and health effects [69]. Three procedures are necessary for the safe handling of phosgene: 1) Ensuring that the level of phosgene in the air is monitored and maintained at a safe level; 2) Using suitable personal protective equipment in the designated work area; 3) Implementing accordance to legal controls of storage, transportation, and waste disposal. The detection of phosgene can be done by chromatography-mass spectrometry techniques or electrochemical assays [70]. Currently, several types of detection methods have been developed for the purpose of monitoring phosgene, including colorimetric, chromatographic, mass spectrometry, and fluorogenic approaches [71,72].

3.2. Carbonation with urea

One of the main benefits associated with the carbonation of glycerol with urea is the readily available, inexpensive basic material, and non-toxic nature of both glycerol and urea. Additionally, this simple method may be performed without any solvents. Furthermore, the carbonation reaction reveals high selectivity and yield of glycerol carbonate under mild reaction conditions [73,74]. Many studies have been undertaken to investigate the synthesis of glycerol carbonate by use of urea. For instance, metal salt catalysts such as $ZnBr_2$, $ZnCl_2$, $ZnSO_4$ [75] were reported for this reaction. Additionally, Mixed metal oxide catalysts were examined to enhance catalytic performance such as zinc-based catalyst (ZnO, Zn/Sn, and Zn/MCM-41) [75–77], magnesium-based catalyst (MgO [78], AuPd/MgO [79], Mg/Al and Mg/Al/Zn [80]), tin-tungsten mixed oxide catalysts [81], and Ionic liquids [82].

Significantly, the reaction between glycerol and urea results in the generation of a substantial amount of ammonia as a by-product, hence limiting its wide usage in industrial stage [27,29]. Urea could be considered an activated form of carbon dioxide. The transformation of ammonia and CO_2 into urea provides the most essential chemical process utilising CO_2. Fig. 11 illustrates the chemical process in the production of glycerol carbonate from urea, as well as the simultaneous consumption of its ammonia by-product by other chemical reaction through the utilisation of CO_2 to generate urea. However, in order to facilitate the shift of the reaction equilibrium towards the right by eliminating ammonia gas, which has the potential to contaminate the surrounding environment. In general, in order to remove the by-product ammonia, the reaction of glycerol with urea needs to be conducted in a vacuum or with the presence of a sweeping gas. Jagadeeswaraiah et al. [81] conducted the reaction under a vacuum to eliminate the ammonia produced during the process. This removal process is carried out at decreased pressure conditions, typically ranging from 0.004 to 0.005 MPa. Consequently, this approach leads to an increase in investment costs [82]. Argon gas (Ar) was employed to purge the ammonia from the reaction system, either by passing it through the reactor or directly through the reaction mixture. This was conducted to minimise the formation of undesired reverse reactions throughout the process [83]. In addition to using an inert gas flow to remove NH_3, another product is synthesised using one of the pathways for NH_3 removal. Costanzo et al. [84] used Q-tube help to eliminate NH_3 during the synthesis of 1,4-dihydropyridine, resulting in the production of water as a by-product.

3.3. Transesterification glycerol with dimethyl carbonate (DMC)

The synthesis of glycerol carbonate by the transesterification of glycerol and organic carbonates has attracted attention in recent times. The raw materials used in the production of glycerol carbonates are ethylene carbonate (EC), propylene carbonate (PC), dimethyl carbonate (DMC), and diethyl carbonate (DEC). Meanwhile, the catalysts utilised in this process include inorganic or basic compounds, as well as lipase catalysts [74].

Dimethyl carbonate (CAS: 616–38-6) is a green and environmentally sustainable chemical[86], which is non-toxic, biodegradable and can be produced via the base catalysed reaction of methanol with CO_2 [87]. Whilst other sources have been reported such as ethylene carbonate, industrial use is limited due to the high boiling points of both ethylene carbonate (261 °C) and the reaction by-product ethylene glycol (197 °C) [88]. Use of homogeneous catalysts such as sodium and potassium hydroxide, ionic liquids and enzymes have also been reported in the literature. With a view towards [89] industrial feasibility the catalyst must be easily separated from the reaction mixture and recyclable when

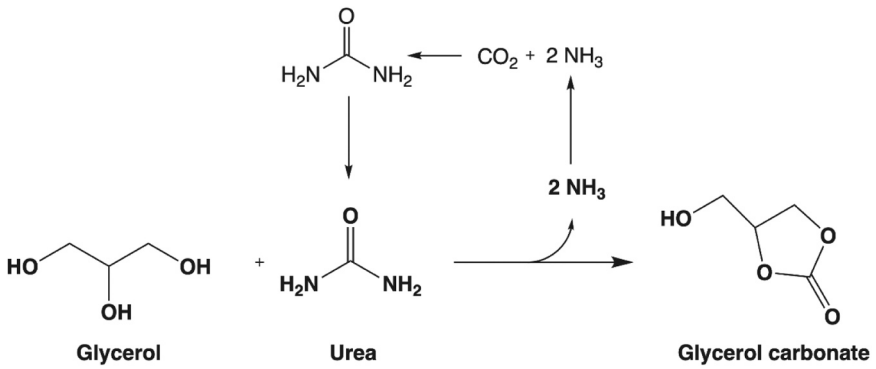

Fig. 11. Schematic of the glycerol carbonate synthesis utilising urea as the CO_2 donor [85].

reused [7]. A simple separation and purification of the desired product is required, which can be aided by high conversion of reactants and high selectivity to a certain product. For this reason, use of heterogeneous catalysis is preferred due to ease of separation from the reaction mixture. If high conversion of glycerol is achieved coupled with high selectivity to either product, separation and purification of the products should be theoretically simple due to the boiling points of the reactants and products. The boiling points of the reactants and products are shown in Table 11.

3.3.1. Mechanism

The effect of acid vs. base catalysis for the reaction was examined by Ochoa-Gómez et al. [90]. Low conversion of glycerol and yield of glycerol carbonate was observed when acid catalysis was employed. After 90 min sulphuric acid gave 10.6 % conversion, para-Toluenesulfonic acid gave 19 % and Amberlyst 131 wet gave 33.9 % conversion. Furthermore, it was shown that the reaction was kinetically controlled, with sulphuric acid obtaining 94.5 % conversion after 24 h. Yield was still quite limited with only 50 % attained.

Conversely when basic catalysis is employed a much higher rate of conversion and selectivity is obtained. Greater than 98 % glycerol conversion and selectivity to glycerol carbonate was achieved when using the homogeneous catalysts potassium and sodium hydroxide. Ochoa-Gómez et al. [90] have suggested the reaction of glycerol and dimethyl carbonate to produce glycerol carbonate involves four steps as follows:

(i) Formation of a glyceroxide anion – one of the primary hydroxyl groups of glycerol undergoes nucleophilic attack by the base catalyst.
(ii) Nucleophilic attack of the carbonyl group of dimethyl carbonates by the glyceroxide anion liberating a methoxide anion.
(iii) The methyl glyceryl carbonate intermediate undergoes cyclisation through a nucleophilic attack of the oxygen from the secondary hydroxyl on the carbonyl carbon to yield glycerol carbonate and methanol.
(iv) Regeneration of the catalyst through reaction of the methoxide anion from step (2) with the conjugate base.

The reaction mechanism for the formation of glycerol carbonate is shown in Fig. 12. Whilst the reaction proceeds mainly via a basic catalytic route, it has been suggested that moderate acidic sites also contribute to the reaction. Zhang et al. [91] have shown that the interaction of acid-base sites is beneficial to the reaction. Whereas strong basic sites lead to the formation of the glyceroxide anion in step (1), moderate acidic sites contribute to the carbonyl activation of dimethyl carbonate in step (2). It is also possible for glycerol carbonate to undergo a further reaction with dimethyl carbonate to produce glycerol dicarbonate as a by-product [92].

The decarboxylation of glycerol carbonate can produce two possible products – glycidol and 3-hydroxyoxetane. Due to the kinetics of ring closure, glycidol is the favoured product. Darensbourg et al. [93] investigated the mechanism of glycidol formation computationally with the mechanism in agreement with that proposed by Ochoa-Gómez et al. [92]. The mechanism suggested by both groups is shown as Fig. 13 follows:

(i) Deprotonation of the hydroxyl group of 1,2-glycerol carbonate by a strong base leading to the formation of a cyclic carbonate alkoxide.
(ii) Loss of the five-membered ring structure due to a nucleophilic substitution reaction leads to formation of a carbonate anion.
(iii) Loss of carbon dioxide from the carbonate anion structure forms 2,3-epoxy-1-propanolate.
(iv) Regeneration of catalyst and formation of glycidol through reaction of conjugate acid with 2,3-epoxy-1-propanolate.

3.3.2. Single component metal oxide catalysts

Single metal oxide catalysts gain activity through the presences of O^{2-} anions, which are Brønsted bases [94]. Often the formation of hydroxyl groups results from the reaction of the O^{2-} anions and water vapour.

3.3.2.1. Calcium oxide. The use of calcium oxide (CaO) for the transesterification of glycerol with dimethyl carbonate was first reported by Ochoa-Gómez et al. [90] who compared the activity of CaO against other basic materials such as magnesium oxide (MgO) and calcium carbonate ($CaCO_3$). The activity of CaO was found to be strongly influenced by calcination temperature. Impurities such as calcium hydroxide and calcium carbonate had a negative effect on the activity of the catalyst, due to their lower basic strength in comparison to that of CaO. Calcination of the material at 900 °C results in the removal of these impurities thereby increasing the activity. The yield of glycerol carbonate could be increased from 64.0 % to 91.1 % after calcination. Despite this CaO suffers from poor reusability if no regeneration or after-treatment is employed. The yield of glycerol carbonate decreases dramatically from 95.3 % to 17.8 % after only 4 reaction cycles. CaO is partially soluble in glycerol and methanol, however the levels of leaching were found to be relatively low with less than 0.34 wt % of the catalyst. It had been

Table 11
Boiling points of reactants and products for the transesterification of glycerol with dimethyl carbonate.

Component	Boiling Point (°C)
Glycerol	290
Dimethyl Carbonate	90
Methanol	65
Glycerol Carbonate	137
Glycidol	167

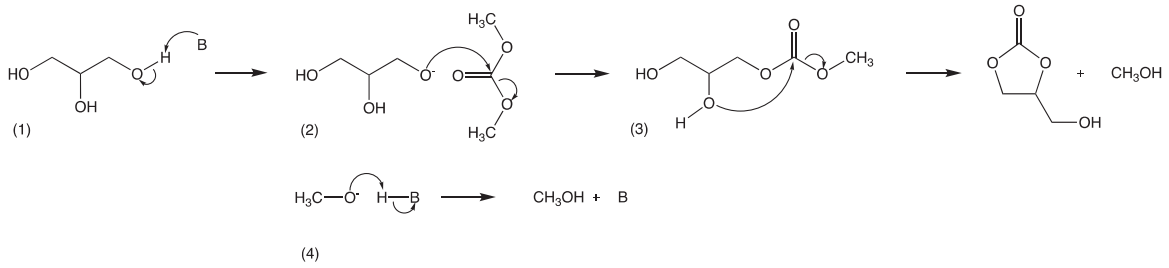

Fig. 12. Reaction mechanism for the formation of glycerol carbonate from glycerol and dimethyl carbonate [90].

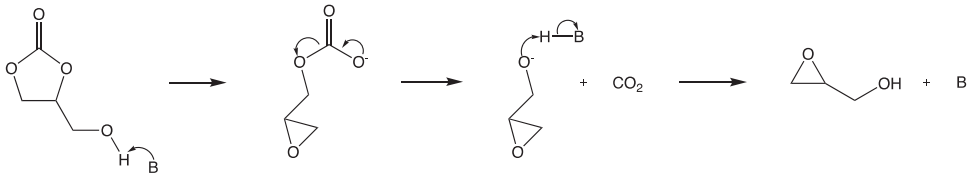

Fig. 13. Reaction mechanism for the base catalysed decarboxylation of glycerol carbonate to glycidol [93].

postulated that the poor reusability was due to carbonation and hydration of CaO when exposed to air as had been reported in the manufacturing of biodiesel [95]. This was found to be false when Li and Wang [96] reported that the deactivation of CaO was due to the formation of a basic calcium carbonate ($Ca_x(OH)_y(CO_3)_2$) after interaction with glycerol and dimethyl carbonate.

To overcome the limitations associated with used CaO catalyst, calcium diglyceroxide was suggested as a reusable catalyst, formed through the reaction of CaO and glycerol. A yield of greater than 95 % could be obtained with excellent reusability observed over 5 reaction cycles. The stability and reusability of CaO can also be improved through use of a support such as activated alumina [97]. Lu et al. [97] reported the use of CaO supported on activated alumina extrudates using polyacrylamide as a pore forming agent. The catalyst showed higher stability than unsupported CaO, with the yield decreasing from 90.57 % to 62.53 % after 6 reaction cycles. This is a marked improvement when compared to unsupported CaO. The introduction of additional basic species on the surface of CaO has also been shown to improve the stability and activity. The doping of the surface of CaO with potassium nitrate increased both the activity and stability when compared with plain CaO [89]. A 15 wt % loading of KNO_3 maintained a glycerol conversion of greater than 95 % over 5 recycles, with a constant glycerol carbonate yield of between 83–85 %. Similarly supporting lithium chloride on CaO increase the yield and stability, with a yield greater than 6.5 % higher than pure CaO [98]. A yield of over 80 % could be maintained over 5 recycles.

One positive aspect of CaO is that it can be prepared from abundant and renewable natural sources, often from materials that would be classified as waste which allows the development of a more circular economy. The use of CaO from renewable sources may offset the limited reusability of the catalyst without calcination to regenerate the active sites. Roschat et al. [99] investigated the use of CaO derived from various renewable sources such as cockle shells, golden apple snail shells and egg shells. Sources such as shells consist of mainly $CaCO_3$ which can be phase transformed to CaO by calcination at high temperature. It was found that CaO derived from cockle shells was the most active catalyst due to a higher surface area and greater number of basic sites, with a 92.1 % yield of glycerol carbonate in 2 h. However, it should be noted that all sources of CaO outperformed commercial CaO catalyst. Another waste, an eggshell is rich in $CaCO_3$. CaO was derived by Praikaew et al. [100] via calcination at 900 °C for 2.5 h in a N_2 atmosphere. The basic strength of CaO eggshell is very high, with a total basicity of 0.481 mmol/g. The highest achieved results were a glycerol conversion of 96 % and a glycerol carbonate yield of 94 %. The effect of CaO synthesis method from waste egg shells was investigated by Changmai et al. [101] who found that microwave synthesis yielded higher activity when compared with furnace and calcination synthesis. The higher level of activity was attributed to a higher surface area and smaller particle size which led to a high density of active sites. Regeneration of active sites could be achieved by calcination of the catalyst at 400 °C for 4 h, resulting in only a marginal decrease in glycerol carbonate yield over 6 reaction cycles.

3.3.2.2. Magnesium oxide. Ochoa-Gómez et al. [90] first used magnesium oxide (MgO) and found it to be less active in comparison to both CaO and $CaCO_3$. The activity of commercial MgO was found to be unaffected by calcination with similar yields obtained by both. To address the low activity of commercial MgO, Simanjuntak et al. [102] synthesised MgO with the use of the surfactant - pluronic F127. MgO generated from $Mg(NO_3)_2.6\ H_2O$ and pluronic F127 was more active (75.4 % yield of glycerol carbonate after 90 min) when compared to MgO prepared from direct calcination (11.1 % yield) and through precipitation with $Mg(NO_3)_2.6\ H_2O$ in potassium hydroxide solution (16.0 % yield). The higher activity was attributed to greater concentration of basic sites 0.48 mmol/g ($H_- \geq 9.8$) and highly basic sites 0.38 mmol g-1 ($H_- \geq 15$) in comparison with MgO from calcination 0.09 mmol g-1 ($H_- \geq 9.8$) due to a higher amount of surface O^{2-} species.

The morphology of MgO also has a marked effect on the catalytic activity [103]. Trapezoidal MgO exhibited a higher activity (95 % yield after 1 h at 70 °C) in comparison to rod-like, spherical, flower and nest-like morphologies (<6.5 %). Converse to previous catalysts reported the high activity of trapezoidal MgO could not be attributed to a higher basicity, as it illustrated the weakest basicity of all morphologies. Higher reaction efficiency was linked to a smaller ratio of O:Mg (1.02) which gave ride to better interactions with the reactants – higher number of oxygen atoms would result in a greater electron repulsion force. Impregnation of MgO with K_2CO_3 is also effective in increasing the efficiency for the reaction [104]. A 20 wt % loading can increase the yield of glycerol carbonate from 15.2 % to 98.6 % with 1 wt % catalyst loading at 80 °C after 2 h.

3.3.2.3. Other single metal oxides. Alumina (Al_2O_3) based catalysts have also been reported for glycerol carbonate synthesis. Whilst alumina itself has a low level of activity for the reaction, it can be functionalized through the impregnation of other active species. Sandesh et al. [105] found that γ-Al_2O_3 was the most effective support for impregnating potassium fluoride (KF) out of the supports tested (α-Al_2O_3, SiO_2, H-beta zeolite, ZnO, ZrO_2 and carbon). The activity is attributed to the higher

amount of strong basic sites formed with γ-Al_2O_3. These strong basic sites were attributed to the presence of F^- and OH^- species formed by the interaction of KF with Al_2O_3. Impregnation of Al_2O_3 with sodium hydroxide (NaOH) is also an effective way of increasing the activity of alumina [106]. A 20 wt % loading of NaOH increased the basicity of the catalyst to 1.63 mmol/g. Interestingly further increase in NaOH loading resulted in a decrease in basicity, due to the formation of sodium aluminate from NaOH and Al_2O_3. Furthermore, Elhaj et al. [107] conducted the preparation of KNO_3/Al_2O_3 nanoparticles using the impregnation method. Active species of K_2O are well dispersed on Al_2O_3 support. At medium and high temperatures, the peaks of the KNO_3/Al_2O_3 TPD profile are more pronounced, and it has the highest CO_2 adsorption volume at 1.38 mmol/g. After each run, the KNO_3/Al_2O_3 recycling studies were subjected to calcination at a temperature of 800 °C for a duration of 5 h. In the fourth cycle of catalyst recycling, the glycerol conversion and glycerol carbonate output achieved percentages of 90.32 %g % and 58.08 % respectively.

Lanthanum oxide (La_2O_3) has also been reported for the reaction. The activity of pure La_2O_3 could be enhanced through hydrothermal preparation using polyethylene glycol (PEG) as a pore-expanding agent [108]. Using PEG-20000 as the pore expanding agent (5 times excess of metal nitrate precursor) the basic strength and number of basic sites of La_2O_3 was improved when compared to La_2O_3 prepared without the use of PEG-20000. This effect is highlighted in the increase in yield of glycerol carbonate from 40 % to 99.4 % under similar reaction conditions. Surface area, pore diameter and pore volume all increased as a result of the use of a pore-expanding agent. Similarly impregnation of La_2O_3 with lithium (Li) can also improve the activity due to an increase in strong basic sites [109]. A 3.5 mol % loading of Li/ La_2O_3 calcined at 600 °C gives 94.4 % glycerol conversion with 92.1 % glycerol carbonate selectivity (85 °C, mole ratio glycerol to dimethyl carbonate of 1:3, 0.1 g catalyst, 3 h). To improve the basicity of La_2O_3, it was doped with alkali and alkaline earth metals (Li, Na, K, Mg, Ca, Sr, and Ba) at a concentration of 25 mol % and doped La_2O_3 was calcined at 600 °C. The Na doping La_2O_3 had the highest glycerol conversion (85 %) and glycerol carbonate yield (60 %) [110].

Functionalization of both zirconium oxide (ZrO_2) and zinc oxide (ZnO) with Li has been reported for the reaction. Kaur et al. [111] found that Li was the most active out of a range of alkali and alkaline metals (Li, Na, K, Ca and Mg) when loaded on ZrO_2. Interestingly it was found that a wet impregnation method provided a more active catalyst than that prepared by co-precipitation. This was due to the formation of monoclinic Li_2ZrO_3 as the major phase when wet impregnation was used. Song et al. found that the activity of Li doped ZnO catalysts could be attributed to the substitution of Zn^{2+} by Li^+ in the ZnO lattice and the presence of [Li^+O^-] species [112]. Calcination temperature was key to catalyst activity, with higher temperatures promoting the substitution in the lattice, transforming weak and medium basic sites into strong basic sites. Optimal calcination temperature was found to be 500 °C, with further increase resulting in the destruction of strong basic sites. Liu et al. [113] prepared catalysts, including ZrO_2–KOH-CP, ZrO_2–KOH and ZrO_2–NH_4OH. The ZrO_2–NH_4OH catalyst had a maximum BET surface area of 247 m^2/g, whereas the ZrO_2–KOH sample showed a slightly lower BET surface area of 209 m^2/g. However, it is interesting that the ZrO_2-KOH catalyst exhibited a much higher total basicity compared to the other catalysts. The best results of 99.43 % glycerol conversion and glycerol carbonate yield were achieved with 100 % of selectivity.

Titanium-based materials were used as a catalyst in the process of transesterification. The Na/TiO_2 catalysts were synthesised using the wetness incipient approach, as reported by Jaiswal et al. [114]. The use of a TiO_2 support, along with a 10 wt % Na loading and a calcination temperature of 900 °C, results in the formation of the pure sodium hexatitanate ($Na_2Ti_6O_{13}$). The presence of sodium metal within the TiO_2 lattice results in a reduction in both the BET surface area and pore volume. Nevertheless, it has been found that the basic strength of 10TNO lies in the range of 15 <H_< 18.4, resulting in an increase of the amount of basic sites to 30.5 mmol/g. The catalyst loading was at 3 wt % exhibited a selectivity of 96.4 % for glycerol carbonate, with a yield of 94.5 % and a conversion rate of 98.5 %. Pristinedosium titanate nanotube (NaTNT) was prepared by Scheid et al. [115] with different calcination temperatures. Additionally, a significant decrease in both the specific surface area and total pore size was observed at temperatures reaching 500 °C. Conversely, using NaTNT, NaTNT500, and NaTNT700, which revealed higher values of glycerol conversion (100 %), GC yield (96 %) and GC selectivity (96 %). (Tables 12–14).

3.3.3. Mixed Metal Oxide Catalysts

Mixed metal oxides (MMOs) are oxides which contain two or more different metal cations [116]. MMOs are synthesised with a view of increasing catalytic activity through increased amounts of basic sites or increased surface area. Typically MMOs catalysts are synthesised using a co-precipitation method, although methods such as impregnation and sol-gel can also be used [94]. First the metal salts are precipitated from solution by the addition of a base at an appropriate pH. The obtained solid metal hydroxides are then calcined under a specific atmosphere to obtain the mixed metal oxide catalyst.

3.3.3.1. Binary Systems. Binary mixed metal oxide systems are those consisting of two different metal cations. For the production of glycerol carbonate from DMC and glycerol, significant research has focused on lanthanum (La) as one of the binary components. Simanjuntak et al. [117] prepared magnesium-lanthanum mixed oxide catalysts by a co-precipitation method. Surface area of the catalysts increased with increasing magnesium to lanthanum mole ratio, however catalyst activity was found not to be proportional to surface area. Mg_3La_1 exhibited the highest basicity (0.39 mmol/g) and was 2.1 times more active than pure lanthanum oxide. Interestingly the catalyst activity was affected by choice of precipitating agent, with a mixture of potassium hydroxide and potassium carbonate the most effective. Zinc-lanthanum mixed oxides have also been reported with both Zn_4La_1 and Zn_2La_1 providing reasonably high conversion and selectivity [118]. Zn_4La_1 gave a glycerol carbonate yield of 95.7% at 150 °C, dimethyl carbonate to glycerol mole ratio of 6:1, 0.5 wt% catalyst and 2 h reaction time. Whilst the catalyst exhibited deactivation upon reuse it could be regenerated through calcination. Similarly with calcium-lanthanum mixed oxides increasing the calcium to lanthanum mole ratio resulted in increased activity [119]. The catalyst 3CaLa yielded 74% glycerol carbonate at 90 °C, dimethyl carbonate to glycerol mole ratio of 5:1, 0.217 g catalyst and 1.5 h reaction time. Song et al. [120] prepared porous lanthanum-zirconium catalysts using P123 as a soft template. The prepared La-Zr catalyst was not as active as pristine La_2O_3 giving only 15.97% glycerol conversion compared to 70% under similar conditions. The activity could be increased with impregnation of a 0.3 mass ratio of potassium fluoride. The interaction of KF with La-Zr lead to the formation of a Lewis base yielding strong and super basic sites, increasing yield to 91.77% under similar conditions. A lanthanum-cobaltite perovskite material was prepared by sol-gel method by Phadtare et al. [121]. It was found that metal oxide precursor, ratio and crucible material had a strong effect on the catalyst activity. Lanthanum nitrate and cobalt acetate were found to be the best precursors in a 1:2 ratio using a porcelain crucible and calcined at 900 °C. These preparation conditions resulted in the formation of a highly crystalline $LaCoO_3$ perovskite phase with 40% La_2O_3 phase also contributing to the basicity. Continuous synthesis of glycerol carbonate has been reported by Pattanaik et al. [122] using iron and lanthanum mixed oxides prepared by co-precipitation. A highly active $LaFeO_3$ phase could be obtained at a 1:1 molar ratio of metals, giving a greater number of strong acidic and basic sites. The catalyst exhibited excellent stability with 100 h on stream, yielding 71% glycerol carbonate at 240 °C, dimethyl carbonate to glycerol mole ratio of 4:1 and 1 g of catalyst.

Magnesium is another binary component which has been extensively

Table 12
Physical properties and performance of different single component metal oxides catalysts for the transesterification of glycerol with DMC.

Catalyst	Physical properties		Operating parameter					Performance	Ref
	BET surface area (m^2/g)	Total basic site amount (mmol CO_2/g catalyst)	Temp (°C)	Time (min)	Mole Ratio of DMC to glycerol	Catalyst loading	Solvent		
CaO – calcined at 900 °C	-	-	75	90	5:1	10 mol %	-	C = 94.1 % Y = 91.1 %	[90]
CaO (waste cockle shells) – calcined at 800 °C	3.5	0.2074	80	120	3:1	3 wt %	-	Y = 92.1 %	[99]
CaO (waste eggshells) – calcined at 900 °C	4.92	0.481	60	180	2.5:1	9 mol %	-	Y = 94 % C = 96 % S = 100 %	[100]
CaO/Al_2O_3 (polya,3) – calcined at 800 °C	29.35	-	80	300	3:1	15 mol %	-	C = 95.39 % Y = 90.57 %	[97]
5 wt % KNO_3/CaO – calcined at 700 °C	-	0.12	70	120	3:1	10 mol %	-	C = 99.23 % Y = 89.38 %	[89]
10 wt % LiCl/CaO – calcined at 600 °C	3.2822	-	65	20	1:1	10 wt %	Ethanol	Y = 94.2 %	[98]
MgO – calcined at 900 °C	-	-	75	90	5:1	10 mol %	-	C = 12.4 % Y = 12.1 % %	[90]
MgO – pluronic F127	47	0.39	90	90	2:1	5 wt %	-	Y = 75.4 %	[102]
Trapezoidal MgO	31.8	-	90	120	1:3	3 wt %	Ethanol	Y = 96.2 %	[103]
20 wt % K_2CO_3/MgO	25.74	-	80	120	2.5:1	1 wt %	-	Y = 99.0 %	[104]
3.8 mmol KF/γ-Al_2O_3	20.4	2.17	75	120	2:1	5 wt %	DMF	Y = 95.8 %	[105]
80 wt % NaOH/γ-Al_2O_3	21.7	0.50	78	60	2:1	3 wt%	-	C = 97.9 % S = 99.0 %	[106]
30 wt % KNO_3/Al_2O_3 – calcined at 800 °C	5.90	1.38	70	120	2:1	0.75 mol % 5 wt %	-	Y = 31.60 % C = 95.12 %	[107]

Catalyst	Physical properties		Operating parameter					Performance	Ref
	BET surface area (m^2/g)	Total basic site amount (mmol CO_2/g catalyst)	Temp (°C)	Time (min)	Mole Ratio of DMC to glycerol	Catalyst loading	Solvent		
La_2O_3 (PEG 20000)	11.27	-	85	30	5:1	5 wt %	-	Y = 99.4 %	[108]
3.5 mol% Li/La_2O_3	1.9	0.7409	85	180	3:1	0.1 g	-	C = 94.4 % S = 92.1 %	[109]
25 mol% Na/La_2O_3 – calcined at 600 °C	31.94	5.6 μmol m^{-2}	70	120	3:1	0.10 g 3.33% wt	-	Y = 60 % C = 85 %	[110]
20 wt% Li/ZrO_2	-	2.10	95	120	3:1	5 wt%	-	Y = 91 %	[111]
1 wt% $LiNO_3$/ZnO	-	-	95	240	2:1	5 wt%	-	Y = 95.8 %	[112]
ZrO_2–KOH	209	1.226	80	120	3:1	3 wt%	-	Y = 99.43 % C = 99.43 % S = 100 %	[113]
10 wt% Na/TiO_2	7.721	30.5	90	90	2:1	3 wt%	-	Y = 94.5 % C = 98.5 % S = 96.4 %	[114]
NaTNT– calcined at 700ºC	19	-	75	90	2:1	2 wt%	-	Y = 96 % C = 100 % S = 96 %	[115]

Note: Y = yield of glycerol carbonate, C = conversion of glycerol, S = selectivity of glycerol carbonate, DMC = dimethyl carbonate

researched. Khayoon et al. [123] reported the use of magnesium-calcium mixed oxide catalysts prepared by a co-precipitation method. All Mg-Ca mixed oxide catalysts prepared exhibited higher basicity when compared to pristine MgO and CaO. It was found that by increasing the ratio of Mg that the surface area, pore volume, and number of basic sites all increased. The catalyst $Mg_{1.2}Ca_{0.8}O_2$ had the highest activity of the prepared catalysts, exhibited higher activity than conventional hydrotalcite under the same reaction conditions. Li/Mg composite was reported by Liu et al. [124]. As the molar ratio of Li to Mg increased, the weak basic sites were transformed into the medium and strong sites, respectively. The maximal glycerol yield (90.61%) was achieved at a molar ratio of 4 between Li and Mg. MgO was also synthesised by co-precipitation with CuO, MnO_2 and CrO_2, reported by Jaiswal et al. [125] By doping Mg onto MnO_2, the surface area can be increased. $MgCu_4O_5$had a pore diameter of 64.25 nm, which was considerably larger than $MgMn_2O_4$ (58.65 nm). MnO_2 and CuO doped to Mg, which improved the total basicity and basic strength of the catalyst. $MgCu_4O_5$ exhibited a lower basic site than $MgCu_4O_5$ (18.86 mmol/g). According to Pradhan et al. [126], $MgCr_2O_4$ exhibited remarkable catalytic activity and contributed to a 98% conversion of glycerol, which is significantly higher than MgV_2O_4 (82% conversion of glycerol). In contrast to MgV_2O_4, $MgCr_2O_4$ exhibited a significantly higher efficiency due to its higher crystallite size and higher total basicity (17.63 mmol/g), both of which are fundamental properties that enhance the catalytic activity of heterogeneous catalysts. Magnesium titanate ($MgTiO_3$) catalyst was synthesised by simple co-precipitation route. The main reasons for its 88% selectivity and 93% conversion are its high surface area and strong basicity catalyst [127]. The presence of MgO to the g-C_3N_4 resulted in an increase in the specific surface area, pore volume, and pore size. According to the results report by Reisi and Chermahini [128], the catalyst 6MgO/C_3N_4 shown the best catalytic activity due to its good basic strength. The total CO_2 desorption was measured to be 0.196 mmol/g. Consequently, the conversion, yield, and selectivity were determined to be 98.3%, 97.1%, and 95.5%, respectively. Magnesium-zirconium catalysts can be prepared via a self-induced assembly route with Pluronic P123 as a structure directing

Table 13
Physical properties and performance of different mixed metal oxide catalysts for the transesterification of glycerol with DMC.

Catalyst	Physical properties		Operating parameter					Performance	Ref
	BET surface area (m^2/g)	Total basic site amount (mmol CO_2/g catalyst)	Temp (°C)	Time (min)	Mole Ratio of DMC to glycerol	Catalyst loading	Solvent		
Mg_3La_1	43.4	0.39	85	90	2:1	5 wt%	-	Y = 81.3 %	[117]
Zn_4La_1	33.54	0.256	150	120	6:1	0.5 wt %	-	Y = 95.7 % C = 98.5 % S = 97.2 %	[118]
3CaLa	33	0.771	90	90	5:1	0.217 g	-	Y = 74.0 % C = 94.0 %	[119]
0.3 wt% KF/LaZr	14.49	-	80	60	2:1	1 wt%	-	Y = 91.77 % S = 99.00 %	[120]
$LaCoO_3$	7.89	0.2503	120	90	3:1	5 wt%	DMF	C = 98.0 % S = 77.0 %	[121]
$LaFeO_3$ – on stream	16.4	1.413	240	6000	2:1	1 g	-	Y = 71 % S = 100 %	[122]
$Mg_{1.2}Ca_{0.8}O_2$	31.7	1.486	70	90	2:1	0.30 g	-	Y = 100 % C = 100 %	[123]
Mg_1Zr_2	54.19	-	70	180	5:1	15 wt%	-	Y = 88 %	[129]
Li/Mg: 4 molar ratio – calcined at 100 °C	13.62	-	80	120	3:1	4 wt%	-	Y = 90.61 % C = 92.05 % S = 98.44 %	[124]
$MgMn_2O_4$ – calcined at 400 °C	14.94	18.86	90	75	4:1	5 wt%	-	Y = 94 % C = 97 %	[125]
$MgCu_4O_5$ – calcined at 400 °C	2.64	10.56	90	75	4:1	5 wt%	-	Y = 71 % C = 83 %	[125]

Catalyst	Physical properties		Operating parameter					Performance	Ref
	BET surface area (m^2/g)	Total basic site amount (mmol CO_2/g catalyst)	Temp (°C)	Time (min)	Mole Ratio of DMC to glycerol	Catalyst loading	Solvent		
$MgCr_2O_4$	28.7	17.63	85	80	4:1	5 wt%	-	Y = 95.7 % C = 98 % S = 96.48 %	[126]
$MgTiO_3$ – calcined at 800 °C	27.58	11.46	90	180	6:1	12 wt%	-	C = 93 % S = 88	[127]
6MgO/g-C_3N_4	43.4	0.196	80	240	3:1	30 mg	-	Y = 97.1 % C = 98.3 % S = 95.5 %	[128]
Mg_3Ce_1	122	0.291	90	90	5:1	15 wt%	-	Y = 86 % S = 100 %	[131]
Mg_3Ni_1	27	0.511	90	90	4:1	4 wt%	-	Y = 82 %	[132]
$Ca_{0.6}Zr_1$	167	0.138	90	LHSV = 1.5 h^{-1}	3:1	3 mL	-	C = 97 % S = 93 %	[133]
1:2 Ni/CaO (NDW)	-	35.65	90	90	3:1	3 wt% 300 mg	-	Y = 94.02 % C = 99.2% S = 95 %	[134]
SiO_2-Na_2O (2:1)	6.2	16.4	75	90	4:1	4 wt%	-	Y = 94.1 % C = 96.3 %	[135]
Al_2O_3-ZrO_2-1 F	168	0.1053	110	90	2:1	0.1 g	-	Y = 95.2 % C = 100 % S = 95.2 %	[136]
$Mg_3Al_1Zr_1$	-	-	75	90	5:1	10 wt%	-	Y = 94 %	[137]

Catalyst	Physical properties		Operating parameter					Performance	Ref
	BET surface area (m^2/g)	Total basic site amount (mmol CO_2/g catalyst)	Temp (°C)	Time (min)	Mole Ratio of DMC to glycerol	Catalyst loading	Solvent		
$Mg_3Zr_1Sr_1$	-	-	90	90	5:1	0.3 g	-	C = 96 % S = 56 %	[138]
$Mg_{2.4}Al_{1.0}Cu_{0.6}$	165.2	0.98	90	90	5:1	15 wt%	-	Y = 91.2 % C = 96.4 %	[139]
5 wt% Ce/CaO-MgO	5.80	2.50	85	90	4:1	4 wt%	-	Y = 91.74 % C = 95.57 %	[140]
$CoFe_2O_4$/CaO-ZnO	11.58	-	85	150	5:1	5 wt%	-	C = 97.7 % S = 99.2 %	[91]

Note: Y = yield of glycerol carbonate, C = conversion of glycerol, S = selectivity of glycerol carbonate, DMC = dimethyl carbonate.

agent [129]. A magnesium to zirconium ratio of 1:2 exhibited the highest activity. This was attributed to its highly basic nature with a lower pore size and well dispersed MgO. The catalyst gave a glycerol carbonate yield of 88% after 3 h at 70 °C, dimethyl carbonate to glycerol mole ratio of 5:1 and 15 wt% of catalyst. Li et al. [130] also studied the effects of the preparation method (co-precipitation, hydrothermal process) and Mg/Zr ratio. The molar ratio of Mg/Zr exerts a substantial influence on the basicity of catalysts that consist of Mg-Zr oxide. Among all the catalysts, Mg_1Zr_2 has the highest number of total basic sites. In addition, the catalyst that was synthesised using the hydrothermal

Table 14
Physical properties and performance of different layered double hydroxides catalysts for the transesterification of glycerol with DMC.

Catalyst	Physical properties		Operating parameter					Performance	Ref
	BET surface area (m^2/g)	Total basic site amount (mmol CO_2/g catalyst)	Temp (°C)	Time (min)	Mole Ratio of DMC to glycerol	Catalyst loading	Solvent		
Mg_5Al_1	-	0.64	100	60	5:1	0.1 g	-	Y = 98 %	[143]
Mg_4Al_1 (hierarchical)	223.52	0.0146	90	240	5:1	10 wt%	-	Y = 84 %	[146]
0.5 mmol/g Ni/ Mg_2Al_1	248	0.55	100	120	3:1	10 wt%	-	Y = 55 % S = 100 %	[147]
$(AlF_6)^{3-}$/MgAl	177	0.269	110	180	3:1	0.3 g	-	Y = 95.3 % C = 100 % S = 95.3 %	[148]
Mg_2Al_1	219	0.51	100	120	3:1	10 wt%	1,4-butanediol	Y = 66 % S = 100 %	[149]
5 wt% Li/$Mg_4Al_1O_{5.5}$	52	3.11	80	90	3:1	4 wt%	-	Y = 96.28 % C = 100 % S = 96.28 %	[150]
$Ca_{1.5}Mg_{1.5}Al_{1.0}$	-	-	80	180	3:1	5 wt%	-	Y = 45 %	[151]
5 wt% KF/ $Ca_{1.5}Mg_{1.5}Al_{1.0}$	-	-	80	30	3:1	5 wt%	-	Y = 99 %	[151]
CaMgAl (S95 steel slag)	40.27	0.99	75	90	3:1	3 wt%	-	Y = 96.2 % C = 98.3 % S = 97.9	[152]
[BMIM][OH]/ CaMgAl (S95 steel slag)	-	-	75	120	3:1	3 wt%	-	Y = 95 % C = 96.1 %	[153]
[APmim]OH/ZIF-8/ LDH	431.66	1.47	75	80	3:1	3 wt%	-	Y = 96.5 % C = 98.6 %	[154]

Catalyst	Physical properties		Operating parameter					Performance	Ref
	BET surface area (m^2/g)	Total basic site amount (mmol CO_2/g catalyst)	Temp (°C)	Time (min)	Mole Ratio of DMC to glycerol	Catalyst loading	Solvent		
CaAl	16	-	90	180	3.5:1	0.15 g	-	C = 79 % S = 60 %	[155]
CaAl – calcined at 750 °C	4	-	90	180	3.5:1	0.15 g	-	C = 97 % S = 85 %	[156]
MMO-$Cu_{15}Zn_{15}$	218	3.28	85	270	2:1	7.5 wt %	-	Y = 85.1 % C = 95.6 % S = 89.0 %	[157]

Note: Y = yield of glycerol carbonate, C = conversion of glycerol, S = selectivity of glycerol carbonate, DMC = dimethyl carbonate

method has a larger specific surface area, smaller grain size, and higher dispersion. The catalyst Mg_1Zr_2-HT, after undergoing calcination at 600 °C in a nitrogen atmosphere, exhibited the best catalytic activity, achieving a conversion of 99% and a selectivity of 96.1%. Parameswaram et al. [131] investigated the use of magnesium-cerium mixed oxide catalysts. Increasing the amount of Mg led to increased activity of the catalysts, with Mg_3Ce_1 the most active exhibiting strong basic sites. The presence of cerium was found to be important to increase the yield of glycerol carbonate, with magnesium important for glycerol conversion. A calcination temperature of 650 °C produced well formed CeO_2 phases and well dispersed MgO. A similar trend of increased basic strength with increased magnesium amount was found by Pradhan et al. [132] when preparing nickel-magnesium mixed oxide catalysts. A Mg_3Ni_1 catalyst exhibited the highest activity due to a higher basic strength because of the increased magnesium loading. An 82% yield of glycerol carbonate was achieved after 90 min at 90 °C, dimethyl carbonate to glycerol mole ratio of 4:1 and 4 wt% of catalyst.

Mesoporous calcium-zirconium mixed metal oxides have also been prepared through template free co-precipitation [133]. Zhang et al. [133] found that increasing the amount of Ca present resulted in an increase in the basic strength of the prepared catalysts with $Ca_{0.6}Zr_1$ having 138 μmol/g of basic sites compared to 43 μmol/g of pure zirconia. The contribution of strong basic sites is roughly 4 times higher in $Ca_{0.6}Zr_1$ than pure ZrO_2. When employed in a continuous flow set-up the $Ca_{0.6}Zr_1$ catalyst exhibited 97% glycerol conversion and 93% selectivity towards glycerol carbonate at 90 °C, dimethyl carbonate to glycerol mole ratio of 3:1, 3 mL of catalyst and a liquid hourly space velocity (LHSV) of 1.5 h^{-1}. In addition, a nickle oxide was doped into CaO to synthesised Ni-modified distillation waste (NDW) by the wet impregnation process with 2:1 Ni/ca atomic ratio [134]. The catalyst consists of two types of CaO and NiO crystals, each with an average particle size of 25.68 nm, exhibiting a varied spheroidal shape. The moderate basicity of the catalyst is indicated by the 35.65 mmol/g of basic sites. The catalysts revealed an increased conversion of 99.2% for glycerol carbonate and a higher selectivity of 95%, with a yield of 94.02%.

Mixed metal oxides of SiO_2 and Na_2O known as water glass have been prepared by Xu et al. [135] with differing modulus values (the ratio of SiO_2 to Na_2O). The catalyst with a modulus value of 2 was chosen as the best catalyst due to a high surface area, relatively high total basicity and due to less sodium hydroxide being required during preparation. The catalyst exhibited a 94.1% yield after 90 min at 75 °C, dimethyl carbonate to glycerol mole ratio of 4:1 and 4 wt% of catalyst. Wang et al. [136] reported another mixed metal oxide consisting of ZrO_2 and Al_2O_3, with the same Al^{3+}/Zr^{4+} atomic ratio of 0.2 and different F/Al molar ratios (n = 0, 0.5, 1, 2). It is noted that the presence of Al^{3+} and $(AlF_6)^{3-}$ to ZrO_2 not only increased the acidity but also significantly enhanced the basicity of the Al_2O_3-ZrO_2-nF catalysts. Additionally, F content also impacted both the strength and the distribution of acidic-basic sites on the catalysts. Glycerol carbonate was produced with a high selectivity of 95.2%, a glycerol conversion of 100%, and a yield of 95.2% through Al_2O_3-ZrO_2-1 F.

3.3.3.2. Non-Binary Systems. Mixed metal oxide catalysts can also be made of three (ternary) or four (quaternary) different metal

components. Malyaadri et al. [137] reported the use of a ternary mixed metal oxide consisting of magnesium, aluminium and zirconium. The most active catalyst consisted of Mg as the main component with a Mg:Al:Zr ratio of 3:1:1. MAZ-311 yielded 94% glycerol carbonate after 90 min at 75 °C, dimethyl carbonate to glycerol mole ratio of 5:1 and 10 wt% of catalyst. A similar ternary mixed metal oxide was reported by Parameswaram et al. [138] consisted of magnesium, zirconium and strontium. Again, a high loading of magnesium was found in the most active catalyst with a Mg:Zr:Sr ratio of 3:1:1. However this catalyst suffered from low selectivity to glycerol carbonate compared to that reported by Malyaadri et al. [137]. A glycerol conversion of 96% and selectivity of glycerol carbonate of 56% was achieved after 90 min at 90 °C, dimethyl carbonate to glycerol mole ratio of 5:1 and 0.3 g of catalyst. A copper based mixed metal oxide consisting of magnesium, aluminium and copper has also been investigated [139]. The catalyst consisting of $Mg_{2.4}Al_{1.0}Cu_{0.6}$ had the highest density of strong Lewis basic sites yielding 91.2% of glycerol carbonate after 90 min at 90 °C, dimethyl carbonate to glycerol mole ratio of 5:1 and 15 wt% of catalyst. Arora et al. [140] synthesised a ternary system through the calcination of marble waste to give a mixture of calcium and magnesium oxide, which was then loaded with cerium oxide through a wet impregnation method. Whilst loading ceria decreased the surface area of the catalyst, the presence of both Ce^{3+} and Ce^{4+} species were shown to create oxygen vacancies which increased both the catalyst activity and stability. A 5 wt% loading of Ce calcined at 850 °C gave a glycerol carbonate yield of 91.74% after 90 min at 85 °C, dimethyl carbonate to glycerol mole ratio of 4:1 and 4 wt% of catalyst.

One quaternary system has been reported by Zhang et al. [91] consisting of a magnetic mesoporous $CoFe_2O_4$ supported on calcium and zinc oxide. CaO-ZnO was found to be the best support when compared to $CoFe_2O_4$/CaO-CeO_2 and $CoFe_2O_4/Ca_{12}Al_{14}O_{33}$. This was due to the higher peak strength and therefore the presence of more moderate acidic sites. The magnetic nature of the catalyst also offers easy separation from the reaction mass. The catalyst achieved a 97.7% conversion of glycerol and a 99.2% selectivity towards glycerol carbonate after 2.5 h at 85 °C, dimethyl carbonate to glycerol mole ratio of 5:1 and 5 wt% of catalyst.

3.3.4. Layered double hydroxides

Layered double hydroxides (LDHs), hydrotalcite-like materials or anionic clays, are a type of layered material consisting of positively charged brucite-like layers with an interlayer region containing charge compensating anions and solvation molecules [141]. A general formula for a LDH is $[M^{2+}_{1-x}M^{3+}(OH)_2][A^{n-}]_{x/n}.zH_2O$ where M2 + is typically Mg^{2+}, Zn^{2+} or Ni^{2+}, M^{3+} is typically Al^{3+}, Ga^{3+}, Fe^{3+} or Mn^{3+}, A^{n-} is typically CO_3^{2-}, Cl^-, SO_4^{2-} or RCO^{2-} and x is typically between 0.2 and 0.4. Layered double hydroxides have a number of interesting properties including their ease of synthesis, uniform distribution of metal cations, surface hydroxyl groups, flexible tunability and high chemical and thermal stability to name a few [142]. They can be synthesised through co-precipitation, ion-exchange or reconstruction/rehydration synthesis methods.

The mineral, hydrotalcite, was one of the first LDHs discovered with a formula $[Mg_6Al_2(OH)_{16}](CO)_3.4\ H_2O$. The use of an uncalcined MgAl hydrotalcite prepared by co-precipitation was first reported by Takagaki et al. [143]. When ranging the Mg/Al ratio from 2 to 5, a higher ratio of 5 was found to give the highest basicity of 0.64 mmol/g. This high ratio was found to also form a hydromagnesite phase of $Mg_5(CO_3)_4(OH)_2.4\ H_2O$. The activity of the catalyst was attributed to the hydrotalcite formed, with the hydromagnesite exhibiting poor activity. The hydromagnesite however was shown to absorb glycerol, bringing it closer to the active sites of the hydrotalcite and improving the activity. Hsu et al. [144] also found that basicity increased with increasing Mg/Al ratio, with a Mg/Al ratio of 5 was also found to be the most active catalyst.

This promotional effect of hydromagnesite was further investigated by Kumar et al. [145]. Through glycerol absorption studies it was found that hydomagnesite absorbed 0.68 mmol of glycerol compared to 0.52 absorbed by pure hydrotalcite, with a mixture of both absorbing 1.22 mmol of glycerol. It was found that whilst glycerol carbonate yield increased throughout the reaction, almost complete uptake of glycerol was observed at the initial stage of the reaction facilitated through the adsorption of glycerol onto hydromagnesite.

The effect of MgAl layered double hydroxide morphology was investigated by Sun et al. [146] through the preparation of three-dimensional hierarchical flowerlike catalysts. The catalysts were prepared through a sacrificial template coprecipitation method using γ-Al_2O_3 with an Mg/Al ratio of 4. When comparing conventional LDH with the 3D hierarchical structure, conversion could be increased from 13% to 26.3% under similar conditions due to an increase in both surface area, and more importantly basicity which increases from 0.3 μmol/g to 1.29 μmol/g. Surface area and basicity of the 3D hierarchical structures could be further increased by calcination at 500 °C achieving a surface area of 223.52 m^2/g and high basicity of 14.64 μmol/g. As a result of this glycerol conversion increased to 85.6%. The increase in activity from calcination is attributed to the presence of OH^- Brønsted sites, Mg/MO pairs and strong O^{2-} Lewis basic sites.

To further increase the activity of Mg/Al LDHs Liu et al. [147] investigated the effect of metal doping. The catalysts were prepared by a homogeneous precipitation method and doped with metals (Cr, Mn, Fe, Co, Ni, Cu and Zn) using a calcination-reconstruction process. Using 0.5 mmol metal/g hydrotalcite precursor lithium was found to be the most active dopant. Similarly, Zhang et al. [148] investigated MgAl LDH promotion through modification with fluorine containing $(AlF_6)^{3-}$. The basic strength and number of basic sites increased with the fluorine content, until a ratio of F/Al of 1. With loading of fluorine, the glycerol conversion could be increased from 57.8% of pure MgAl LDH to complete conversion.

It is also possible to prepare mixed metal oxide materials from LDHs through calcination. Liu et al. [149] prepared MgAl LDHs through a co-precipitation method and subsequent calcination to give mixed oxide catalysts. The surface area of the LDHs decreased with increasing Mg/Al ratio with a similar trend found in the mixed oxide catalysts. However, calcination of the LDHs to mixed oxides resulted in an increase in the surface area. For a Mg/Al ratio of 6, the LDH had a surface area of 16 m^2/g with the mixed oxide having a surface area of 155 m^2/g. A good correlation between the number of basic sites and activity was found with a Mg/Al ratio of 2 calcined at 600 °C giving the highest basicity of 2.3 μmol/g. The high activity of the calcined catalyst was attributed to the presence of weak OH^- sites, medium Mg-O pair sites and strong O^{2-} sites. A similar trend of increased LDH activity by calcination to mixed oxides was found by Liu et al. [150]. The activity of the calcined LDH (Mg/Al ratio of 4) could be further enhanced through incorporation of lithium nitrate ($LiNO_3$) resulting in an increase in the number of basic sites. The MgAl oxide gave a 52.09% yield of glycerol carbonate which could be increased to 96.28% yield through incorporation of 5 wt% $LiNO_3$. For comparison 5 wt% $LiNO_3$ on MgAl LDH gave 88.35% glycerol carbonate yield.

Calcium, magnesium and aluminium LDHs have also been reported for the reaction [151]. A CaMgAl LDH with a ratio of 1.5/1.5/1 exhibited low activity for the reaction, with only 45% glycerol carbonate yield after 3 h at 80 °C, a dimethyl carbonate to glycerol mole ratio of 3:1 and 5 wt% catalyst loading. The activity of CaMgAl LDH could be dramatically improved through loading of 5 wt% KF, giving a 99% glycerol carbonate yield in 30 min under the same conditions. The effect of solvents was also found to inhibit the formation of glycerol carbonate. It is possible to synthesis CaMgAl hydrotalcite type mixed oxides from waste material, such as waste steel slag [152]. The catalysts were prepared through acidolysis, co-precipitation and calcination from S95 steel slag. The basicity of the prepared catalysts was found to increase with increasing calcination temperature. A high calcination temperature of 800 °C was found to increase glycidol formation, therefore 600 °C

was found to be optimum giving a 96.2% glycerol carbonate yield after 90 min at 75 °C, a dimethyl carbonate to glycerol mole ratio of 3:1 and 3 wt% catalyst loading. The activity of the waste steel slag catalyst could be improved through intercalation with basic ionic liquids [153]. Liu et al. [153] tested 5 different ionic liquids – [BMIM][CH_3COO], [BMIM][HCOO], [BMIM][OH], [BMIM][Br] and ChOH. [BMIM][OH] was found to be the most active and drastically improved the activity of the catalyst. Liu et al. [154] also synthesised ZIF-8 modified by ionic liquid and dispersed evenly in the CaMgAl hydrotalcites to prepare [APmim]OH/ZIF-8/LDH. The dispersion of [APmim]OH/ZIF-8 among hydrotalcites serves to improve the alkaline strength of catalyst and prevent the aggregation of ZIF-8. Furthermore, it should be noted that hydrotalcites exhibit an increased specific surface area of 431.66 m^2/g. The glycerol conversion achieved a high value of 98.6%, while the yield of glycerol carbonate reached 96.5% at 75 °C and the reaction time was 80 min

Granados-Reyes et al. [155] reported the use of CaAl LDHs for the reaction. The effect of metal salt precursor and ageing techniques such as microwave, conventional heating, refluxing of autoclave was investigated. However no significant differences were found in any of the catalysts synthesised, with similar surface and basic characteristics. The effect of calcination temperature on these catalysts was further studied by Granados-Reyes et al. [156]. Calcination temperature and duration was found to have a marked effect on the activity of the catalyst. Calcination of the catalyst for longer than 15 h at 450 °C in an air or inert atmosphere was shown to improve glycerol conversion and glycerol carbonate selectivity. This could be further improved at higher calcination temperatures such as 750 °C due to the formation of a CaO phase in the catalysts.

Argüello et al. [157] prepared quaternary (Cu-Zn-Mg-Al) precursors. Layered double hydroxides (LDHs) are used as the precursor materials for the synthesis of multi metallic oxides. Subsequently, the precursor materials were calcined at 450 °C for 9 h, resulting in the formation of MMO. The presence of Zn in the MMO-Cu_{15}Zny samples resulted in an increase in the number of very strong basic sites. MMO-$Cu_{15}Zn_{15}$ catalyst had the highest glycerol yield (85.1%) due to the presence of the highest number of total basic sites, as well as its larger pore diameter and volume.

3.3.5. Sodium aluminate

Sodium aluminate ($NaAlO_2$) is a strong base, available as both a solid or in solution, which has gained interest recently as a catalyst for biomass conversion, as it is commercially available and relatively inexpensive. $NaAlO_2$ is also reported to be insoluble in alcohols, making it interesting for glycerol carbonate synthesis which produces methanol as a by-product.

The use of $NaAlO_2$ for glycerol carbonate synthesis from glycerol and DMC was first reported by Ramesh et al. [158]. The activity of $NaAlO_2$ microspheres prepared by a spray-drying method was compared with commercial $NaAlO_2$. The basicity of commercial $NaAlO_2$ is lower than that of the spray-dried microspheres. The basicity of the microspheres could be further improved by spray-drying a $NaAlO_2$ and ethanol solution. The microspheres prepared by $NaAlO_2$/ethanol solution has much faster kinetics than the commercial catalysts, yielding 94% of glycerol carbonate after 30 min at 90 °C, a dimethyl carbonate to glycerol mole ratio of 2:1 and 3 wt% catalyst loading. The improved activity was attributed to the smaller crystallite size and higher surface basicity. Production of $NaAlO_2$ was also investigated by Rittiron et al. [159] who used glycerol as a template during production. When comparing spray-drying vs. the conventional hot-air drying method, spray-drying was found to be marginally more active giving 10.4% glycerol carbonate yield vs. 9.4. Contradictory to what is reported by Ramesh et al. [158] it was found that without the use of template, that the commercial $NaAlO_2$ catalyst was more active. When using a template, glycerol was found to produce more active catalysts than polyvinylpyrrolidone (PVP), due to the increased SA and basicity of the catalyst.

Chotchuang et al. [160] investigated the impregnation of CaO onto $NaAlO_2$ in an effort to improve the activity. Loading of CaO resulted in an increase in the activity of the catalyst until a loading of 5 wt% CaO. The activity of the catalysts could be further improved through the use of glycerol as a template in order to improve the surface area. The catalyst synthesised with 45 wt% glycerol as a template and 5 wt% CaO was most active with 91% glycerol carbonate yield after 3 h at 70 °C, a dimethyl carbonate to glycerol mole ratio of 4:1 and 30 wt% catalyst loading. The catalyst exhibited deactivation due to agglomeration and leaching.

Whilst $NaAlO_2$ is highly active in its pure form, it is also highly hygroscopic and corrosive [161]. For this reason, it is desirable to support $NaAlO_2$ to increase the ease of handling. $NaAlO_2$ supported on hydrotalcites have proven to be highly active for the transesterification of glycerol with DMC. A 10 wt% loading of $NaAlO_2$ was found to be the optimum catalyst loading conversion 93% of glycerol after 30 min at 90 °C, a dimethyl carbonate to glycerol mole ratio of 2:1 and 3 wt% catalyst loading.

To further increase activity and stability of $NaAlO_2$, alumina supported sodium aluminate catalysts were synthesis by Keogh et al. [162] using a simple wet impregnation method. Sodium aluminate supported on Al_2O_3 is the most stable catalyst in terms of stability, exhibiting a small decrease in activity when reused. After 60 min of reaction time, the glycerol conversion of pure sodium aluminate is similar to 20 wt% SA/Al_2O_3, at 98% and 96% conversion, respectively. Although the catalysts exhibit similar activity, supported sodium aluminate shows the benefit of being easier to handle in comparison with pure sodium aluminate, which is corrosive and hygroscopic. The reusability of the catalyst was relatively good, as evidenced by a 3.4% reduction in glycerol conversion upon reuse.(Tables 15 and 16).

3.3.6. Silicate materials

Silicates are cheap and effective basic catalysts, which were first reported for this reaction by Wang et al. [163]. Sodium silicate was found to be the most active out of the silicates tested (aluminium, magnesium, calcium, potassium, and sodium). Calcination of the silicates was found to release water by cratering, which created smaller particle sizes. Calcination of $Na_2SiO_3.9\ H_2O$ at 200 °C provided a catalyst with intermediate total basicity and a low amount of strong basic sites.

Silicates are typically used as a support, to provide dispersion for a more active compound. MCM-41 (Mobil Composition of Matter No. 41) is an ordered mesoporous silica with a 2D hexagonal structure [164]. Mg-Al mixed oxides supported on MCM-41 were prepared via co-precipitation followed by thermal decomposition [165]. The supported catalysts were found to be more active than the corresponding pure Mg-Al mixed oxides, due to the increased basicity. MCM-41 has also been reported as a support for lithium prepared through wet impregnation [166]. Out of the metals tested (lithium, lanthanum, cerium, magnesium, and potassium) lithium was found to be the most active. A loading of 5 wt% Li calcined at 450 °C resulted in both decreased surface area and pore volume, but an increase in the basic character of the catalysts from 5.7 mmol/g to 9.8 mmol/g. The low yield of 3.2% glycerol carbonate associated with pristine MCM-41 could be increased to 93.14%. Arora et al. incorporated Co_3O_4 nanoparticles on the synthesised support material by impregnation method [167]. The presence of active metal in MCM-41 resulted in a slight reduction in both surface area and pore volume. However, this did not appear to have a significant impact on the average pore diameter. The conversion of glycerol and the yield of glycerol carbonate increased to 42.1 ± 1.7% and 40.2 ± 2.2%, respectively, while using a 5 wt% loading of active metal cobalt on the MCM-41 catalyst. The observed increase in positivity might perhaps be attributed to the rise in the concentration of the basic site, which reached 8.7 mmol/g. The increase in the basic site concentration to 8.7 mmol/g might be the reason for the positive result.

SBA-15 is another mesoporous silica with uniform hexagonal pores

Table 15
Physical properties and performance of different sodium aluminate catalysts for the transesterification of glycerol with DMC.

Catalyst	Physical properties		Operating parameter					Performance	Ref
	BET surface area (m^2/g)	Total basic site amount (mmol CO_2/g catalyst)	Temp (°C)	Time (min)	Mole Ratio of DMC to glycerol	Catalyst loading	Solvent		
$NaAlO_2$ (microspheres)	-	-	90	30	2:1	3 wt%	-	Y = 94%	[158]
$NaAlO_2$ (glycerol template)	9.5	-	70	120	4:1	30 wt%	-	Y = 85% S = 100%	[159]
5 wt% $CaO/NaAlO_2$	16.11	-	70	180	4:1	30 wt%	-	Y = 91% S = 100%	[160]
10 wt% $NaAlO_2$/ Hydrotalcite	23	1.1	90	30	2:1	3 wt%	-	C = 93%	[161]
20 wt% SA/Al_2O_3	178.25	2.2	90	60	3:1	10% wt	-	C = 96%	[162]

Note: Y = yield of glycerol carbonate, C = conversion of glycerol, S = selectivity of glycerol carbonate, DMC = dimethyl carbonate

Table 16
Physical properties and performance of different silicate materials catalysts for the transesterification of glycerol with DMC.

Catalyst	Physical properties		Operating parameter					Performance	Ref
	BET surface area (m^2/g)	Total basic site amount (mmol CO_2/g catalyst)	Temp (°C)	Time (min)	Mole Ratio of DMC to glycerol	Catalyst loading	Solvent		
$Na_2SiO_3.9\ H_2O$ – calcined at 200 °C	1.3	10.3	75	150	4:1	5 wt%	-	Y = 95.5% C = 97.8% S = 97.6%	[163]
MgAl/MCM-41	657	0.120	100	-	3:1	0.3 g	-	Y = 92.5% C = 98.7%	[165]
5 wt% Li/MCM-41	254	9.80	90	180	3:1	5.5 wt%	-	Y = 93.14% C = 99.00%	[166]
5 wt% Co/MCM-41 – calcined at 400 °C	490	8.7	990	120	3:1	6 wt%	-	Y = 94.1% C = 98.7%	[167]
Ti/SBA-15 (Si/Ti = 4)	1000	-	87.5	240	3:1	5.5 wt%	-	Y = 82% C = 94% S = 87.17%	[169]
Mg_2Al_1/SBA-15	317	0.533	100	120	3:1	30.46 wt%	DMF	C = 78% S = 90%	[170]
0.3CaO-SBA-15	324	-	95	90	4:1	7 wt%	-	Y = 99.0%	[171]
7 wt% K/TUD-1	430	6.68	90	150	5:1	6 wt%	-	Y = 91.5% C = 98.0%	[172]
Mg_2Al_1/HMS	250	-	170	150	3:1	0.002 g/ cm^3	Methanol	Y = 83.4% C = 84.7%	[8]

Note: Y = yield of glycerol carbonate, C = conversion of glycerol, S = selectivity of glycerol carbonate, DMC = dimethyl carbonate

and a narrow pore size distribution [168]. SBA-15 catalysts doped with titanium with varying Si/Ti ratio were prepared by Devi et al. [169] using a sol-gel method. Lower Si/Ti ratios exhibited higher glycerol conversion and glycerol carbonate selectivity when compared to higher ratios. A Ti-SBA-15 catalyst prepared with a Si/Ti ratio of 4 was found to be 10 times more active than pristine SBA-15. The catalyst gave an 82% yield of glycerol carbonate after 4 h at 87.5 °C, a dimethyl carbonate to glycerol mole ratio of 3:1 and 5.5 wt% catalyst loading. LDHs with a Mg/Al ratio of 2 have also been coated on SBA-15 to give different morphologies – rice shape, short rods and long rods [170]. The rice shape morphology was found to be most active, due to a high specific surface area (317 m^2/g) and large pore volume (0.71 cm^3/g). The rice shape also gave mesoporous cavities which resulted in higher dispersibility of the LDH and glycerol. Mesoporous CaO-SBA-15 catalysts (CaO-SBA-15) and impregnation of CaO with SBA-15 (CaO/SBA-15) were reported by Zhu et al. [171] In comparison to 0.3CaO-SBA-15, the surface area and pore volume of 0.3CaO-SBA-15 are noticeably higher, reaching 324 m^2/g and 0.95 mL/g, respectively. Regarding CaO-SBA-15 samples, it was observed that the presence of Ca consistently leads to a reduction in the number of weak basic sites. Increasing Ca content can significantly increase the number of strong and medium basic sites. It was evident that CaO-SBA-15 samples showed significantly higher activity when compared to purified SBA-15 under the same conditions. The 0.3CaO-SBA-15 sample with a Ca/Si molar ratio of 0.3 was found to be the most active catalyst, producing 99.0% glycerol carbonate. Even after 5 cycles, no decrease in glycerol carbonate yield was observed. TUD-1 is another 3D mesoporous silica material which has been loaded with potassium to create a more active catalyst [172]. With loading of potassium, the surface area of TUD-1 decreased from 632 to 430 m^2/g, but both the basicity and activity increased. A loading of 7 wt% potassium provided optimal activity of the catalyst with 91.5% yield after 2.5 h at 90 °C, a dimethyl carbonate to glycerol mole ratio of 5:1 and 6 wt% catalyst loading.

Hexagonal mesoporous silica (HMS) was used as a support for a calcined hydrotalcite with an Al/Mg ratio of 1:2 [8]. The presence of the HMS silica support increased the surface area of the catalyst, however there was some neutralization of basic sites observed. An Al/Mg ratio of 1:2 was found to be most optimum, giving 84.7% glycerol conversion and 83.4% glycerol carbonate yield after 2.5 h at 170 °C, a dimethyl carbonate to glycerol mole ratio of 3:1, 0.002 g/cm^3 catalyst loading and 20 cm^3 methanol.

3.3.7. Zeolites

Zeolites are 3D frameworks typically consisting of SiO_4 and AlO_4 tetrahedra, which are linked at their corners via a common oxygen atom [173]. Pan et al. [174] reported the use of Na-based zeolites as catalysts for the transesterification of glycerol. Using a variety of zeolite catalysts, it was found that smaller pore zeolites such as 3 A, 4 A and NaZSM-5

(consisting of 8 or 10 numbered ring-structured pore channels) were inactive for the reaction. Larger pore zeolites such as NaY and Naβ were more active giving 80% and 37% glycerol conversion, respectively. The poor active was attributed to the small pore size, which restricted the formation of glycerol carbonate. NaY was particularly active due to its larger pore size (0.74 ×0.74 nm) when compared with geometric parameter of glycerol (0.47 nm in diameter and 0.52 nm in length) and DMC (0.37 nm in diameter and 0.45 nm in length) and it had greater number of basic sites (4.2 mmol/g). NaY with bigger pore channel allows for the entrance and diffusion of both reactants, and desired product, resulting in an excellent performance. Methanol was found to enhance glycerol carbonate when compared to a solvent free reaction, and other solvents such as DMSO, DMF and ethanol.

The activity of zeolites can be improved through incorporation of more active species. ETS-10 which is a titanosilicate molecular sieve with a 3D 12-ring structure can be promoted through the incorporation of transition metals [175]. The effect of a porous structure was investigated through the preparation of METS-10, which is a hierarchical porous ETS-10. The introduction of hierarchical pores was found to improve the catalyst activity from ETS-10 and provided a more stable catalyst upon reuse. M3ETS-10 was found to be the most active of the hierarchical catalysts with the largest pore size distribution of 7 nm. Out of the transition metals tested nickel was found to be the most active followed by zinc, manganese, iron, cobalt and finally copper. The Lewis basic sites (TiO_6^{2-}) were found to be enhanced by the presence of Ni^0 species. Incorporation of a 5% nickel loading was found to enhance basicity without a serious loss of zeolite crystallinity yielding 97.1% yield of glycerol carbonate after 2 h at 90 °C, a dimethyl carbonate to glycerol mole ratio of 2:1 and 0.125 g catalyst loading.

Similarly, MgO can be incorporated into the structure of zeolitic imidazolate framework-8 (ZIF-8) [176]. Loading MgO into ZIF-8, did not affect the structure and well dispersed MgO nanoparticles were observed. MgO incorporated ZIF-8 was found to be more active than MgO or ZIF-8. A 50 wt% loading of MgO yielded 21.1 mmol of glycerol carbonate per gram of catalyst after 2 h at 75 °C, a dimethyl carbonate to glycerol mole ratio of 4:1 and 0.2 g catalyst loading.

BPH-type zeolite (Linde Q) was synthesised using hydrothermal treatment with different Si/Al ratios to produce two different size of catalyst; nano-sized and micro-sized [177]. In their study, Kosawatthanakun et al. [177] observed that the nano-sized CsBPH_AP exhibited better efficiency in comparison to the micron-sized KBPH_AP. The ion-exchange process of the BPH-type zeolite, using potassium and cesium, provided similar thermal properties to the parent samples. However, there were differences in terms of basicity and catalytic activity. The catalytic activity of the nano-sized CsBPH_AP, with a catalyst loading of 6 wt%, was found good performance over four runs at 120 °C for 3 h.(Table 17).

3.3.8. Enzymes

Enzymes are known as biological catalysts, or biocatalysts, and consist of 3D structured proteins. Whilst enzymes can catalyst the reaction without being supported [178], the immobilisation of enzymes on a physical support can provide ease of separation and also act as a prevention against denaturation. Kim et al. [179] first reported the use of an immobilised lipase B from *C. antarctica* (Novozym 435). Novozym 435 was found to be most effective out of a range of enzymes tested. Similarly, *C. antarctica* lipase B could be immobilised on magnetic organosilica nanoflowers [180]. A 88.6% glycerol carbonate yield was achieved after 24 h at 50 °C, a dimethyl carbonate to glycerol mole ratio of 20:1, 5 g/L catalyst loading and 0.2 g of molecular sieves.

Tudorache et al. [181] reported the immobilisation of the lipase *Aspergillus niger* on magnetic particles. It was found that the support composition affected the activity of the supported enzyme. Nanoparticles of magnetic Fe_3O_4 functionalized with silicone derivatives with $-NH_2$ terminal groups were found to be most active. The immobilisation of the enzyme resulted in a catalyst which was stable for fifteen reaction cycles (90 h reaction time) whereas free enzymes were only stable for 4 cycles (16 h reaction time). *Aspergillus niger* can also be cross-linked onto magnetic particles using glutaraldehyde as a cross-linker [182]. A 55% glycerol carbonate yield could be achieved after 6 h at 60 °C, a dimethyl carbonate to glycerol mole ratio of 10:1 and 5 wt% catalyst loading. The catalyst also exhibited excellent stability over 20 successive reaction cycles. This was further investigated by Tudorache et al. [183]. The immobilised catalyst had a higher TON than the homogeneous with 20.4 × 105 and 4.64 × 105 respectively. Again, the catalyst exhibited good recyclability over 15 reaction cycles, and could be recovered through use of a magnetic field.

3.3.9. Waste sources

In an effort to promote a more circular economy, production of catalysts from waste sources can repurpose waste into more useful substances and improve the economics of a chemical process.

Das and Mohanty [184] reported the use red mud, which is a waste product from the production of alumina from bauxite. The composition of red mud was mainly hematite phase (Fe_2O_3) with smaller amounts of NaO, CaO, Al_2O_3, SiO_2 and TiO_2. A moderate basic strength was found to be desirable to prevent decomposition of glycerol carbonate to glycidol. The red mud catalyst calcined at 500 °C gave a 92.09% glycerol carbonate yield after 90 min at 90 °C, a dimethyl carbonate to glycerol mole ratio of 3:1 and 12.5 wt% catalyst loading. The promotional effects of potassium, strontium and magnesium on red mud were then investigated [185]. Potassium doped red mud showed both higher activity and stability, when compared to magnesium and strontium doped. A 30 wt% potassium doped red mud had the highest activity and stability, attributed to a high surface concentration of K_2O. Glycerol carbonate yield could be increased to 93.27% with a lower loading of 10 wt%

Table 17
Physical properties and performance of different zeolites catalysts for the transesterification of glycerol with DMC.

Catalyst	Physical properties		Operating parameter					Performance	Ref
	BET surface area (m^2/g)	Total basic site amount (mmol CO_2/g catalyst)	Temp (°C)	Time (min)	Mole Ratio of DMC to glycerol	Catalyst loading	Solvent		
NaY	-	4.2	70	240	3:1	10 wt%	Methanol	C = 80% S = 99%	[174]
Naβ	-	0.64	70	240	3:1	10 wt%	Methanol	C = 37%	[174]
5 wt% Ni/M_3ETS-10	298.5	-	90	120	2:1	0.125 g	-	Y = 97.1% C = 97.7%	[175]
50 wt% MgO/ZIF-8	650	-	75	120	4:1	0.2 g	-	Y = 21.1 mmol/g	[176]
Nano-sized CsBPH_AP ($Cs_{4.2}K_{2.3}Na_{5.5}$) $Si_{16}Al_{12}O_{56}$	196	0.130	120	180	5:1	6 wt%	-	Y = 80% C = 83% S = 96%	[177]

Note: Y = yield of glycerol carbonate, C = conversion of glycerol, S = selectivity of glycerol carbonate, DMC = dimethyl carbonate

catalyst.

Ladle furnace steel slag is another industrial process waste which can be converted into an active catalyst [186]. The composition was mainly $Ca(OH)_2$, $CaCO_3$, CaO and $CaSiO_3$. The steel slag was impregnated with NaOH to increase the basicity, but NaOH was also found to stabilize the leaching of CaO in the catalyst. A 10 wt% loading of NaOH gave 97% yield after 90 min at 75 °C, a dimethyl carbonate to glycerol mole ratio of 2:1 and 3 wt% catalyst loading. Similarly Okoye et al. [187] reported the use of oil palm fuel ash obtained from the burning of oil palm. Calcined at 600 °C the catalyst consists of K_2MgSiO_4, $MgSiO_3$ and $KAlSiO_4$ phases. Deactivation could be attributed to the leaching of magnesium, silica and potassium from the catalyst upon reuse.

Municipal waste such as disposable baby diaper waste has been reported by Wang et al. [188]. The superabsorbent polymer present in the waste was carbonized at 200 to 600 °C under a nitrogen flow. It was found that temperatures greater than 400 °C resulted in thermal decomposition to Na_2CO_3, with 500 and 600 °C having a higher basicity due to increased amounts of Na_2CO_3. A calcination temperature of 500 °C was found to be most effective due to the reduced calcination temperature and appropriate level of basicity.

Food waste is an abundant source of waste material to synthesis catalysts. Corncob can be calcined at 500 °C to produce an effective catalyst [189]. The catalyst is composed mainly of carbon material with alkaline mineral salts. The catalyst was not stable however, due to the leaching of potassium carbonate. Wang et al. [190] reported the use of calcined waste crayfish shell. Chitin and calcium carbonate composed the bulk of the catalyst, with CaO composition increasing with calcination temperature. A calcination temperature of 800 °C gave the best catalyst due to formation of a mainly CaO phase. Olivares et al. [191] also reported the calcination of CaO catalyst from snail shell (*Achatina fulica* sp.) at 900 °C for 4 h under air flow (SNS-900 °C). By reacting SNS-900 °C with Na_3PO_4, an apatite-like catalyst (snail shell apatite, SNS-AP) with a Ca/P ratio of 1.61 was produced. The findings indicated that the catalyst's basicity was increased. Consequently, a glycerol conversion of approximately 94.54% and a glycerol carbonate yield of 96.5% were achieved under optimal reaction conditions of 80 °C for 90 min. Empty fruit bunch can also be activated through calcination [192]. Increasing calcination temperature was found to induce a phase transition from $KAlSiO_4$ to $K_2Mg(SiO_4)$ resulting in increased basic strength and number of basic sites, with 500 °C the optimum calcination temperature. Deactivation of the catalyst was attributed to phase change from $MgSiO_3$ and $K_2Mg(SiO_4)$ to $KAlSiO_4$, $K_2Mg(SiO_4)$ and $CaAl_2SiO_6$ upon reuse. *Musa acuminita* (a species of banana) peel can be burned in open air to produce an active ash [101]. Composed of mainly K_2O with minor components of SiO_2, CaO and MgO. The catalyst was mesoporous in nature with a high surface area and high basicity. The peel of Fresh *Mangifera indica* (mango) can be activated by through calcination, resulting in the production of *Mangifera indica* peel calcined ash (MIPCA) [193]. The MIPCA sample exhibited a high amount of potassium (K) element, with potassium oxide (K_2O) being the primary metal oxide responsible for basic strength to the catalyst. Moreover, MIPCA exhibits a significant amount of CaO and MgO, which possess highly basic properties, hence enhancing its catalytic efficiency. In contrast, the utilisation of microwave-assisted reaction using MIPCA as a catalyst showed a conversion of 98.1%.

Biochars can be produced through the pyrolysis of fish scale and cow dung [194]. Cow dung exhibited higher activity than that of fish scales, with optimum calcination values of 600 and 650 °C respectively. The activity of fish scales could be improved through modification with KF.

3.3.10. Others

Hydroxyapatite ($Ca_{10}(PO_4)_6(OH)_2$) is a mineral which is the main component of bones and teeth. Bai et al. [195] reported the modification of hydroxyapatite prepared by a precipitation method with metal salts such as potassium, lanthanum, zirconium, lithium, cerium and potassium fluoride. Potassium fluoride modified hydroxyapatite was the most active out of the metals tested, with comparable activity to homogeneous KF with a longer reaction time of 2 h compared to 50 min. KF modified hydroxyapatite could be encapsulated on spherical γ-Fe_2O_3 nanoparticles to improve catalyst separation [196]. Again, KF proved most active out of sodium fluoride, potassium carbonate, sodium bicarbonate, cesium carbonate and lanthanum nitrate. CTAB used during synthesis was found to improve the wettability of the catalyst, improving the catalyst contact with the reactants.

Chai et al. [197] reported the use of a covalent organic framework (COF) which was then modified with a N-Heterocyclic carbene (NHC) moiety. A COF of BMIM4FPy modified with $NaCO_3$ provided an active catalyst for the transesterification reaction. A 96% yield could be obtained after 8 h at 70 °C, a dimethyl carbonate to glycerol mole ratio of 3:1 and 5 mol% catalyst loading.

The polyamine DABCO was found to have the highest activity of PMDTA, TMEDA and DMAP [198]. Interactions between the hydroxyls of glycerol and the Cl^- of the immobilised resin led to high activity of the catalyst. Wan et al. [199] found that higher mass fractions of DABCO lead to more hydrophilic polymers with excellent wettability. The high surface area and hierarchical porosity of the catalyst lead to easily accessible catalytic sites for glycerol and DMC.(Table 18).

4. Conclusions and future perspectives

CO_2 concentration in the atmosphere is a global crisis. Transitioning from conventional fuel to green fuel is an effective method of reducing CO_2 emissions. Biodiesel exhibits greater efficacy in reducing carbon dioxide (CO_2) and CO emissions when compared to conventional transport fuels. People become more concerned about environmental issues when biodiesel has been used, leading to increase its production. In fact, biodiesel production continues to emit carbon dioxide into the atmosphere and produces large amounts of glycerol. There are several carbon capture methods which have been used in recent years. It is noteworthy that the process of decreasing CO_2 concentration and enhancing value of glycerol to glycerol carbonate could potentially serve as an effective method for carbon capture due to the utilisation of glycerol carbonate to synthesis value-added compounds, providing commercial and industrial importance. In addition, its biodegradable, edible, non-toxic, and sustainable, glycerol carbonate also has the capacity to be manufactured in large volumes. Nowadays, the increasing acceptance of the potential of glycerol carbonate as a chemical agent has been utilised to enhance a variety of industrial processes. Furthermore, CO_2 is a non-flammable, and inexpensive carbon-oxygen source that can be employed to produce reactants in the glycerol carbonate synthesis process. After the thorough literature review, the important points that require consideration can be summarised as follows:

- The main challenge in the process of direct carbonation glycerol with CO_2 is the synthesis of a suitable catalyst that exhibits high selectivity, activity, and thermal stability. This reaction is limited by thermodynamics, leading to a low production yield that might not support scaling up. To address this limitation, catalysts with excellent properties and dehydrating agents, have been suggested to shift the equilibrium towards glycerol carbonate. The utilisation of heterogeneous catalysts is favoured over homogeneous catalysts due to the ease of recovery and reuse. Nanostructured materials seem to be the most promising catalysts owing to their notably increased surface area. Three main suggestions are required to further improve the catalytic performance and increase the feasibility of using the direct reaction route while maintaining environment friendliness. The first point is dual-functional materials, that consist of basic metal oxides with high dispersion and basicity. These basic metal oxides are doped onto a supporter that has a large surface area which has more active site to alter the reaction. The second point is deep eutectic solvents, which are environmentally friendly solvents, have the ability to absorb carbon dioxide. And the third option is reaction

Table 18
Physical properties and performance of different enzyme, waste source and other catalysts for the transesterification of glycerol with DMC.

Catalyst	Physical properties		Operating parameter					Performance	Ref
	BET surface area (m^2/g)	Total basic site amount (mmol CO_2/g catalyst)	Temp (°C)	Time (min)	Mole Ratio of DMC to glycerol	Catalyst loading	Solvent		
Enzymes									
CALB/magnetic organosilica	-	-	50	24 h	20:1	5 g/L	-	Y = 88.66% C = 94.24% S = 94.13%	[180]
Aspergillus niger/ Fe_3O_4	-	-	60	360	10:1	5 wt%	-	Y = 55% C = 61% S = 90%	[182]
Waste Sources									
Red Mud – Calcined at 500 °C	21.967	32.10	90	90	3:1	12.5 wt %	-	Y = 92.02% C = 95.21% S = 96.64%	[184]
30 wt% K/Red Mud	1.36	33.1	75	90	3:1	10 wt%	-	Y = 93.27% C = 96.8%	[185]
10 wt% NaOH/ Ladle Furnace Steel Slag	29.92	39.60	75	90	2:1	3 wt%	-	Y = 97% C = 99%	[186]
Oil Palm Fuel Ash – Calcined at 600 °C	5.12	12.60	80	112	5:1	5 wt%	-	Y = 94.5% C = 95.03%	[187]
Disposable Baby Diaper Waste	1.1	15.5	75	60	4:1	2 wt%	-	Y = 93.6% C = 95.6% S = 97.9%	[188]
Corncob – Calcined at 500 °C	3.08	8.8	80	90	3:1	3 wt%	-	Y = 94.1% C = 98.1%	[189]
Crayfish Shell – Calcined at 800 °C	13.1	20.4	75	90	6:1	4 wt%	-	Y = 95.3% C = 98.7%	[190]
Catalyst	Physical properties		Operating parameter					Performance	Ref
	BET surface area (m^2/g)	Total basic site amount (mmol CO_2/g catalyst)	Temp (°C)	Time (min)	Mole Ratio of DMC to glycerol	Catalyst loading	Solvent		
Apatite-like catalyst (snail shell apatite, SNS-AP)	-	36.65	80	90	4:1	5 wt%	-	Y = 94.54%	[191]
Empty Fruit Bunch Ash	7	3.38	90	45	3:1	5 wt%	-	Y = 95.65% C = 96.15%	[192]
Musa acuminata Peel - Microwave	539	0.169	75	15	2:1	6 wt%	-	Y = 99.5%	[101]
Magnifera indica peel - Microwave	3.985	-	80	50	3:1	6 wt%	-	C = 98.1% S = 100%	[193]
Cow Dung Biochar	111	3.40	85	90	2:1	3 wt%	-	Y = 97.1% C = 100%	[194]
3 wt% KF/Fish Scale Biochar	117	2.74	85	60	2:1	2 wt%	-	Y = 99.6% C = 100%	[194]
Others									
15 wt% KF/ Hydroxyapatite	10.8	-	78	120	2:1	3 wt%	-	Y = 99% C = 99.3%	[195]
KF-/HAP-γ-Fe_2O_3	-	-	85	150	5:1	5 wt%	-	Y = 97.5% C = 98.3%	[196]
$NaCO_3$/BMIM4F-Py-COF	13256	-	70	480	3:1	5 mol%	-	Y = 96% C = 99%	[197]
([p-DABCO]Cl)	-	-	80	60	2:1	1 wt%	-	Y = 92.5% C = 94.1% S = 98.3%	[198]
P(DVB-DABCO)– 0.4	412	1.54	85	60	3:1	1.5 mol %	-	Y = 95%	[199]

Note: Y = yield of glycerol carbonate, C = conversion of glycerol, S = selectivity of glycerol carbonate, DMC = dimethyl carbonate

engineering solutions, which involve using reactor designs, such as membrane reactors, to increase the rate of a chemical reaction by driving reaction equilibrium through the removal of water.

- Carbonation of glycerol with urea and transesterification of glycerol with alkyl carbonates are both effective processes. In order to further develop the glycerol with urea reaction pathway, it is needed to consider the NH_3 removal process. While it is true that CO_2 has the potential to convert ammonia to urea. Urea is the most often utilised as a nitrogen fertiliser. The manufacture of urea from NH_3 and CO_2 process necessitates the use of high temperatures and pressures. The implementation of an alternative heat source or waste heat recovery system has the potential to make it economically feasible. Furthermore, the amount of ammonia produced is minimal in comparison to the capacity of urea plant; therefore, combining this reaction with other chemical units that consume NH_3 may be one possible solution.
- For transesterification glycerol with DMC, most of research focus on the development of new catalysts that exhibit great catalytic performance, resulting in high yield of glycerol carbonate, particularly heterogeneous catalyst. In addition to catalyst efficiency studies, technological economic analysis should be further investigated so that the glycerol carbonate production process can be operated on an industrial scale.

- Therefore, the process exhibits a possibility for achieving greatly high glycerol carbonate yield. The reaction takes place between the immiscible reactants of hydrophilic glycerol and a hydrophobic carbonate source, could happen in a prolonged reaction time and need a larger amount of catalyst. Furthermore, it is necessary for further study on microwave reactors due to their potential to enhance the efficiency of reaction heating. Despite being presented as a highly efficient technique that greatly reduces reaction time, reactions usually are operated on a small scale. The heating process of a microwave reactor relies on the alteration of dielectric characteristics caused by the motion of electromagnetic fields. However, the use of solid catalysts, particularly heterogeneous catalysts, can lead to the build-up of heat inside these materials, resulting in overheating or the creation of hot spots. Furthermore, the chemicals employed in the procedure possess different characteristics regarding their penetration depth, which depend on the solvent temperature. When scaling up and designing a reactor, it is necessary to consider these factors for maintaining uniform heat distribution and enhancing the efficiency of the catalyst.

CRediT authorship contribution statement

Artioli Nancy: Writing – review & editing. **Manyar Haresh:** Conceptualization, Funding acquisition, Supervision, Writing – review & editing. **Inrirai Patcharaporn:** Writing – original draft. **Keogh John:** Writing – original draft. **Centeno-Pedrazo Ander:** Writing – original draft.

Declaration of Competing Interest

The authors declare that they have no known competing financial interests or personal relationships that could have appeared to influence the work reported in this paper.

Data Availability

Data will be made available on request.

Acknowledgements

The Authors gratefully acknowledge the financial support for PhD scholarship to PI funded by the royal Thai government. HM thankfully acknowledges the funding and support provided by the Leverhulme Trust research grant RPG-2020-301, as well as the UK Catalysis hub via our membership of the UK Catalysis Hub Consortium funded by EPSRC grant: EP/R026645/1.

References

[1] A. Mukhtar, S. Saqib, H. Lin, M.U. Hassan Shah, S. Ullah, M. Younas, M. Rezakazemi, M. Ibrahim, A. Mahmood, S. Asif, A. Bokhari, Current status and challenges in the heterogeneous catalysis for biodiesel production, Renew. Sust. Energ. Rev. 157 (2022) 112012, https://doi.org/10.1016/j.rser.2021.112012.

[2] Y. Zhang, L. Duan, H. Esmaeili, A review on biodiesel production using various heterogeneous nanocatalysts: operation mechanisms and performances, Biomass-.-. Bioenergy 158 (2022) 106356, https://doi.org/10.1016/j.biombioe.2022.106356.

[3] Z. Liu, Z. Deng, S. Davis, P. Ciais, Monitoring global carbon emissions in 2022, Nat. Rev. Earth Env. 4 (4) (2023) 205–206, https://doi.org/10.1038/s43017-023-00406-z.

[4] M. Hajjari, M. Tabatabaei, M. Aghbashlo, H. Ghanavati, A review on the prospects of sustainable biodiesel production: a global scenario with an emphasis on waste-oil biodiesel utilization, Renew. Sust. Energ. Rev. 72 (2017) 445–464, https://doi.org/10.1016/j.rser.2017.01.034.

[5] A.A. Babadi, S. Rahmati, R. Fakhlaei, B. Barati, S. Wang, W. Doherty, K. Ostrikov, Emerging technologies for biodiesel production: processes, challenges, and opportunities, Biomass-.-. Bioenergy 163 (2022) 106521, https://doi.org/10.1016/j.biombioe.2022.106521.

[6] N. Mahbub, E. Gemechu, H. Zhang, A. Kumar, The life cycle greenhouse gas emission benefits from alternative uses of biofuel coproducts, Sustain. Energy Technol. 34 (2019) 173–186, https://doi.org/10.1016/j.seta.2019.05.001.

[7] J.R. Ochoa-Gómez, O. Gómez-Jiménez-Aberasturi, C. Ramírez-López, M. Belsué, A brief review on industrial alternatives for the manufacturing of glycerol carbonate, a green chemical, Org. Process Res. Dev. 16 (3) (2012) 389–399, https://doi.org/10.1021/op200369v.

[8] G.D. Yadav, P.A. Chandan, A green process for glycerol valorization to glycerol carbonate over heterogeneous hydrotalcite catalyst, Catal. Today 237 (2014) 47–53, https://doi.org/10.1016/j.cattod.2014.01.043.

[9] H.W. Tan, A.R. Abdul Aziz, M.K. Aroua, Glycerol production and its applications as a raw material: a review, Renew. Sust. Energ. Rev. 27 (2013) 118–127, https://doi.org/10.1016/j.rser.2013.06.035.

[10] S. Sahani, S.N. Upadhyay, Y.C. Sharma, Critical review on production of glycerol carbonate from byproduct glycerol through transesterification, Ind. Eng. Chem. Res. 60 (1) (2021) 67–88, https://doi.org/10.1021/acs.iecr.0c05011.

[11] P. de Caro, M. Bandres, M. Urrutigoïty, C. Cecutti, S. Thiebaud-Roux, Recent progress in synthesis of glycerol carbonate and evaluation of its plasticizing properties, Front. Chem. 7 (2019), https://doi.org/10.3389/fchem.2019.00308.

[12] G. Galletti, P. Prete, S. Vanzini, R. Cucciniello, A. Fasolini, J. De Maron, F. Cavani, T. Tabanelli, Glycerol carbonate as a versatile alkylating agent for the synthesis of β-aryloxy alcohols, ACS Sustain. Chem. Eng. 10 (33) (2022) 10922–10933, https://doi.org/10.1021/acssuschemeng.2c02795.

[13] M. Delarmelina, G. Deshmukh, A. Goguet, C.R.A. Catlow, H. Manyar, Role of sulfation of zirconia catalysts in vapor phase ketonization of acetic acid, J. Phys. Chem. C. 125 (50) (2021) 27578–27595, https://doi.org/10.1021/acs.jpcc.1c06920.

[14] J. Ethiraj, D. Wagh, H. Manyar, Advances in upgrading biomass to biofuels and oxygenated fuel additives using metal oxide catalysts, Energy Fuels 36 (3) (2022) 1189–1204, https://doi.org/10.1021/acs.energyfuels.1c03346.

[15] K. Pandit, C. Jeffrey, J. Keogh, M.S. Tiwari, N. Artioli, H.G. Manyar, Techno-economic assessment and sensitivity analysis of glycerol valorization to biofuel additives via esterification, Ind. Eng. Chem. Res. 62 (23) (2023) 9201–9210, https://doi.org/10.1021/acs.iecr.3c00964.

[16] J. Keogh, C. Jeffrey, M.S. Tiwari, H. Manyar, Kinetic analysis of glycerol esterification using tin exchanged tungstophosphoric acid on K-10, Ind. Eng. Chem. Res. (2022), https://doi.org/10.1021/acs.iecr.2c01930.

[17] M.S. Tiwari, D. Wagh, J.S. Dicks, J. Keogh, M. Ansaldi, V.V. Ranade, H. G. Manyar, Solvent free upgrading of 5-hydroxymethylfurfural (HMF) with levulinic acid to HMF levulinate using tin exchanged tungstophosphoric acid supported on K-10 catalyst, ACS Org. Inorg. Au 3 (1) (2023) 27–34, https://doi.org/10.1021/acsorginorgau.2c00027.

[18] G.D. Yadav, H.G. Manyar, Synthesis of a novel redox material UDCaT-3: an efficient and versatile catalyst for selective oxidation, hydroxylation and hydrogenation reactions, Adv. Synth. Catal. 350 (14-15) (2008) 2286–2294, https://doi.org/10.1002/adsc.200800313.

[19] I.J. McManus, H. Daly, H.G. Manyar, S.F.R. Taylor, J.M. Thompson, C. Hardacre, Selective hydrogenation of halogenated arenes using porous manganese oxide (OMS-2) and platinum supported OMS-2 catalysts, JFaraday Discuss. 188 (2016) 451–466, https://doi.org/10.1039/C5FD00227C.

[20] T. Jakubek, K. Ralphs, A. Kotarba, H. Manyar, Nanostructured potassium-manganese oxides decorated with Pd nanoparticles as efficient catalysts for low-temperature soot oxidation, Catal. Lett. 149 (1) (2019) 100–106, https://doi.org/10.1007/s10562-018-2585-z.

[21] J. Salisu, N. Gao, C. Quan, J. Yanik, N. Artioli, Co-gasification of rice husk and plastic in the presence of CaO using a novel ANN model-incorporated Aspen plus simulation, J. Energy Inst. 108 (2023) 101239, https://doi.org/10.1016/j.joei.2023.101239.

[22] C. Quan, G. Zhang, N. Gao, S. Su, N. Artioli, D. Feng, Behavior study of migration and transformation of heavy metals during oily sludge pyrolysis, Energy Fuels 36 (15) (2022) 8311–8322, https://doi.org/10.1021/acs.energyfuels.2c01283.

[23] E.L. Byrne, R. O'Donnell, M. Gilmore, N. Artioli, J.D. Holbrey, M. Swadźba-Kwaśny, Hydrophobic functional liquids based on trioctylphosphine oxide (TOPO) and carboxylic acids, Phys. Chem. Chem. Phys. 22 (42) (2020) 24744–24763, https://doi.org/10.1039/D0CP02605K.

[24] L. Castoldi, R. Matarrese, L. Kubiak, M. Daturi, N. Artioli, S. Pompa, L. Lietti, In-depth insights into N_2O formation over Rh- and Pt-based LNT catalysts, Catal. Today 320 (2019) 141–151, https://doi.org/10.1016/j.cattod.2018.01.026.

[25] M.T. Yilleng, E.C. Gimba, G.I. Ndukwe, I.M. Bugaje, D.W. Rooney, H.G. Manyar, Batch to continuous photocatalytic degradation of phenol using TiO_2 and Au-Pd nanoparticles supported on TiO_2, J. Environ. Chem. Eng. 6 (5) (2018) 6382–6389, https://doi.org/10.1016/j.jece.2018.09.048.

[26] R. O'Donnell, K. Ralphs, M. Grolleau, H. Manyar, N. Artioli, Doping manganese oxides with ceria and ceria zirconia using a one-pot sol–gel method for low temperature diesel oxidation catalysts, Top. Catal. 63 (3) (2020) 351–362, https://doi.org/10.1007/s11244-020-01250-x.

[27] N. Rozulan, S.A. Halim, N. Razali, S.S. Lam, A review on direct carboxylation of glycerol waste to glycerol carbonate and its applications, Biomass-.-. Convers. Bior. 12 (10) (2022) 4665–4682, https://doi.org/10.1007/s13399-022-02540-y.

[28] S. Lukato, G.N. Kasozi, B. Naziriwo, E. Tebandeke, Glycerol carbonylation with CO_2 to form glycerol carbonate: a review of recent developments and challenges, Curr. Res. Green. Sustain. Chem. 4 (2021) 100199, https://doi.org/10.1016/j.crgsc.2021.100199.

[29] M.O. Sonnati, S. Amigoni, E.P. Taffin de Givenchy, T. Darmanin, O. Choulet, F. Guittard, Glycerol carbonate as a versatile building block for tomorrow: synthesis, reactivity, properties and applications, Green. Chem. 15 (2) (2013) 283–306, https://doi.org/10.1039/C2GC36525A.

[30] S. Christy, A. Noschese, M. Lomelí-Rodriguez, N. Greeves, J.A. Lopez-Sanchez, Recent progress in the synthesis and applications of glycerol carbonate, Curr.

Opin. Green. Sustain. Chem. 14 (2018) 99–107, https://doi.org/10.1016/j.cogsc.2018.09.003.
[31] G.E. Rossi, J.M. Winfield, N. Meyer, D.H. Jones, R.H. Carr, D. Lennon, Phosgene formation via carbon monoxide and dichlorine reaction over an activated carbon catalyst: towards a reaction model, Appl. Catal. A. 609 (2021) 117900, https://doi.org/10.1016/j.apcata.2020.117900.
[32] F. Barzagli, F. Mani, M. Peruzzini, From greenhouse gas to feedstock: formation of ammonium carbamate from CO_2 and NH_3 in organic solvents and its catalytic conversion into urea under mild conditions, Green. Chem. 13 (5) (2011) 1267–1274, https://doi.org/10.1039/C0GC00674B.
[33] J. Ding, R. Ye, Y. Fu, Y. He, Y. Wu, Y. Zhang, Q. Zhong, H.H. Kung, M. Fan, Direct synthesis of urea from carbon dioxide and ammonia, Nat. Commun. 14 (1) (2023) 4586, https://doi.org/10.1038/s41467-023-40351-5.
[34] K. Kohli, B.K. Sharma, C.B. Panchal, Dimethyl carbonate: review of synthesis routes and catalysts used, Energies 15 (14) (2022) 5133, https://doi.org/10.3390/en15145133.
[35] A. Dibenedetto, A. Angelini, M. Aresta, J. Ethiraj, C. Fragale, F. Nocito, Converting wastes into added value products: from glycerol to glycerol carbonate, glycidol and epichlorohydrin using environmentally friendly synthetic routes, Tetrahedron 67 (6) (2011) 1308–1313, https://doi.org/10.1016/j.tet.2010.11.070.
[36] Y. Li, H. Liu, Z. Zheng, Z. Fu, D. He, Q. Zhang, Synthesis of glycerol carbonate via alcoholysis of urea with glycerol: current status and future prospects, Ind. Eng. Chem. Res. 61 (17) (2022) 5698–5711, https://doi.org/10.1021/acs.iecr.2c00667.
[37] S.M. Gade, V.B. Saptal, B.M. Bhanage, Perception of glycerol carbonate as green chemical: synthesis and applications, Catal. Commun. 172 (2022) 106542, https://doi.org/10.1016/j.catcom.2022.106542.
[38] J. Gao, J.-W. Yang, T. Ma, J. Wang, D. Xia, B. Du, Y. Cui, C. Yang, Mechanism study on direct synthesis of glycerol carbonate from CO_2 and glycerol over shaped CeO2 model catalysts, Chin. Chem. Lett. 34 (12) (2023) 108395, https://doi.org/10.1016/j.cclet.2023.108395.
[39] A. Kojčinović, B. Likozar, M. Grilc, Heterogeneous catalytic materials for carboxylation reactions with CO_2 as reactant, J. CO_2 Util. 66 (2022) 102250, https://doi.org/10.1016/j.jcou.2022.102250.
[40] J. Liu, Y. Li, H. Liu, D. He, Transformation of CO_2 and glycerol to glycerol carbonate over CeO_2ZrO_2 solid solution —— effect of Zr doping, Biomass-.-. Bioenergy 118 (2018) 74–83, https://doi.org/10.1016/j.biombioe.2018.08.004.
[41] L.P. Ozorio, C.J.A. Mota, Direct carbonation of glycerol with CO_2 catalyzed by metal oxides, ChemPhysChem 18 (22) (2017) 3260–3265, https://doi.org/10.1002/cphc.201700579.
[42] X. Su, W. Lin, H. Cheng, C. Zhang, Y. Wang, X. Yu, Z. Wu, F. Zhao, Metal-free catalytic conversion of CO_2 and glycerol to glycerol carbonate, Green. Chem. 19 (7) (2017) 1775–1781, https://doi.org/10.1039/C7GC00260B.
[43] Y. Li, H. Liu, L. Ma, J. Liu, D. He, Transforming glycerol and CO_2 into glycerol carbonate over $La_2O_2CO_3$–ZnO catalyst — a case study of the photo-thermal synergism, Catal. Sci. Technol. 11 (3) (2021) 1007–1013, https://doi.org/10.1039/D0CY01821J.
[44] J. Liu, D. He, Transformation of CO_2 with glycerol to glycerol carbonate by a novel $ZnWO_4$-ZnO catalyst, J. CO_2 Util. 26 (2018) 370–379, https://doi.org/10.1016/j.jcou.2018.05.025.
[45] N. Kulal, R. Vetrivel, N.S. Ganesh Krishna, G.V. Shanbhag, Zn-Doped CeO_2 Nanorods for Glycerol Carbonylation with CO_2, ACS Appl. Nano Mater. 4 (5) (2021) 4388–4397, https://doi.org/10.1021/acsanm.0c03166.
[46] L. Lei, Y. Wang, Z. Zhang, J. An, F. Wang, Transformations of Biomass, Its Derivatives, and Downstream Chemicals over Ceria Catalysts, ACS Catal. 10 (15) (2020) 8788–8814, https://doi.org/10.1021/acscatal.0c01900.
[47] Y. Shan, Y. Liu, Y. Li, W. Yang, A review on application of cerium-based oxides in gaseous pollutant purification, Sep. Purif. Technol. 250 (2020) 117181, https://doi.org/10.1016/j.seppur.2020.117181.
[48] X. Huang, K. Zhang, B. Peng, G. Wang, M. Muhler, F. Wang, Ceria-Based Materials for Thermocatalytic and Photocatalytic Organic Synthesis, ACS Catal. 11 (15) (2021) 9618–9678, https://doi.org/10.1021/acscatal.1c02443.
[49] P. Priecel, J.A. Lopez-Sanchez, Advantages and Limitations of Microwave Reactors: From Chemical Synthesis to the Catalytic Valorization of Biobased Chemicals, ACS Sustain. Chem. Eng. 7 (1) (2019) 3–21, https://doi.org/10.1021/acssuschemeng.8b03286.
[50] J. Liu, Y. Li, J. Zhang, D. He, Glycerol carbonylation with CO_2 to glycerol carbonate over CeO_2 catalyst and the influence of CeO_2 preparation methods and reaction parameters, Appl. Catal., A. 513 (2016) 9–18, https://doi.org/10.1016/j.apcata.2015.12.030.
[51] H. Li, D. Gao, P. Gao, F. Wang, N. Zhao, F. Xiao, W. Wei, Y. Sun, The synthesis of glycerol carbonate from glycerol and CO_2 over $La_2O_2CO_3$–ZnO catalysts, Catal. Sci. Technol. 3 (10) (2013) 2801–2809, https://doi.org/10.1039/C3CY00335C.
[52] H. Li, X. Jiao, L. Li, N. Zhao, F. Xiao, W. Wei, Y. Sun, B. Zhang, Synthesis of glycerol carbonate by direct carbonylation of glycerol with CO_2 over solid catalysts derived from Zn/Al/La and Zn/Al/La/M (M = Li, Mg and Zr) hydrotalcites, Catal. Sci. Technol. 5 (2) (2015) 989–1005, https://doi.org/10.1039/C4CY01237B.
[53] C. Hu, C.-W. Chang, M. Yoshida, K.-H. Wang, Lanthanum nanocluster/ZIF-8 for boosting catalytic CO_2/glycerol conversion using $MgCO_3$ as a dehydrating agent, J. Mater. Chem. A 9 (11) (2021) 7048–7058, https://doi.org/10.1039/D0TA12413C.
[54] J. Zhang, D. He, Surface properties of Cu/La_2O_3 and its catalytic performance in the synthesis of glycerol carbonate and monoacetin from glycerol and carbon dioxide, J. Colloid Interface Sci. 419 (2014) 31–38, https://doi.org/10.1016/j.jcis.2013.12.049.
[55] J. Zhang, D. He, Synthesis of glycerol carbonate and monoacetin from glycerol and carbon dioxide over Cu catalysts: the role of supports, J. Chem. Technol. Biotechnol. 90 (6) (2015) 1077–1085, https://doi.org/10.1002/jctb.4414.
[56] J.M.H. Al-Kurdhani, H. Wang, The Synthesis of Glycerol Carbonate from Glycerol and Carbon Dioxide over Supported CuO-Based Nanoparticle Catalyst, Molecules 28 (10) (2023) 4164, https://doi.org/10.3390/molecules28104164.
[57] J.C. Védrine, Importance, features and uses of metal oxide catalysts in heterogeneous catalysis, Chin. J. Catal. 40 (11) (2019) 1627–1636, https://doi.org/10.1016/S1872-2067(18)63162-6.
[58] A.B. Kehoe, D.O. Scanlon, G.W. Watson, Role of Lattice Distortions in the Oxygen Storage Capacity of Divalently Doped CeO_2, Chem. Mater. 23 (20) (2011) 4464–4468, https://doi.org/10.1021/cm201617d.
[59] P.H. Pandey, H.S. Pawar, Mingled Metal Oxides Catalyst for Direct Carbonylation of Glycerol into Glycerol Carbonate, ChemistrySelect 7 (12) (2022) e202104264, https://doi.org/10.1002/slct.202104264.
[60] J.N. Appaturi, E.-P. Ng, F. Adam, Solid imidazolium halide catalysts for the solvent free synthesis of glycerol carbonate, J. CO_2 Util. 6 (2014) 69–74, https://doi.org/10.1016/j.jcou.2014.01.002.
[61] Z. Gao, M. Xiang, M. He, W. Zhou, J. Chen, J. Lu, Z. Wu, Y. Su, Transformation of CO_2 with Glycerol to Glycerol Carbonate over ETS-10 Zeolite-Based Catalyst, Molecules 28 (5) (2023) 2272, https://doi.org/10.3390/molecules28052272.
[62] C. Luo, J. Wang, H. Lu, K. Wu, Y. Liu, Y. Zhu, B. Wang, B. Liang, Atmospheric-pressure synthesis of glycerol carbonate from CO_2 and glycerol catalyzed by protic ionic liquids, Green. Chem. 24 (21) (2022) 8292–8301, https://doi.org/10.1039/D2GC02674K.
[63] J. George, Y. Patel, S.M. Pillai, P. Munshi, Methanol assisted selective formation of 1,2-glycerol carbonate from glycerol and carbon dioxide using $^nBu_2SnO$ as a catalyst, J. Mol. Catal. A: Chem. 304 (1) (2009) 1–7, https://doi.org/10.1016/j.molcata.2009.01.010.
[64] A. Álvarez, M. Borges, J.J. Corral-Pérez, J.G. Olcina, L. Hu, D. Cornu, R. Huang, D. Stoian, A. Urakawa, CO_2 Activation over Catalytic Surfaces, ChemPhysChem 18 (22) (2017) 3135–3141, https://doi.org/10.1002/cphc.201700782.
[65] Q. Zhang, H.-Y. Yuan, X.-T. Lin, N. Fukaya, T. Fujitani, K. Sato, J.-C. Choi, Calcium carbide as a dehydrating agent for the synthesis of carbamates, glycerol carbonate, and cyclic carbonates from carbon dioxide, Green. Chem. 22 (13) (2020) 4231–4239, https://doi.org/10.1039/D0GC01402H.
[66] K. Takeuchi, K. Matsumoto, N. Fukaya, K. Sato, J.-C. Choi, Synthesis of Glycerol Carbonate from Glycerol and CO_2 Using CaO as a Dehydrating Agent, Asian J. Org. Chem. 11 (11) (2022) e202200212, https://doi.org/10.1002/ajoc.202200212.
[67] M. Aresta, A. Dibenedetto, F. Nocito, C. Pastore, A study on the carboxylation of glycerol to glycerol carbonate with carbon dioxide: The role of the catalyst, solvent and reaction conditions, J. Mol. Catal. A: Chem. 257 (1) (2006) 149–153, https://doi.org/10.1016/j.molcata.2006.05.021.
[68] S. Franklin, Carbonate-haloformate of glycerol and method of producing same, United States, 1948.
[69] A.K. Sharma, N. Kumar, Chapter 25 - Phosgene: Risk assessment, environmental, and health hazard, in: J. Singh, R.D. Kaushik, M. Chawla (Eds.), Hazardous Gases, Academic Press, 2021, pp. 313–325, https://doi.org/10.1016/B978-0-323-89857-7.00016-5.
[70] A. Tsuda, In situ photo-on-demand phosgenation reactions with chloroform for syntheses of polycarbonates and polyurethanes, Polym. J. 55 (9) (2023) 903–912, https://doi.org/10.1038/s41428-023-00800-w.
[71] Y. Zhang, X. Qiu, B. Wang, X. Liu, Y. Cheng, X. Rong, Y. Kuang, L. Sun, J. Liu, R. L. Luck, H. Liu, An effective fluorescent probe for detection of phosgene based on naphthalimide dyes in liquid and gaseous phases, Spectrochim. Acta Part A: Mol. Biomol. Spectrosc. 289 (2023) 122189, https://doi.org/10.1016/j.saa.2022.122189.
[72] J. Tan, Z. Li, Z. Lu, R. Chang, Z. Sun, J. You, Recent progress in the development of chemodosimeters for fluorescence visualization of phosgene, Dyes Pigments 193 (2021) 109540, https://doi.org/10.1016/j.dyepig.2021.109540.
[73] H. Zhang, H. Li, A. Wang, C. Xu, S. Yang, Progress of Catalytic Valorization of Bio-Glycerol with Urea into Glycerol Carbonate as a Monomer for Polymeric Materials, Adv. Polym. Tech. 2020 (2020) 7207068, https://doi.org/10.1155/2020/7207068.
[74] D. Procopio, M.L. Di Gioia, An Overview of the Latest Advances in the Catalytic Synthesis of Glycerol Carbonate, Catalysts 12 (1) (2022) 50, https://doi.org/10.3390/catal12010050.
[75] S.-i Fujita, Y. Yamanishi, M. Arai, Synthesis of glycerol carbonate from glycerol and urea using zinc-containing solid catalysts: A homogeneous reaction, J. Catal. 297 (2013) 137–141, https://doi.org/10.1016/j.jcat.2012.10.001.
[76] P. Manjunathan, R. Ravishankar, G.V. Shanbhag, Novel Bifunctional Zn–Sn Composite Oxide Catalyst for the Selective Synthesis of Glycerol Carbonate by Carbonylation of Glycerol with Urea, ChemCatChem 8 (3) (2016) 631–639, https://doi.org/10.1002/cctc.201501088.
[77] S.E. Kondawar, R.B. Mane, A. Vasishta, S.B. More, S.D. Dhengale, C.V. Rode, Carbonylation of glycerol with urea to glycerol carbonate over supported Zn catalysts, Appl. Petrochem. Res. 7 (1) (2017) 41–53, https://doi.org/10.1007/s13203-017-0177-2.
[78] G.P. Fernandes, G.D. Yadav, Selective glycerolysis of urea to glycerol carbonate using combustion synthesized magnesium oxide as catalyst, Catal. Today 309 (2018) 153–160, https://doi.org/10.1016/j.cattod.2017.08.021.
[79] M. Hasbi Ab Rahim, Q. He, J.A. Lopez-Sanchez, C. Hammond, N. Dimitratos, M. Sankar, A.F. Carley, C.J. Kiely, D.W. Knight, G.J. Hutchings, Gold, palladium

and gold–palladium supported nanoparticles for the synthesis of glycerol carbonate from glycerol and urea, Catal. Sci. Technol. 2 (9) (2012) 1914–1924, https://doi.org/10.1039/C2CY20288C.
[80] Y. Sun, X. Tong, Z. Wu, J. Liu, Y. Yan, S. Xue, A Sustainable Preparation of Glycerol Carbonate from Glycerol and Urea Catalyzed by Hydrotalcite-Like Solid Catalysts, Energy Technol. 2 (3) (2014) 263–268, https://doi.org/10.1002/ente.201300135.
[81] K. Jagadeeswaraiah, C.R. Kumar, P.S.S. Prasad, S. Loridant, N. Lingaiah, Synthesis of glycerol carbonate from glycerol and urea over tin-tungsten mixed oxide catalysts, Appl. Catal., A. 469 (2014) 165–172, https://doi.org/10.1016/j.apcata.2013.09.041.
[82] J. Chen, C. Wang, B. Dong, W. Leng, J. Huang, R. Ge, Y. Gao, Ionic liquids as eco-friendly catalysts for converting glycerol and urea into high value-added glycerol carbonate, Chin. J. Catal. 36 (3) (2015) 336–343, https://doi.org/10.1016/S1872-2067(14)60257-6.
[83] K. Ptaszyńska, A. Malaika, K. Kozigrodzka, M. Kozłowski, A Green Approach to Obtaining Glycerol Carbonate by Urea Glycerolysis Using Carbon-Supported Metal Oxide Catalysts, Molecules 28 (18) (2023) 6534, https://doi.org/10.3390/molecules28186534.
[84] P. Costanzo, C. Calandruccio, M.L. Di Gioia, M. Nardi, M. Oliverio, A. Procopio, First multicomponent reaction exploiting glycerol carbonate synthesis, J. Clean. Prod. 202 (2018) 504–509, https://doi.org/10.1016/j.jclepro.2018.08.120.
[85] C. Hammond, J.A. Lopez-Sanchez, M. Hasbi Ab Rahim, N. Dimitratos, R. L. Jenkins, A.F. Carley, Q. He, C.J. Kiely, D.W. Knight, G.J. Hutchings, Synthesis of glycerol carbonate from glycerol and urea with gold-based catalysts, Dalton Trans. 40 (15) (2011) 3927–3937, https://doi.org/10.1039/C0DT01389G.
[86] I. Banu, G. Bumbac, D. Bombos, S. Velea, A.-M. Gălan, G. Bozga, Glycerol acetylation with acetic acid over Purolite CT-275. Product yields and process kinetics, Renew. Energ. 148 (2020) 548–557, https://doi.org/10.1016/j.renene.2019.10.060.
[87] S. Fang, K. Fujimoto, Direct synthesis of dimethyl carbonate from carbon dioxide and methanol catalyzed by base, Appl. Catal., A. 142 (1) (1996) L1–L3, https://doi.org/10.1016/0926-860X(96)00081-6.
[88] G. Fiorani, A. Perosa, M. Selva, Dimethyl carbonate: a versatile reagent for a sustainable valorization of renewables, Green. Chem. 20 (2) (2018) 288–322, https://doi.org/10.1039/C7GC02118F.
[89] K. Hu, H. Wang, Y. Liu, C. Yang, KNO_3/CaO as cost-effective heterogeneous catalyst for the synthesis of glycerol carbonate from glycerol and dimethyl carbonate, J. Ind. Eng. Chem. 28 (2015) 334–343, https://doi.org/10.1016/j.jiec.2015.03.012.
[90] J.R. Ochoa-Gómez, O. Gómez-Jiménez-Aberasturi, B. Maestro-Madurga, A. Pesquera-Rodríguez, C. Ramírez-López, L. Lorenzo-Ibarreta, J. Torrecilla-Soria, M.C. Villarán-Velasco, Synthesis of glycerol carbonate from glycerol and dimethyl carbonate by transesterification: Catalyst screening and reaction optimization, Appl. Catal., A. 366 (2) (2009) 315–324, https://doi.org/10.1016/j.apcata.2009.07.020.
[91] P. Zhang, Y. Chen, M. Zhu, C. Yue, Y. Dong, Y. Leng, M. Fan, P. Jiang, Acidic–Basic Bifunctional Magnetic Mesoporous $CoFe_2O_4$@(CaO–ZnO) for the Synthesis of Glycerol Carbonate, Catal. Lett. 150 (10) (2020) 2863–2872, https://doi.org/10.1007/s10562-020-03191-2.
[92] J.R. Ochoa-Gómez, O. Gómez-Jiménez-Aberasturi, C. Ramírez-López, B. Maestro-Madurga, Synthesis of glycerol 1,2-carbonate by transesterification of glycerol with dimethyl carbonate using triethylamine as a facile separable homogeneous catalyst, Green. Chem. 14 (12) (2012) 3368–3376, https://doi.org/10.1039/C2GC35992H.
[93] D.J. Darensbourg, A.D. Yeung, Kinetics and thermodynamics of the decarboxylation of 1,2-glycerol carbonate to produce glycidol: computational insights, Green. Chem. 16 (1) (2014) 247–252, https://doi.org/10.1039/C3GC41643G.
[94] J.C. Védrine, Heterogeneous Catalysis on Metal Oxides, Catalysts 7 (11) (2017) 341, https://doi.org/10.3390/catal7110341.
[95] M. Kouzu, T. Kasuno, M. Tajika, S. Yamanaka, J. Hidaka, Active phase of calcium oxide used as solid base catalyst for transesterification of soybean oil with refluxing methanol, Appl. Catal., A. 334 (1) (2008) 357–365, https://doi.org/10.1016/j.apcata.2007.10.023.
[96] J. Li, T. Wang, On the deactivation of alkali solid catalysts for the synthesis of glycerol carbonate from glycerol and dimethyl carbonate, React. Kinet. Mech. Catal. 102 (1) (2011) 113–126, https://doi.org/10.1007/s11144-010-0259-y.
[97] P. Lu, H. Wang, K. Hu, Synthesis of glycerol carbonate from glycerol and dimethyl carbonate over the extruded CaO-based catalyst, Chem. Eng. J. 228 (2013) 147–154, https://doi.org/10.1016/j.cej.2013.04.109.
[98] Y. Tang, Y. Xue, Z. Li, T. Yan, R. Zhou, Z. Zhang, Heterogeneous synthesis of glycerol carbonate from glycerol and dimethyl carbonate catalyzed by LiCl/CaO, J. Saudi Chem. Soc. 23 (4) (2019) 494–502, https://doi.org/10.1016/j.jscs.2018.11.003.
[99] W. Roschat, S. Phewphong, T. Kaewpuang, V. Promarak, Synthesis of glycerol carbonate from transesterification of glycerol with dimethyl carbonate catalyzed by CaO from natural sources as green and economical catalyst, Mater. Today Proc. 5 (6, Part 1) (2018) 13909–13915, https://doi.org/10.1016/j.matpr.2018.02.039.
[100] W. Praikaew, W. Kiatkittipong, F. Aiouache, V. Najdanovic-Visak, M. Termtanun, J.W. Lim, S.S. Lam, K. Kiatkittipong, N. Laosiripojana, S. Boonyasuwat, S. Assabumrungrat, Mechanism of CaO catalyst deactivation with unconventional monitoring method for glycerol carbonate production via transesterification of glycerol with dimethyl carbonate, Int. J. Energy Res. 46 (2) (2022) 1646–1658, https://doi.org/10.1002/er.7281.
[101] B. Changmai, I.B. Laskar, S.L. Rokhum, Microwave-assisted synthesis of glycerol carbonate by the transesterification of glycerol with dimethyl carbonate using Musa acuminata peel ash catalyst, J. Taiwan Inst. Chem. Eng. 102 (2019) 276–282, https://doi.org/10.1016/j.jtice.2019.06.014.
[102] F.S.H. Simanjuntak, S.R. Lim, B.S. Ahn, H.S. Kim, H. Lee, Surfactant-assisted synthesis of MgO: Characterization and catalytic activity on the transesterification of dimethyl carbonate with glycerol, Appl. Catal., A. 484 (2014) 33–38, https://doi.org/10.1016/j.apcata.2014.06.028.
[103] Z. Bai, Y. Zheng, W. Han, Y. Ji, T. Yan, Y. Tang, G. Chen, Z. Zhang, Development of a trapezoidal MgO catalyst for highly-efficient transesterification of glycerol and dimethyl carbonate, CrystEngComm 20 (29) (2018) 4090–4098, https://doi.org/10.1039/C8CE00808F.
[104] M. Du, Q. Li, W. Dong, T. Geng, Y. Jiang, Synthesis of glycerol carbonate from glycerol and dimethyl carbonate catalyzed by K_2CO_3/MgO, Res. Chem. Intermed. 38 (3) (2012) 1069–1077, https://doi.org/10.1007/s11164-011-0443-3.
[105] S. Sandesh, G.V. Shanbhag, A.B. Halgeri, Transesterification of Glycerol to Glycerol Carbonate Using KF/Al_2O_3 Catalyst: The Role of Support and Basicity, Catal. Lett. 143 (11) (2013) 1226–1234, https://doi.org/10.1007/s10562-013-1043-1.
[106] R. Bai, Y. Wang, S. Wang, F. Mei, T. Li, G. Li, Synthesis of glycerol carbonate from glycerol and dimethyl carbonate catalyzed by NaOH/γ-Al_2O_3, Fuel Process. Technol. 106 (2013) 209–214, https://doi.org/10.1016/j.fuproc.2012.07.027.
[107] E. Elhaj, H. Wang, M. Imran, S.E.F. Hegazi, M. Hassan, M.A. Eldoma, J. Hakami, W.A. Wani, A.A. Chaudhary, Nanocatalyst-Assisted Facile One-Pot Synthesis of Glycidol from Glycerol and Dimethyl Carbonate, ACS Omega 7 (36) (2022) 31778–31788, https://doi.org/10.1021/acsomega.2c02381.
[108] C. Yue, M. Fan, P. Zhang, L. Liu, P. Jiang, Monodisperse mesoporous La_2O_3 flakes for the synthesis of glycerol carbonate by efficiently catalyzing the transesterification of dimethyl carbonate with glycerol, React. Kinet. Mech. Catal. 128 (2) (2019) 763–778, https://doi.org/10.1007/s11144-019-01635-4.
[109] Y. Li, J. Liu, D. He, Catalytic synthesis of glycerol carbonate from biomass-based glycerol and dimethyl carbonate over Li-La_2O_3 catalysts, Appl. Catal., A. 564 (2018) 234–242, https://doi.org/10.1016/j.apcata.2018.07.032.
[110] J. Yu, K. Wang, S. Shao, W. Li, S. Du, X. Chen, C. Chao, X. Fan, Effect of ionic radius and valence state of alkali and alkaline earth metals on promoting the catalytic performance of La_2O_3 catalysts for glycerol carbonate production, Chem. Eng. J. 458 (2023) 141486, https://doi.org/10.1016/j.cej.2023.141486.
[111] A. Kaur, A. Ali, Lithium Zirconate as a Selective and Cost-Effective Mixed Metal Oxide Catalyst for Glycerol Carbonate Production, Ind. Eng. Chem. Res. 59 (7) (2020) 2667–2679, https://doi.org/10.1021/acs.iecr.9b05747.
[112] X. Song, Y. Wu, F. Cai, D. Pan, G. Xiao, High-efficiency and low-cost Li/ZnO catalysts for synthesis of glycerol carbonate from glycerol transesterification: The role of Li and ZnO interaction, Appl. Catal., A. 532 (2017) 77–85, https://doi.org/10.1016/j.apcata.2016.12.019.
[113] Y. Liu, Z. Yin, Z. Wang, R. Mou, Z. Wei, Synthesis of glycerol carbonate with high surface area ZrO_2–KOH catalyst, Res. Chem. Intermed. 48 (6) (2022) 2557–2573, https://doi.org/10.1007/s11164-022-04725-6.
[114] S. Jaiswal, S. Sahani, Y.C. Shar, Enviro-benign synthesis of glycerol carbonate utilizing bio-waste glycerol over Na-Ti based heterogeneous catalyst: Kinetics and E- metrics studies, J. Environ. Chem. Eng. 10 (3) (2022) 107485, https://doi.org/10.1016/j.jece.2022.107485.
[115] C.M. Scheid, W.F. Monteiro, M.O. Vieira, L. Alban, L. Luza, D. Eberhardt, R. V. Gonçalves, A.F. Feil, J.E.A. de Lima, R.A. Ligabue, Glycerol carbonate synthesis over nanostructured titanate catalysts: Effect of morphology and structure of catalyst, Chem. Eng. Res. Des. 197 (2023) 392–404, https://doi.org/10.1016/j.cherd.2023.07.039.
[116] M.B. Gawande, R.K. Pandey, R.V. Jayaram, Role of mixed metal oxides in catalysis science—versatile applications in organic synthesis, Catal. Sci. Technol. 2 (6) (2012) 1113–1125, https://doi.org/10.1039/C2CY00490A.
[117] F.S.H. Simanjuntak, V.T. Widyaya, C.S. Kim, B.S. Ahn, Y.J. Kim, H. Lee, Synthesis of glycerol carbonate from glycerol and dimethyl carbonate using magnesium–lanthanum mixed oxide catalyst, Chem. Eng. Sci. 94 (2013) 265–270, https://doi.org/10.1016/j.ces.2013.01.070.
[118] D. Singh, B. Reddy, A. Ganesh, S. Mahajani, Zinc/Lanthanum Mixed-Oxide Catalyst for the Synthesis of Glycerol Carbonate by Transesterification of Glycerol, Ind. Eng. Chem. Res. 53 (49) (2014) 18786–18795, https://doi.org/10.1021/ie5011564.
[119] P. Kumar, P. With, V.C. Srivastava, R. Gläser, I.M. Mishra, Glycerol Carbonate Synthesis by Hierarchically Structured Catalysts: Catalytic Activity and Characterization, Ind. Eng. Chem. Res. 54 (50) (2015) 12543–12552, https://doi.org/10.1021/acs.iecr.5b03644.
[120] X. Song, D. Pan, Y. Wu, P. Cheng, R. Wei, L. Gao, J. Zhang, G. Xiao, Synthesis of glycerol carbonate over porous La-Zr based catalysts: The role of strong and super basic sites, J. Alloy. Compd. 750 (2018) 828–837, https://doi.org/10.1016/j.jallcom.2018.03.392.
[121] D. Phadtare, S. Kondawar, A. Athawale, C. Rode, Crystalline $LaCoO_3$ perovskite as a novel catalyst for glycerol transesterification, Mol. Catal. 475 (2019) 110496, https://doi.org/10.1016/j.mcat.2019.110496.
[122] P.P. Pattanaik, P.M. Kumar, N. Raju, N. Lingaiah, Continuous Synthesis of Glycerol Carbonate by Transesterification of Glycerol with Dimethyl Carbonate Over Fe–La Mixed Oxide Catalysts, Catal. Lett. 151 (5) (2021) 1433–1443, https://doi.org/10.1007/s10562-020-03397-4.
[123] M.S. Khayoon, B.H. Hameed, $Mg_{1+x}Ca_{1-x}O_2$ as reusable and efficient heterogeneous catalyst for the synthesis of glycerol carbonate via the transesterification of glycerol with dimethyl carbonate, Appl. Catal., A. 466 (2013) 272–281, https://doi.org/10.1016/j.apcata.2013.06.044.

[124] Z. Liu, B. Li, F. Qiao, Y. Zhang, X. Wang, Z. Niu, J. Wang, H. Lu, S. Su, R. Pan, Y. Wang, Y. Xue, Catalytic Performance of Li/Mg Composites for the Synthesis of Glycerol Carbonate from Glycerol and Dimethyl Carbonate, ACS Omega 7 (6) (2022) 5032–5038, https://doi.org/10.1021/acsomega.1c05968.
[125] S. Jaiswal, S. Maurya, Y.C. Sharma, Studies on role of support metal in glycerol conversion to glycerol carbonate through Mg/MnO_2 and Mg/CuO heterogeneous catalyst, Mol. Catal. 546 (2023) 113243, https://doi.org/10.1016/j.mcat.2023.113243.
[126] G. Pradhan, S. Jaiswal, Y.C. Sharma, Exploring the promotional effect of transition metals (Cr and V) on the catalytic activity of MgO for glycerol carbonate synthesis, Mol. Catal. 526 (2022) 112332, https://doi.org/10.1016/j.mcat.2022.112332.
[127] G. Pradhan, S. Maurya, S. Pradhan, Y.C. Sharma, An accelerated route for synthesis of Glycerol carbonate using $MgTiO_3$ perovskite as greener and cheaper catalyst, Mol. Catal. 545 (2023) 113162, https://doi.org/10.1016/j.mcat.2023.113162.
[128] B. Reisi, A. Najafi Chermahini, Modification g-C_3N_4 by MgO and its application for glycerol carbonate synthesis from glycerol and dimethyl carbonate, Environ. Prog. Sustain. Energy 42 (2) (2023) e14007, https://doi.org/10.1002/ep.14007.
[129] M. Varkolu, D.R. Burri, S.R.R. Kamaraju, S.B. Jonnalagadda, W.E. Van Zyl, Transesterification of glycerol with dimethyl carbonate over nanocrystalline ordered mesoporous MgO–ZrO_2 solid base catalyst, J. Porous Mater. 23 (1) (2016) 185–193, https://doi.org/10.1007/s10934-015-0069-8.
[130] Y. Li, H. Zhao, W. Xue, F. Li, Z. Wang, Transesterification of Glycerol to Glycerol Carbonate over Mg-Zr Composite Oxide Prepared by Hydrothermal Process, Nanomater 12 (12) (2022) 1972, https://doi.org/10.3390/nano12121972.
[131] G. Parameswaram, P.S.N. Rao, A. Srivani, G.N. Rao, N. Lingaiah, Magnesia-ceria mixed oxide catalysts for the selective transesterification of glycerol to glycerol carbonate, Mol. Catal. 451 (2018) 135–142, https://doi.org/10.1016/j.mcat.2017.12.006.
[132] G. Pradhan, Y. Chandra Sharma, Studies on green synthesis of glycerol carbonate from waste cooking oil derived glycerol over an economically viable $NiMgO_x$ heterogeneous solid base catalyst, J. Clean. Prod. 264 (2020) 121258, https://doi.org/10.1016/j.jclepro.2020.121258.
[133] X. Zhang, S. Wei, X. Zhao, Z. Chen, H. Wu, P. Rong, Y. Sun, Y. Li, H. Yu, D. Wang, Preparation of mesoporous CaO-ZrO_2 catalysts without template for the continuous synthesis of glycerol carbonate in a fixed-bed reactor, Appl. Catal., A. 590 (2020) 117313, https://doi.org/10.1016/j.apcata.2019.117313.
[134] S. Jaiswal, Y.C. Sharma, Ni modified distillation waste derived heterogeneous catalyst utilized for the production of glycerol carbonate from a biodiesel by-product glycerol: Optimization and green metric studies, Waste Manag. 156 (2023) 148–158, https://doi.org/10.1016/j.wasman.2022.11.003.
[135] L. Xu, S. Wang, P.U. Okoye, J. Wang, S. Li, L. Zhang, A. Zhang, T. Tang, Water glass derived catalyst for the synthesis of glycerol carbonate via the transesterification reaction between glycerol and dimethyl carbonate, J. Serb. Chem. Soc. 84 (6) (2019) 609–622. ⟨https://www.shd-pub.org.rs/index.php/JSCS/article/view/7299⟩.
[136] D. Wang, D. Bai, J. Xiong, Z. Chen, X. Zhao, H. Wu, J. Shan, S. Wei, X. Zhang, The atom-efficient production of glycerol carbonate via transesterification between dimethyl carbonate and glycerol over fluorinated Al_2O_3-ZrO_2 solid solution catalysts with suitable acidic-basic property, Appl. Catal., A. 665 (2023) 119370, https://doi.org/10.1016/j.apcata.2023.119370.
[137] M. Malyaadri, K. Jagadeeswaraiah, P.S. Sai Prasad, N. Lingaiah, Synthesis of glycerol carbonate by transesterification of glycerol with dimethyl carbonate over Mg/Al/Zr catalysts, Appl. Catal., A. 401 (1) (2011) 153–157, https://doi.org/10.1016/j.apcata.2011.05.011.
[138] G. Parameswaram, M. Srinivas, B. Hari Babu, P.S. Sai Prasad, N. Lingaiah, Transesterification of glycerol with dimethyl carbonate for the synthesis of glycerol carbonate over Mg/Zr/Sr mixed oxide base catalysts, Catal. Sci. Technol. 3 (12) (2013) 3242–3249, https://doi.org/10.1039/C3CY00532A.
[139] M. Marimuthu, P. Marimuthu, A.K. S.K, S. Palanivelu, V. Rajagopalan, Tuning the basicity of Cu-based mixed oxide catalysts towards the efficient conversion of glycerol to glycerol carbonate, Mol. Catal. 460 (2018) 53–62, https://doi.org/10.1016/j.mcat.2018.09.002.
[140] S. Arora, V. Gosu, U.K.A. Kumar, T.C. Zhang, V. Subbaramaiah, A novel Ce-CaO/MgO catalyst derived from marble waste through green synthesis route for glycerol carbonate synthesis, React. Kinet. Mech. Catal. 132 (2) (2021) 839–858, https://doi.org/10.1007/s11144-021-01930-z.
[141] Q. Wang, D. O'Hare, Recent Advances in the Synthesis and Application of Layered Double Hydroxide (LDH) Nanosheets, Chem. Rev. 112 (7) (2012) 4124–4155, https://doi.org/10.1021/cr200434v.
[142] G. Mishra, B. Dash, S. Pandey, Layered double hydroxides: A brief review from fundamentals to application as evolving biomaterials, Appl. Clay Sci. 153 (2018) 172–186, https://doi.org/10.1016/j.clay.2017.12.021.
[143] A. Takagaki, K. Iwatani, S. Nishimura, K. Ebitani, Synthesis of glycerol carbonate from glycerol and dialkyl carbonates using hydrotalcite as a reusable heterogeneous base catalyst, Green. Chem. 12 (4) (2010) 578–581, https://doi.org/10.1039/B925404H.
[144] Y.-T. Hsu, J.C.S. Wu, V.-H. Nguyen, MgxAl-LDHs layered double hydroxides catalysts for boosting catalytic synthesis of biodiesel and conversion of by-product into valuable glycerol carbonate, J. Taiwan Inst. Chem. Eng. 104 (2019) 219–226, https://doi.org/10.1016/j.jtice.2019.09.020.
[145] A. Kumar, K. Iwatani, S. Nishimura, A. Takagaki, K. Ebitani, Promotion effect of coexistent hydromagnesite in a highly active solid base hydrotalcite catalyst for transesterifications of glycols into cyclic carbonates, Catal. Today 185 (1) (2012) 241–246, https://doi.org/10.1016/j.cattod.2011.08.016.
[146] Y. Sun, X. Gao, N. Yang, X. Tantai, X. Xiao, B. Jiang, L. Zhang, Morphology-Controlled Synthesis of Three-Dimensional Hierarchical Flowerlike Mg–Al Layered Double Hydroxides with Enhanced Catalytic Activity for Transesterification, Ind. Eng. Chem. Res. 58 (19) (2019) 7937–7947, https://doi.org/10.1021/acs.iecr.9b00703.
[147] P. Liu, M. Derchi, E.J.M. Hensen, Promotional effect of transition metal doping on the basicity and activity of calcined hydrotalcite catalysts for glycerol carbonate synthesis, Appl. Catal., B: Envi. 144 (2014) 135–143, https://doi.org/10.1016/j.apcatb.2013.07.010.
[148] X. Zhang, D. Wang, J. Ma, W. Wei, Fluorinated Mg–Al Hydrotalcites Derived Basic Catalysts for Transesterification of Glycerol with Dimethyl Carbonate, Catal. Lett. 147 (5) (2017) 1181–1196, https://doi.org/10.1007/s10562-017-2013-9.
[149] P. Liu, M. Derchi, E.J.M. Hensen, Synthesis of glycerol carbonate by transesterification of glycerol with dimethyl carbonate over MgAl mixed oxide catalysts, Appl. Catal., A. 467 (2013) 124–131, https://doi.org/10.1016/j.apcata.2013.07.020.
[150] Z. Liu, J. Wang, M. Kang, N. Yin, X. Wang, Y. Tan, Y. Zhu, Structure-activity correlations of $LiNO_3$/$Mg_4AlO_{5.5}$ catalysts for glycerol carbonate synthesis from glycerol and dimethyl carbonate, J. Ind. Eng. Chem. 21 (2015) 394–399, https://doi.org/10.1016/j.jiec.2014.02.051.
[151] M. Hong, L. Gao, G. Xiao, An Efficient and Green Transesterification of Glycols into Cyclic Carbonates Catalysed by KF/Ca–Mg–Al Hydrotalcite, J. Chem. Res. 38 (11) (2014) 679–681, https://doi.org/10.3184/174751914X14138850796063.
[152] G. Liu, J. Yang, X. Xu, Synthesis of hydrotalcite-type mixed oxide catalysts from waste steel slag for transesterification of glycerol and dimethyl carbonate, Sci. Rep. 10 (1) (2020) 10273, https://doi.org/10.1038/s41598-020-67357-z.
[153] G. Liu, J. Yang, X. Xu, Synthesis of Hydrotalcites from Waste Steel Slag with [Bmim]OH Intercalated for the Transesterification of Glycerol Carbonate, Molecules 25 (19) (2020) 4355, https://doi.org/10.3390/molecules25194355.
[154] G. Liu, J. Yang, Y. Zhao, X. Xu, Embedded ionic liquid modified ZIF-8 in CaMgAl hydrotalcites for bio-glycerol transesterification, RSC Adv. 12 (7) (2022) 4408–4416, https://doi.org/10.1039/D1RA08928E.
[155] J. Granados-Reyes, P. Salagre, Y. Cesteros, CaAl-layered double hydroxides as active catalysts for the transesterification of glycerol to glycerol carbonate, Appl. Clay Sci. 132-133 (2016) 216–222, https://doi.org/10.1016/j.clay.2016.06.008.
[156] J. Granados-Reyes, P. Salagre, Y. Cesteros, Effect of the preparation conditions on the catalytic activity of calcined Ca/Al-layered double hydroxides for the synthesis of glycerol carbonate, Appl. Catal., A. 536 (2017) 9–17, https://doi.org/10.1016/j.apcata.2017.02.013.
[157] D.S. Argüello, L.C. Cabana Saavedra, S.M. Mendoza, M.I. Oliva, E. Rodríguez-Castellón, N.F. Bálsamo, G.A. Eimer, M.E. Crivello, Layered double hydroxides modified by transition metals for sustainable glycerol valorization to glycerol carbonate, Catal. Today 427 (2024) 114415, https://doi.org/10.1016/j.cattod.2023.114415.
[158] S. Ramesh, D.P. Debecker, Room temperature synthesis of glycerol carbonate catalyzed by spray dried sodium aluminate microspheres, Catal. Commun. 97 (2017) 102–105, https://doi.org/10.1016/j.catcom.2017.04.034.
[159] P. Rittiron, C. Niamnuy, W. Donphai, M. Chareonpanich, A. Seubsai, Production of Glycerol Carbonate from Glycerol over Templated-Sodium-Aluminate Catalysts Prepared Using a Spray-Drying Method, ACS Omega 4 (5) (2019) 9001–9009, https://doi.org/10.1021/acsomega.9b00805.
[160] A. Chotchuang, P. Kunsuk, A. Phanpitakkul, S. Chanklang, M. Chareonpanich, A. Seubsai, Production of glycerol carbonate from glycerol over modified sodium-aluminate-doped calcium oxide catalysts, Catal. Today 388-389 (2022) 351–359, https://doi.org/10.1016/j.cattod.2020.06.007.
[161] S. Ramesh, F. Devred, L. van den Biggelaar, D.P. Debecker, Hydrotalcites Promoted by $NaAlO_2$ as Strongly Basic Catalysts with Record Activity in Glycerol Carbonate Synthesis, ChemCatChem 10 (6) (2018) 1398–1405, https://doi.org/10.1002/cctc.201701726.
[162] J. Keogh, G. Deshmukh, H. Manyar, Green synthesis of glycerol carbonate via transesterification of glycerol using mechanochemically prepared sodium aluminate catalysts, Fuel 310 (2022) 122484, https://doi.org/10.1016/j.fuel.2021.122484.
[163] S. Wang, P. Hao, S. Li, A. Zhang, Y. Guan, L. Zhang, Synthesis of glycerol carbonate from glycerol and dimethyl carbonate catalyzed by calcined silicates, Appl. Catal., A. 542 (2017) 174–181, https://doi.org/10.1016/j.apcata.2017.05.021.
[164] D. Kumar, K. Schumacher, C. du Fresne von Hohenesche, M. Grün, K.K. Unger, MCM-41, MCM-48 and related mesoporous adsorbents: their synthesis and characterisation, Colloids Surf. Physicochem. Eng. Asp. 187-188 (2001) 109–116, https://doi.org/10.1016/S0927-7757(01)00638-0.
[165] G.D. Wu, X.L. Wang, Z.L. Zhai, A.Y. Cao, Synthesis of Glycerol Carbonate by Transesterification of Glycerol with Dimethyl Carbonate over Mg-Al Mixed Oxides Supported on MCM-41, Adv. Mat. Res. 1008-1009 (2014) 319–322, https://doi.org/10.4028/www.scientific.net/AMR.1008-1009.319.
[166] S. Arora, V. Gosu, U.K.A. Kumar, V. Subbaramaiah, Valorization of glycerol into glycerol carbonate using the stable heterogeneous catalyst of Li/MCM-41, J. Clean. Prod. 295 (2021) 126437, https://doi.org/10.1016/j.jclepro.2021.126437.
[167] S. Arora, V. Gosu, V. Subbaramaiah, T.C. Zhang, Catalytic transesterification of glycerol with dimethyl carbonate to glycerol carbonate with Co_3O_4 nanoparticle incorporated MCM-41 derived from rice husk, Can. J. Chem. Eng. 100 (8) (2022) 1868–1883, https://doi.org/10.1002/cjce.24284.
[168] D. Zhao, J. Feng, Q. Huo, N. Melosh, G.H. Fredrickson, B.F. Chmelka, G.D. Stucky, Triblock Copolymer Syntheses of Mesoporous Silica with Periodic 50 to 300

Angstrom Pores, Science 279 (5350) (1998) 548–552, https://doi.org/10.1126/science.279.5350.548.
[169] P. Devi, U. Das, A.K. Dalai, Production of glycerol carbonate using a novel Ti-SBA-15 catalyst, Chem. Eng. J. 346 (2018) 477–488, https://doi.org/10.1016/j.cej.2018.04.030.
[170] Q.M. She, W.J. Huang, A. Talebian-Kiakalaieh, H. Yang, C.H. Zhou, Layered double hydroxide uniformly coated on mesoporous silica with tunable morphorlogies for catalytic transesterification of glycerol with dimethyl carbonate, Appl. Clay Sci. 210 (2021) 106135, https://doi.org/10.1016/j.clay.2021.106135.
[171] J. Zhu, D. Chen, Z. Wang, Q. Wu, Z. Yin, Z. Wei, Synthesis of glycerol carbonate from glycerol and dimethyl carbonate over CaO-SBA-15 catalyst, Chem. Eng. Sci. 258 (2022) 117760, https://doi.org/10.1016/j.ces.2022.117760.
[172] S. Arora, V. Gosu, V. Subbaramaiah, One-pot synthesis of glycerol carbonate from glycerol using three-dimensional mesoporous silicates of K/TUD-1 under environmentally benign conditions, Mol. Catal. 496 (2020) 111188, https://doi.org/10.1016/j.mcat.2020.111188.
[173] J. Weitkamp, Zeolites and catalysis, Solid State Ion. 131 (1) (2000) 175–188, https://doi.org/10.1016/S0167-2738(00)00632-9.
[174] S. Pan, L. Zheng, R. Nie, S. Xia, P. Chen, Z. Hou, Transesterification of Glycerol with Dimethyl Carbonate to Glycerol Carbonate over Na–based Zeolites, Chin. J. Catal. 33 (11) (2012) 1772–1777, https://doi.org/10.1016/S1872-2067(11)60450-6.
[175] M. Xiang, D. Wu, Transition metal-promoted hierarchical ETS-10 solid base for glycerol transesterification, RSC Adv. 8 (58) (2018) 33473–33486, https://doi.org/10.1039/C8RA06811A.
[176] C.-W. Chang, Z.-J. Gong, N.-C. Huang, C.-Y. Wang, W.-Y. Yu, MgO nanoparticles confined in ZIF-8 as acid-base bifunctional catalysts for enhanced glycerol carbonate production from transesterification of glycerol and dimethyl carbonate, Catal. Today 351 (2020) 21–29, https://doi.org/10.1016/j.cattod.2019.03.007.
[177] S. Kosawatthanakun, E.B. Clatworthy, S. Ghojavand, N. Sosa, J. Wittayakun, S. Mintova, Application of a BPH zeolite for the transesterification of glycerol to glycerol carbonate: effect of morphology, cation type and reaction conditions, Inorg. Chem. Front. 10 (2) (2023) 579–590, https://doi.org/10.1039/D2QI02023H.
[178] K.H. Lee, C.-H. Park, E.Y. Lee, Biosynthesis of glycerol carbonate from glycerol by lipase in dimethyl carbonate as the solvent, Bioprocess Biosyst. Eng. 33 (9) (2010) 1059–1065, https://doi.org/10.1007/s00449-010-0431-9.
[179] S.C. Kim, Y.H. Kim, H. Lee, D.Y. Yoon, B.K. Song, Lipase-catalyzed synthesis of glycerol carbonate from renewable glycerol and dimethyl carbonate through transesterification, J. Mol. Catal. B: Enzym. 49 (1) (2007) 75–78, https://doi.org/10.1016/j.molcatb.2007.08.007.
[180] Y. Du, J. Gao, W. Kong, L. Zhou, L. Ma, Y. He, Z. Huang, Y. Jiang, Enzymatic Synthesis of Glycerol Carbonate Using a Lipase Immobilized on Magnetic Organosilica Nanoflowers as a Catalyst, ACS Omega 3 (6) (2018) 6642–6650, https://doi.org/10.1021/acsomega.8b00746.
[181] M. Tudorache, L. Protesescu, A. Negoi, V.I. Parvulescu, Recyclable biocatalytic composites of lipase-linked magnetic macro-/nano-particles for glycerol carbonate synthesis, Appl. Catal., A. 437-438 (2012) 90–95, https://doi.org/10.1016/j.apcata.2012.06.016.
[182] M. Tudorache, A. Nae, S. Coman, V.I. Parvulescu, Strategy of cross-linked enzyme aggregates onto magnetic particles adapted to the green design of biocatalytic synthesis of glycerol carbonate, RSC Adv. 3 (12) (2013) 4052–4058, https://doi.org/10.1039/C3RA23222K.
[183] M. Tudorache, A. Negoi, L. Protesescu, V.I. Parvulescu, Biocatalytic alternative for bio-glycerol conversion with alkyl carbonates via a lipase-linked magnetic nano-particles assisted process, Appl. Catal., B: Envi. 145 (2014) 120–125, https://doi.org/10.1016/j.apcatb.2012.12.033.
[184] B. Das, K. Mohanty, A green and facile production of catalysts from waste red mud for the one-pot synthesis of glycerol carbonate from glycerol, J. Environ. Chem. Eng. 7 (1) (2019) 102888, https://doi.org/10.1016/j.jece.2019.102888.
[185] B. Das, K. Mohanty, Exploring the promotional effects of K, Sr, and Mg on the catalytic stability of red mud for the synthesis of glycerol carbonate from renewable glycerol, Ind. Eng. Chem. Res. 58 (35) (2019) 15803–15817, https://doi.org/10.1021/acs.iecr.9b00420.
[186] P.U. Okoye, A.Z. Abdullah, B.H. Hameed, Stabilized ladle furnace steel slag for glycerol carbonate synthesis via glycerol transesterification reaction with dimethyl carbonate, Energy Convers. Manag. 133 (2017) 477–485, https://doi.org/10.1016/j.enconman.2016.10.067.
[187] P.U. Okoye, S. Wang, W.A. Khanday, S. Li, T. Tang, L. Zhang, Box-Behnken optimization of glycerol transesterification reaction to glycerol carbonate over calcined oil palm fuel ash derived catalyst, Renew. Energ. 146 (2020) 2676–2687, https://doi.org/10.1016/j.renene.2019.08.072.
[188] S. Wang, J. Wang, P. Sun, L. Xu, P.U. Okoye, S. Li, L. Zhang, A. Guo, J. Zhang, A. Zhang, Disposable baby diapers waste derived catalyst for synthesizing glycerol carbonate by the transesterification of glycerol with dimethyl carbonate, J. Clean. Prod. 211 (2019) 330–341, https://doi.org/10.1016/j.jclepro.2018.11.196.
[189] S. Wang, J. Wang, P.U. Okoye, S. Chen, X. Li, L. Duan, H. Zhou, S. Li, T. Tang, L. Zhang, Application of corncob residue-derived catalyst in the transesterification of glycerol with dimethyl carbonate to synthesize glycerol carbonate, BioResources 15 (1) (2020) 142–158, https://doi.org/10.15376/biores.15.1.142-158.
[190] J. Wang, H. Liu, Z. Chen, Y. Sun, S. Wang, Using waste crayfish shell derived catalyst to synthesize glycerol carbonate by transesterification reaction between glycerol and dimethyl carbonate, React. Kinet. Mech. Catal. 133 (1) (2021) 191–208, https://doi.org/10.1007/s11144-021-01973-2.
[191] R.D. Ortiz Olivares, P.U. Okoye, J.F. Ituna-Yudonago, C.N. Njoku, B.H. Hameed, W. Song, S. Li, A. Longoria, P.J. Sebastian, Valorization of biodiesel byproduct glycerol to glycerol carbonate using highly reusable apatite-like catalyst derived from waste Gastropoda Mollusca, Biomass-.-. Convers. Bior. 13 (2) (2023) 619–631, https://doi.org/10.1007/s13399-020-01122-0.
[192] P.U. Okoye, S. Wang, L. Xu, S. Li, J. Wang, L. Zhang, Promotional effect of calcination temperature on structural evolution, basicity, and activity of oil palm empty fruit bunch derived catalyst for glycerol carbonate synthesis, Energy Convers. Manag. 179 (2019) 192–200, https://doi.org/10.1016/j.enconman.2018.10.013.
[193] A. Das, D. Shi, G. Halder, S. Lalthazuala Rokhum, Microwave-assisted synthesis of glycerol carbonate by transesterification of glycerol using Mangifera indica peel calcined ash as catalyst, Fuel 330 (2022) 125511, https://doi.org/10.1016/j.fuel.2022.125511.
[194] K. Shikhaliyev, B.H. Hameed, P.U. Okoye, Utilization of biochars as sustainable catalysts for upgrading of glycerol from biodiesel production, J. Environ. Chem. Eng. 9 (2) (2021) 104768, https://doi.org/10.1016/j.jece.2020.104768.
[195] R. Bai, S. Wang, F. Mei, T. Li, G. Li, Synthesis of glycerol carbonate from glycerol and dimethyl carbonate catalyzed by KF modified hydroxyapatite, J. Ind. Eng. Chem. 17 (4) (2011) 777–781, https://doi.org/10.1016/j.jiec.2011.05.027.
[196] M. Zhu, C. Yue, P. Zhang, M. Fan, P. Jiang, Y. Dong, W. Sun, Surface modification of KF Immobilized on spherical magnetite nanoparticle with ctab for glycerol carbonate production, ChemistrySelect 4 (4) (2019) 1214–1219, https://doi.org/10.1002/slct.201803670.
[197] Y. Chai, Y. Li, H. Hu, C. Zeng, S. Wang, H. Xu, Y. Gao, N-heterocyclic carbene functionalized covalent organic framework for transesterification of glycerol with dialkyl carbonates, Catalysts 11 (4) (2021) 423, https://doi.org/10.3390/catal11040423.
[198] F.S.H. Simanjuntak, J.S. Choi, G. Lee, H.J. Lee, S.D. Lee, M. Cheong, H.S. Kim, H. Lee, Synthesis of glycerol carbonate from the transesterification of dimethyl carbonate with glycerol using DABCO and DABCO-anchored Merrifield resin, Appl. Catal., B: Envi. 165 (2015) 642–650, https://doi.org/10.1016/j.apcatb.2014.10.071.
[199] Y. Wan, Y. Lei, G. Lan, D. Liu, G. Li, R. Bai, Synthesis of glycerol carbonate from glycerol and dimethyl carbonate over DABCO embedded porous organic polymer as a bifunctional and robust catalyst, Appl. Catal. A. 562 (2018) 267–275, https://doi.org/10.1016/j.apcata.2018.06.022.